CANADIAN THESES ON MICROFICHE

THÈSES CANADIENNES SUR MICROFICHE

National Library of Canada
Collections Development Branch

Canadian Theses on
Microfiche Service

Ottawa, Canada
K1A 0N4

Bibliothèque nationale du Canada
Direction du développement des collections

Service des thèses canadiennes
sur microfiche

NOTICE

The quality of this microfiche is heavily dependent upon the quality of the original thesis submitted for microfilming. Every effort has been made to ensure the highest quality of reproduction possible.

If pages are missing, contact the university which granted the degree.

Some pages may have indistinct print especially if the original pages were typed with a poor typewriter ribbon or if the university sent us an inferior photocopy.

Previously copyrighted materials (journal articles, published tests, etc.) are not filmed.

Reproduction in full or in part of this film is governed by the Canadian Copyright Act, R.S.C. 1970, c. C-30. Please read the authorization forms which accompany this thesis.

AVIS

La qualité de cette microfiche dépend grandement de la qualité de la thèse soumise au microfilmage. Nous avons tout fait pour assurer une qualité supérieure de reproduction.

S'il manque des pages, veuillez communiquer avec l'université qui a conféré le grade.

La qualité d'impression de certaines pages peut laisser à désirer, surtout si les pages originales ont été dactylographiées à l'aide d'un ruban usé ou si l'université nous a fait parvenir une photocopie de qualité inférieure.

Les documents qui font déjà l'objet d'un droit d'auteur (articles de revue, examens publiés, etc.) ne sont pas microfilmés.

La reproduction, même partielle, de ce microfilm est soumise à la Loi canadienne sur le droit d'auteur, SRC 1970, c. C-30. Veuillez prendre connaissance des formules d'autorisation qui accompagnent cette thèse.

THIS DISSERTATION
HAS BEEN MICROFILMED
EXACTLY AS RECEIVED

LA THÈSE A ÉTÉ
MICROFILMÉE TELLE QUE
NOUS L'AVONS REÇUE

Canada

NL 339 (r. 85/09)

THE UNIVERSITY OF ALBERTA

Aspects of Physisorption Kinetics

by

David Bruce Jack

(C)

A THESIS

SUBMITTED TO THE FACULTY OF GRADUATE STUDIES AND RESEARCH

IN PARTIAL FULFILMENT OF THE REQUIREMENTS FOR THE DEGREE

OF Doctor of Philosophy

IN

Theoretical Physics

Department of Physics

EDMONTON, ALBERTA

FALL 1986

Permission has been granted to the National Library of Canada to microfilm this thesis and to lend or sell copies of the film.

The author (copyright owner) has reserved other publication rights, and neither the thesis nor extensive extracts from it may be printed or otherwise reproduced without his/her written permission.

L'autorisation a été accordée à la Bibliothèque nationale du Canada de microfilmer cette thèse et de prêter ou de vendre des exemplaires du film.

L'auteur (titulaire du droit d'auteur) se réserve les autres droits de publication; ni la thèse ni de longs extraits de celle-ci ne doivent être imprimés ou autrement reproduits sans son autorisation écrite.

ISBN 0-315-32601-8

THE UNIVERSITY OF ALBERTA

RELEASE FORM

NAME OF AUTHOR David Bruce Jack

TITLE OF THESIS Aspects of Physisorption Kinetics

DEGREE FOR WHICH THESIS WAS PRESENTED Doctor of Philosophy

YEAR THIS DEGREE GRANTED FALL 1986

Permission is hereby granted to THE UNIVERSITY OF ALBERTA LIBRARY to reproduce single copies of this thesis and to lend or sell such copies for private, scholarly or scientific research purposes only.

The author reserves other publication rights, and neither the thesis nor extensive extracts from it may be printed or otherwise reproduced without the author's written permission.

(SIGNED) David Jack

PERMANENT ADDRESS:

239 Dolphin Court

Oakville, Ontario

L6J 5S7

DATED June 20 1986

THE UNIVERSITY OF ALBERTA

FACULTY OF GRADUATE STUDIES AND RESEARCH

The undersigned certify that they have read, and recommend to the Faculty of Graduate Studies and Research, for acceptance, a thesis entitled Aspects of Physisorption Kinetics submitted by David Bruce Jack in partial fulfilment of the requirements for the degree of Doctor of Philosophy in Theoretical Physics.

John Stephenson
.....

Supervisor

.....

.....

.....

.....

External Examiner

Date..... 20 JUNE 1986 .....

Abstract

In this thesis Langmuir's phenomenological rate equation for physisorption and microscopic expressions for its component kinetic coefficients, namely, the desorption rate, the sticking coefficient, and the readsorption coefficient, are derived from kinetic theory. This derivation is unique in that the gas phase is allowed to vary in time rather than maintain an equilibrium distribution during the processes of adsorption and desorption. It is argued that this feature leads to an expression for the sticking coefficient which never exceeds the value one, thus correcting a salient deficiency in quantum mechanical theories of physisorption. The readsorption coefficient, which is introduced to the field of physisorption kinetics for the first time, is a necessary consequence of the derivation of the phenomenological rate equation and takes into account the possibility of a gas particle readsorbing after having desorbed.

The expressions for the kinetic coefficients are evaluated both numerically and analytically using the phonon cascade model of physisorption. The analytic work is made possible through the development of the phonon cascade Fokker-Planck equation. This equation, along with the radiative boundary condition appropriate for desorption, is derived according to the methods of van Kampen's large parameter expansion. It is shown that under suitable conditions the classically derived Kramers equation can be obtained from the phonon cascade Fokker-Planck equation. This correspondence yields an expression for the energy space friction coefficient in terms of the microscopic parameters which characterize the gas-solid system, and which differs from the expression derived from linear response theory by a constant factor. This difference raises questions concerning the validity of linear response theory. The desorption rate is found to follow the Frenkel-Arrhenius law and exhibit a temperature dependent compensation effect. It is also found that the readsorption coefficient can decrease the effective desorption rate considerably. The analytic and numerical results for the sticking coefficient are found to be in qualitative agreement with the experimental results and appear to guarantee values less than one. It is concluded that this theory provides a consistent, general framework from which to analyse experimental work and embark on further theoretical investigations.

Acknowledgements

I have benefitted greatly from the association with my two supervisors, Profs. H.J.Kreuzer and Prof. Z.W.Gortel. I was introduced to the field of Physisorption Kinetics by Prof. H.J.Kreuzer, who suggested most of the topics discussed in this thesis. In the past year Prof. Z.W.Gortel's has been an energetic source of comments, suggestions and enthusiasm. I am also grateful to Prof. J.Stephenson for being my acting supervisor during my thesis defence.

The numerical work is based on computer codes written by Bob Teshima. John Nesbit was kind enough to guide me through the labyrinth of the MTS textformatting system which was used to produce this work.

Financial support has come from a variety of sources. First and foremost I would like to thank the Izaak Walton Killam Foundation. I am also grateful for the support received from the Natural Sciences and Engineering Research Council (Canada). Profs. Kreuzer and Gortel have also contributed to my financial support.

I would also like to thank the Webber family for their gift of several physics texts which I found quite useful in the course of my research.

Last, but not least, I wish to thank my wife Siri for her sacrifice of time and energy which enabled me to finish this thesis.

Table of Contents

Chapter		Page
1.	Introduction and Review	1
	1.1 The Nature and Importance of Physisorption	1
	1.2 The Phenomenological Rate Equation	2
	1.3 The Phonon Cascade Model of Physisorption	7
	1.4 The Kramers Approach to Physisorption	18
	1.5 A Derivation of the Phenomenological Rate Equation	24
2.	Macroscopic Equations for Physisorption	29
	2.1 The Macroscopic Law of Friction for Physisorption	30
	2.2 A Numerical Study	34
3.	A Microscopic Theory of the Phenomenological Rate Equation	36
	3.1 Derivation of the Phenomenological Rate Equation	36
	3.2 The Sticking Coefficient	42
	3.3 The Effective Desorption Rate and Readsorption Coefficient	47
4.	The Phonon Cascade Fokker-Planck Equation	50
	4.1 Derivation of the Phonon Cascade Fokker-Planck Equation	51
	4.2 Connection with the Kramers Equation	58
	4.3 Properties of the Phonon Cascade Fokker-Planck Equation	62
5.	Boundary Conditions for Ideal Desorption	65
	5.1 Temporal Boundary Conditions	66
	5.2 Use of the Auxiliary Conditions	67
	5.3 The Radiative Boundary Condition	67
6.	Ideal Desorption Rate and Distribution Function	72
	6.1 Small Eigenvalue Expansion	73
	6.2 Variational Method	78
	6.3 Numerical Comparison	79
7.	Preliminary Results for the Kinetic Coefficients	84

7.1 An Algebraic Expression for the Sticking Coefficient 84

7.2 Numerical Comparison 87

8. Summary and Conclusions 90

References 127

Appendix A 134

Appendix B 136

Appendix C 139

Appendix D 143

Appendix E 148

Appendix F 150

List of Figures

Figure — Page

1 Phase Portrait of the Macroscopic Equations of Physisorption 96

2 Time evolution of a Nonequilibrium Adsorbate at 202.5°K 98

3 Time evolution of a Nonequilibrium Adsorbate at 405°K 100

4 Time evolution of the adparticle distribution at 202.5°K 102

5 Time evolution of the adparticle distribution at 405°K 104

6 Transition Rates 106

7 Transition Rates near the Origin 108

8 Reduced Distribution Function for Xe/W 110

9 Reduced Distribution Function for Ar/Ag 112

10 Scaled Prefactor and Heat of Adsorption for Xe/W 114

11 Scaled Prefactor and Heat of Adsorption for Ar/Ag 116

12 Desorption Rate for He/LiF 118

13 Sticking Coefficient for He/Ar 120

14 Sticking and Readsorption Coefficient for Xe/W 122

15 Sticking and Readsorption Coefficient for Xe/W 124

16 Sticking and Readsorption Coefficient for Ar/Ag 126

1. Introduction and Review

1.1 The Nature and Importance of Physisorption

There has been considerable interest in the process of physisorption in the past years, with little end in sight. As physical devices become smaller and the need to manipulate matter at the atomic level increases, it becomes of great importance to understand the nature of solid surfaces and their interactions with other media and with matter in a different state. For instance, if a chemical vapour deposition technique is used to deposit material onto the surface of a semiconductor it is useful to understand the mechanisms by which the rate of deposition can be adjusted[1]. Although the deposited material is eventually strongly bonded to the surface through a chemical process, it is initially bound to the surface through the process of physical adsorption[2], or physisorption for short. In order to attempt to manipulate the rate of deposition in the above example one must understand the kinetics of physisorption[3].

The basis of physisorption is the existence of a surface potential which can confine a gas particle to a region near the surface of a solid[2-4]. This potential originates from the interaction of the gas particle with the solid. At large distances this interaction is dominated by the van der Waals attraction between an individual gas atom and the atoms of the solid. At short range the overlap of the electron orbitals of the gas atom and the solid gives rise to a strongly repulsive force. Because the attractive portion of the surface potential originates from the weak van der Waals interaction, the physisorption binding energies are typically of the order of a hundredth to a tenth of an electron-Volt. This is in contrast to the case of chemisorption where, due to the formation of chemical bonds, typical binding energies are of the order of a tenth to a few electron-Volts. Occasionally gas-solid systems are met which exhibit properties of physisorption but are very strongly bound. Conversely, there are chemisorbed systems which are rather weakly bound. It is convenient to think of chemisorption and physisorption as being at the two ends of the spectrum of gas-solid interactions but with no sharp dividing line between the two.

The kinetics of both physisorption and chemisorption are governed by the exchange of energy between the solid and the particles bound at the solid surface. The dynamical mechanism underlying the kinetics is thought to differ for these two cases. Physisorption is considered to be mediated by the coupling of the adsorbed gas particle (adparticle) to the lattice vibrations of the solid. In quantum mechanical theories this means that the exchange of energy between a gas and a solid is mediated through the creation and destruction of phonons. In the case of chemisorption the chemisorbed particles are coupled to the electronic degrees of freedom of the solid. The electronic processes responsible for the exchange of energy include the creation and destruction of electron-hole pairs, plasmons, and charge transfer etc.[5-8] . The difference in underlying mechanisms aside, it is apparent that physisorption is a simpler phenomenon whose study can, through analogy, shed some light on the more complicated process of chemisorption.

Of course physisorption is an important process in its own right. As is illustrated by the example in the opening paragraph, physisorption is thought[2-3] to be the precursor state for a variety of processes which take place at solid surfaces such as molecular dissociation and chemisorption. This then means that physisorption is an underlying phenomenon for processes like catalysis[2, 9, 10], the epitaxial growth of crystals[11],and the deposition of metals on semiconductors[1].These processes are all of obvious industrial importance. Physisorption is also fundamental for understanding the nature of gas flow past solid bodies, and so may eventually make contributions to the field of aerodynamics[12].

1.2 The Phenomenological Rate Equation

Physisorption kinetics is a broad topic. In this thesis only some aspects of the kinetics of adsorption and desorption will be discussed. Even this limited area can be very involved. Much of this complication arises when the detailed nature of a real surface is considered; a realistic surface has a definite lattice structure as well as inherent dislocations, vacancies, grain boundaries, and impurities etc.[13]. To successfully incorporate these features would mean that the interaction of a gas particle with the surface of the solid would become highly site

specific, and hence would necessitate a case by case study. The true nature of the surface is not the only complication involved. The presence of a physisorbed gas molecule at the solid surface may induce changes in the properties of the surface, such as an alteration of the vibrational spectrum of the solid lattice. If there are many adparticles on the surface then the mutual interaction of these particles also becomes important. It is advantageous, however, to first gain a thorough understanding of the kinetics of physisorption for a simpler situation before attempts at a fully realistic situation are made. Fortunately, some simplifications for this purpose can be made.

In order to facilitate such a study the following assumptions are made throughout this thesis. First, the surface is assumed to be an infinite flat plane. This can be justified on the grounds that for many systems, and helium on most substrates in particular[14], the surface potential does not vary much over the surface of the solid[3]. Physically this yields a situation where, for submonolayer coverages, the adsorbate is highly mobile. Even when one considers that the surface of the solid is vibrating this assumption remains valid because the root mean square displacement of a surface atom of the solid is on the order of a hundredth to a tenth of an Ångstrom[15] while the range of the surface potential is on the order of an Ångstrom. It is also assumed that the surface density of the adsorbate is so low that the individual adsorbed gas particles never interact with one another. This is known as the low coverage limit. If the conservation of lateral momentum within the adsorbate is also assumed then these assumptions lead to a one dimensional theory appropriate to a highly mobile adsorbate[3]. Even with such an array of simplifications there remains a great deal of interesting and challenging physics to be pursued.

Langmuir has postulated[16-17] that the macroscopic behaviour of a gas at a solid surface can be described by the phenomenological rate equation

$$\Theta(t) = S \frac{P}{N_S(2\pi m k_B T)^{\frac{1}{2}}} - \lambda\Theta(t), \qquad (1.1)$$

where $\theta(t)$ is the surface coverage (or simply the coverage) at time t, m is the mass of an

individual gas particle, T is the temperature of the gas, P is the pressure of the gas, and the kinetic coefficients λ and S are the desorption rate and the sticking coefficient, respectively. Originally, Langmuir considered the adsorbed particles to be localized at specific sites on the surface so that N_s denoted the number of adsorption sites per unit area on the surface. Since a mobile adsorbate is considered in this work N_s will be the number of adsorbed particles per unit area at monolayer coverage of the surface.

The coverage is defined as the surface density of gas particles adsorbed on the solid surface divided by the maximum surface density achieved when a full monolayer of gas particles covers the solid surface. Obviously, when there is a full monolayer of particles on the surface the coverage is one.

The sticking coefficient, or sticking probability, is defined as the proportion of an incident thermal flux of gas particles which are actually adsorbed after striking the solid surface. It therefore is always less than or equal to one. Typically, the sticking coefficient is a function of temperature and coverage. Langmuir assumed that the sticking coefficient takes the form $S=S_0(1-\theta)$, where S_0 is a constant. Experimental work[18-19] has shown that the dependence of the sticking coefficient on the surface coverage is not necessarily so simple. The expression multiplying the sticking coefficient in Eq. (1.1) is the number of gas particles per adsorption site which are striking the solid surface per second. The first term in Eq. (1.1) is therefore the rate of change of the surface coverage due to adsorption.

The desorption rate, as its name suggests, is the rate at which the adparticles leave the surface. It is typically expressed in terms of the Frenkel-Arrhenius law[20] for thermally activated processes, i.e.

$$\lambda = \nu \exp(-Q/k_B T), \tag{1.2}$$

where the heat of adsorption, Q, and the prefactor, ν, are also functions of temperature and coverage. In their theoretical studies on multilayer physisorption[21-26], Sommer and Kreuzer found that Q and ν are strongly coverage dependent near monolayer coverage. Since the

desorption rate depends exponentially upon Q one would expect the desorption rate to change dramatically with a change in Q. The prefactor ν, however, varies with θ so as to compensate for the change in Q. This compensation effect maintains λ within a relatively narrow range of values for a given temperature. This effect has been experimentally observed by Sinvani *et al.*[27] in their measurements of the desorption kinetics of helium at low temperatures. The temperature dependence of Q and ν will be discussed in Chap. 6 of this thesis where evidence of a temperature dependent compensation effect is presented. Classically, the prefactor ν has been interpreted as the attempt frequency with which the desorbing adparticle tries to escape from the surface potential while the heat of adsorption Q is regarded as the activation energy needed by the adparticle in order to desorb. The heat of adsorption is therefore taken to be equal to the depth of the potential well U_o. The inverse of the desorption rate is called the desorption time, i. e. $t_d = \lambda^{-1}$.

In most calculations of the desorption rate it is assumed that the once a gas particle escapes from the surface potential it never returns. This situation is thought to be realized in isothermal desorption experiments which are performed as follows[21]. In a vacuum chamber a chopped molecular beam is allowed to physisorb onto the surface of the solid under study. The resulting desorption flux is monitored by a mass spectrometer. The rate at which the mass spectrometer's signal decays is then identified as the desorption rate. It is also possible to do so called flash desorption experiments where the temperature of the solid is quickly raised causing some of the adsorbate to desorb. In this case, however, the resulting desorption rate is not the rate required for the phenomenological rate equation. It should be emphasized once again that it is usually assumed that the gas particles do not readsorb. It will be seen in chapters 6 and 7 of this thesis that this assumption is not always valid.

Keeping in mind the definitions given above, it is evident that the phenomenological rate equation (1.1) simply states that the rate of change of the coverage in time is the rate at which particles are deposited on the surface minus the rate at which they escape from the surface. It is the task of physisorption kinetics to derive this equation from microscopic theory and thus obtain expressions for the macroscopic kinetic coefficients, i.e. the sticking

coefficient and the desorption rate, in terms of the microscopic parameters which characterize the gas-solid system. These coefficients must then be calculated within the framework of a given model of physisorption. Such a program, with the phonon cascade model of physisorption being used to calculate the kinetic coefficients, is the major theme of this thesis.

This thesis is presented as follows. In chapter 2 some preliminary studies done on the process of equilibration of the adsorbate at the macroscopic level are shown. This will lead to the introduction of the friction coefficient which controls the equilibration process. The friction coefficient is introduced at this early stage because it turns out to be an integral component of the kinetic coefficients which occur in the phenomenological rate equation. This being done, chapter 3 is devoted to the derivation of the phenomenological rate equation and general expressions for the kinetic coefficients. Chapters 4 and 5 are spent developing the mathematical machinery necessary for the evaluation of the above mentioned coefficients within the framework of the phonon cascade model of physisorption. In chapters 6 and 7 expressions for the desorption rate and the sticking coefficient are evaluated and compared with some preliminary numerical results and with experimental data where possible.

Before starting, it will be useful to review in the remainder of this chapter some of the work previously done to derive the phenomenological rate equation and the kinetic coefficients for physisorption. Special attention is paid to the phonon cascade model of physisorption since it will form the basis of calculations done in this thesis. In the next section the phonon cascade model is presented so as to establish notation and introduce the master equation. Other quantum mechanical models are also mentioned. In the following section some of the classical theories of physisorption are reviewed with particular attention being paid to those which use the Kramers equation. And finally, in the last section an attempted derivation of the phenomenological rate equation is reviewed and evaluated. It will be found in chapter 3 that by modifying this derivation the phenomenological rate equation with the desired properties will result.

1.3 The Phonon Cascade Model of Physisorption

One of the most successful models put forward to describe the kinetics of physisorption is the phonon cascade model of Kreuzer and Gortel[29-31]. It is based on many-body quantum theory and has many features in common with the original quantum mechanical theory of physisorption put forward by Lennard-Jones, Devonshire, and Strachan[32-40]. The phonon cascade model is an improvement on this earlier theory by virtue of its formulation in terms of a master equation at the kinetic level. This framework has allowed Kreuzer, Gortel, and coworkers to tackle a host of problems in the area of physisorption kinetics[21-26 41-43] and branch out into related fields such as laser induced photodesorption[44-47]. A very similar theory has been put forward by Jedrzejek, Metiu *et al.*[48-54].

So far, the phenomenological rate equation has not been derived using the phonon cascade model. The only kinetic coefficient to be calculated within this theory is the desorption rate. Numerical results[29] which match experimental data have been obtained, as well as some approximate analytic expressions suitable in a limited temperature range, but an approximate analytic expression[31] for the desorption rate valid for a wide range of temperatures has yet to be developed. This will be done in chapter 6 of this thesis. Before presenting the phonon cascade model the development of the various quantum mechanical models of physisorption will be outlined.

In a series of articles on *The Interaction of Atoms and Molecules with Solid Surfaces* Lennard-Jones, Devonshire, and Strachan (LJDS) presented the first microscopic theory of physisorption. Although they did not derive the phenomenological rate equation of Langmuir they did obtain microscopic expressions for the sticking coefficient and the desorption rate. These expressions were obtained for the case of a highly mobile adsorbate[34 36] as well as the situation of localized adsorption at an individual site on the surface[35]. In order to calculate these quantities they assumed that the surface potential could be represented as a Morse potential and that the exchange of energy between a gas particle and the solid was mediated by the creation and destruction of phonons. The mediating phonons were limited to those which displaced the surface atoms in a direction perpendicular to the surface and were

assumed to have the same spectrum of those of the bulk. The rate at which the gas particles undergo transitions from the continuum to bound states and *vice versa* was determined by employing first order perturbation theory. The kinetic coefficients were then determined by assuming that the energy level from which the particle was leaving was occupied according to the Boltzmann distribution with the resulting formulas expressed in terms of sums and integrals which were to be evaluated numerically. The resulting expression for the sticking coefficient does not guarantee that it will not take on values greater than one (See Eq. (1.31).). Although the rates of adsorption and desorption were calculated the investigation of the kinetics of physisorption was limited to the assumption that the gas particles were always in equilibrium. The assumption that only one phonon events are important for the determination of the kinetic coefficients was investigated by Strachan[40]. He concluded that multiphonon effects were not important.

Besides calculating the above-mentioned quantities Lennard-Jones and Devonshire also investigated the scattering of atoms by solid surfaces both elastically[36] and inelastically[39]. From the former investigation it was found that there are elastic scattering events which can lead to the adsorption of a gas particle. In the latter investigation the accomodation coefficient, which is a measure of the efficacy with which the gas can transfer energy to the solid, was calculated according to the techniques used to calculate the other kinetic coefficients. It too was expressible only in terms of integrals and sums. In the case of no bound states the expression could be calculated explicitly.

This theory has been critically reviewed by Goodman in Ref. 55 where he reports of previously published criticism[56]. Most of the criticism of the former article is aimed at the derivation of the accomodation coefficient, although it might hold equally well for the derivation of the other the coefficients. In particular, the use of a one dimensional surface potential and single phonon events were objected to. More seriously, however, is the apparently valid criticism that the principle of unitarity is violated in the treatment of the scattering of the gas by the solid surface. An attempt to rectify this problem through the use of scattering theory was put forward by Cabrera *et al.*[57] and Goodman[58]. Efforts were also

made to include bound state to continuum transitions[59] as well as multiphonon effects[60] in the expression for the accomodation coefficient. These developments and others are reviewed in Refs. 61 and 62 . In all of these developments the adsorbate is assumed to maintain an equilibrium configuration during the desorption process. On the whole, these modifications represent relatively minor changes to the LJDS theory.

In 1978 Schaich[63] extended a portion of the LJDS theory to three dimensions. He found that the extended theory could not account for experimental results concerning the angular dependence of the energy distribution of desorbing gas particles. In extending the theory to three dimensions it was assumed that the adsorbed gas particles had an equilibrium distribution in both the lateral and perpendicular direction with respect to the surface. This, coupled with the inability of the expression for the sticking coefficient to guarantee a value less than one, implied that to proceed any farther the adparticle distribution must be allowed to deviate from equilibrium. In order to tackle such a problem the theory of physisorption must be formulated at the kinetic level. The first step towards this was taken by Montroll and Shuler.

In 1958 Montroll and Shuler[64], drawing upon Kramers' ideas on chemical kinetics[65] (See Sec. 1.4 of this thesis.), proposed a much simpler, but less realistic model, for desorption. This theory was intended to model chemical kinetics in general, and molecular dissociation in particular, but is equally applicable to physisorption kinetics. They assumed that the surface potential could be represented by a truncated harmonic oscillator potential. When the adsorbed gas particle reached the top of the potential it was assumed to desorb. In terms of molecular dissociation this condition was interpreted as the molecular bond stretching to a critical distance at which it ruptures. To reach the top of the potential the adparticle was allowed to jump between adjacent energy levels by exchanging energy with a thermal reservoir. In other words the adparticle was executing Brownian motion in energy space[64]. The distribution function of the adparticle energy obeyed a Pauli master equation where the rate at which the particle changed energy levels was calculated quantum mechanically. From the master equation the mean first passage time could be calculated analytically. This approach

had the advantage of being able to express the desorption rate in terms of the microscopic parameters of the system whereas the Kramers approach contains an undetermined coefficient. The result of Montroll and Shuler was generalized by Kim[66] to potentials with the same type of anharmonicity as is found in the Morse potential. Having an analytic form for the approximate desorption rate shed some light on the problem but was limited to the realm of qualitative understanding due to the extreme assumptions made regarding the surface potential. More important though was the introduction of the master equation to the study of physisorption kinetics. Unfortunately this approach was not pursued for another twenty years.

During the 1960's there was no work done on quantum mechanical models other than the fine tuning of the LJDS theory. Ironically, the truncated harmonic potential used by Montroll and Shuler seems to have sparked interest in classical models of the like which are solvable or at least amenable to analytic approximations. Finally, in the early seventies, there was renewed interest in the quantum theory of physisorption. Besides the work of Goodman and others on the LJDS theory[57-63], a new quantum theory was presented by Bendow and Ying[67-70]. Their theory was a three dimensional version of localized physisorption. The coupling of the adparticle to the solid lattice was expressed in terms of the autocorrelation function of the lattice displacement. In principle their theory contains multiphonon effects to all orders, but these effects could only be examined numerically. The most severe limitation, however, is their assumption that the desorption process took place from only a single bound state. Kreuzer and Gortel[3] have pointed out that this assumption leads to desorption rates which are orders of magnitude too small when systems with more than one bound state are considered. To handle systems with several bound states requires the use of kinetic theory.

A kinetic approach to chemisorption and physisorption was initiated by d'Agliano *et al.*[71-72] shortly after the presentation of the theory of Bendow and Ying. Taking up the idea of regarding the adsorbed particle as executing Brownian motion in energy space, Schaich[73] showed that the kinetics of a heavy adparticle coupled to a reservoir of light particles can be described by the classically derived Kramers' equation[65] (See Eq. (1.11).). This derivation

closely followed Mazur and Oppenheim's[74-75] work on Brownian motion where a stochastic equation of motion is derived from the Liouville-von Neumann equations of motion for the density matrix through the use of projection operators[76]. The friction coefficient which occurs in the Kramers equation can be expressed in terms of a time integral over the autocorrelation function of the force which the adparticle experiences due to the thermal vibrations of the lattice. By extensively using linear response theory[77] d'Agliano *et al.*[72] calculated the friction coefficients for a variety of physical processes such as electronic damping. The friction coefficient for an adparticle coupled to the lattice vibrations of the solid was also calculated using the soft cube model (For comments on the soft cube model see sec. 1.4). The expression for the friction coefficient can then be used in the Kramers expression (See Eq. (1.12).) for the desorption rate. Expressions for the desorption rate and sticking coefficient then depend on what can be extracted from the Kramers equation. This then means that approximate expressions must suffice since the Kramers equation can be solved exactly only for potentials like the harmonic oscillator. Because the condition that the adparticle be much heavier than the thermal resevoir particles is readily realized when the thermal resevoir particles are taken to be electrons, this theory is more appropriate for chemisorption than physisorption.

At the end of the 1970's three different groups started to investigate the kinetics of physisorption from a purely quantum mechanical point of view. Two of the groups (Gortel, Kreuzer *et al.*; and Jedrzejek, Metiu *et al.*) produced similar theories. The third group, Brenig *et al.*, took a different approach initially but now seems to be moving toward the approach taken by the other two groups.

The main feature of the Brenig group's approach is to include multiphonon effects in a simple way. By analysing the energy spectrum of a gas particle scattering from a solid surface Brenig and Böheim[78-79] concluded that the transition rates between energy levels could be described by a Gaussian distribution which obeyed the principle of detailed balance. It was subsequently assumed that transitions between energy levels of the surface potential could also be described in such a manner. Using this assumption as well as the results of the classical

theory of Iche and Nozières[40] (See Sec. 1.4 .) Brenig *et al.*[81-83] were able to examine the sticking coefficient in the classical and quantum regimes. They found that the sticking coefficient differed little in these two regimes, except at temperatures so low that it is not practical to do the experiments. Stutzki and Brenig[84] have examined the role of Rayleigh surface modes in the process of sticking and found that they indeed make an important contribution. Work on the sticking coefficient and accomodation coefficient continues[85].

The master equation has been employed by Brenig[86] in an attempt to derive the phenomenological rate equation. It seems that this is the only attempted derivation to date and has done much to reveal the link between the kinetic and macroscopic regimes of physisorption. This work is of sufficient importance that Sec. 1.5 of this thesis is spent on its presentation.

Leuthäusser[87-89] has also used the master equation in the Iche-Nozières-Brenig approach to give a general formulation of physisorption kinetics. From this starting point he is able to obtain the desorption rate, and the sticking and accomodation coefficients, as well as the angular dependence of the energy distribution of desorbing particles. All of these expressions contain two adjustable parameters which arise from the use of the Gaussian transition rates. These parameters have yet to be derived from microscopic theory. This degree of freedom in the choice of the value of the parameters has been exploited to obtain good agreement with the experimental data. The arbitrariness of these parameters has led to some criticism[3] though.

The use of the master equation has brought the work of this group in line with the approach taken by the other two main groups. As mentioned earlier the work of the other two groups is rather similar. The work of Jedrzejek, Metiu *et al.*[49-54] is a more complicated version of the phonon cascade model and has been shown[49, 52] to reduce to the phonon cascade model under the conditions appropriate to physisorption. In particular, the Pauli master equation is derived from a generalized master equation which includes memory effects. Multiphonon effects are included through the use of correlation functions in the manner of Bendow and Ying, but are found to contribute little compared to the one phonon contribution in keeping

with Strachan's findings[40]. The surface potential is assumed to be the sum of the interactions between the gas particle and the individual atoms of the solid and thus yields a temperature dependent surface potential. This temperature dependence was, however, found to be rather weak. Owing to the detailed nature of this model only numerical results could be obtained. In order to do any analytic work the approximations which yield the phonon cascade model must be invoked.

At the beginning of the 1980's, Gortel and Kreuzer[29-31] developed the phonon cascade model for physisorption. In this model one assumes that the net interaction of a solid with a gas particle at the solid surface gives rise to a surface potential which has several, if not many, discrete bound states. Gas particles trapped in the bound states of the surface potential are referred to as adparticles and constitute the adsorbate. If a gas particle, which occupies one of the continuum states of the gas phase, loses enough energy to the solid it will fall into the surface potential and be trapped in a bound state. This process is called adsorption while the reverse process is called desorption. In these processes the exchange of energy between a gas particle and the solid is mediated by the creation and destruction of phonons. During adsorption the adsorbing particle may cascade through a number of bound states before reaching the state with the lowest energy near the bottom of the potential well (This is not to say that all particles reside at the bottom of the potential; it is, however, the most probable situation.). In this case a sequence of phonons is incoherently emitted by the gas particle. For desorption to occur a sequence of phonons must be incoherently absorbed by the adparticle. Overall, one views the gas particle as executing Brownian motion in energy space under the influence of the phonon heat reservoir of the solid.

Regarding this motion in energy space as being a Markovian process, Gortel, Kreuzer *et al.* assumed that the kinetics of physisorption can be describe by a Pauli master equation[29] In discrete form it is often referred to as the rate equation and may be written as,

$$\dot{n}_i(t) = \sum_{j=0}^{N-1} W_{ij} n_j(t) + \sum_{k=-\infty}^{\infty} W_{ik} n_k(t) - \sum_{j=0}^{N-1} W_{ji} n_i(t) - \sum_{k=-\infty}^{\infty} W_{ki} n_i(t). \quad (1.3)$$

To avoid confusion with the phenomenological rate equation, (1.1), the equation above, (1.3), will be referred to as the discrete master equation, or master equation for short. Here the distribution function $n_i(t)$ describes the number of gas particles in state i at time t, and $n_k(t)$ gives the number of particles in a continuum state k at time t. The summations are over the continuum states of the gas phase and the bound states of number N. The function W_{ij} is the rate at which particles make a transition from state j to i, etc. . To calculate the transition rates W_{ij} the surface potential was chosen to be a Morse potential. By numerically diagonalizing Eq. (1.3) with the continuum to bound state transitions set equal to zero, Gortel and Kreuzer[29] were able to determe the smallest eigenvalue which was subsequently identified as the isothermal desorption time. The values of the desorption time were in good agreement with the experimental results.

In order to describe the kinetics of physisorption of gas-solid systems with a large number of bound states Gortel, Kreuzer *et al.*[30] found it necessary to use the continuous form of the master equation,

$$\dot{\tilde{n}}(E,t) = \int_{-U_o}^{\infty} dE' \tilde{\rho}(E') \tilde{W}(E,E') \tilde{n}(E',t) - \int_{-U_o}^{\infty} dE' \tilde{\rho}(E') \tilde{W}(E',E) \tilde{n}(E,t). \qquad (1.4)$$

Here the distribution function $\tilde{n}(E,t)$ describes the number of gas particles with energy E at time t. Gas particles with a negative energy are bound in the surface potential while those with a positive energy occupy one of the continuum states of the gas phase. The surface potential is considered to have a depth U_o and a large number of bound states which, in the continuum limit, have a density $\tilde{\rho}(E')$. The function $\tilde{W}(E,E')$ is the rate at which a gas particle makes a transition from a state of energy E' to a state of energy E.

To calculate the transition rates $\tilde{W}(E,E')$ it is necessary to specify models for both the vibrational spectrum of the solid and the surface potential. Since analytic calculations involving the transition rates must be performed, it is convenient to choose the Debye model

with cutoff frequency ω_D for the former, and the Morse potential,

$$U(z) = U_o \left[e^{-2\gamma(z-z_o)} - 2e^{-\gamma(z-z_o)} \right], \tag{1.5}$$

for the latter. Here the variable z represents the distance perpendicular to the solid surface, z_o is the distance of the potential minimum from the solid surface, and the quantity γ^{-1} is the range of the potential. Using these assumptions the transition rates have been calculated in Ref. 29 and are listed in the Appendix C of this thesis.

In order to extract a desorption time and associated distribution from Eq. (1.4) analytic methods must be employed. For the low temperature regime Kreuzer and Teshima[31] assumed that equilibrium is maintained in the adsorbate during the desorption process. This leads to a perturbation expansion of the master equation (1.4) from which the isothermal desorption rate, t_d^{-1}, was estimated to be

$$\lambda = t_d^{-1} \approx \tfrac{1}{2}\eta\sigma_o e^{\beta U_o}, \tag{1.6}$$

with

$$\beta = [k_B T]^{-1}, \tag{1.7}$$

where their results have been cast in terms of the friction coefficient η and the Morse potential parameter σ_o. The friction coefficient is defined in chapter 4 (See Eq. 4.16). The dimensionless parameter

$$\sigma_o = \frac{(2mU_o)^{\frac{1}{2}}}{\hbar\gamma} \tag{1.8}$$

is a measure of the number of bound states N of the Morse potential, i.e.

$$\sigma_o - \frac{3}{2} < N < \sigma_o - \frac{1}{2} \ . \tag{1.9}$$

Equation (1.6) follows the Frenkel-Arrhenius parametrization (See Eq. (1.2).) which is typical of thermally activated processes. It is worth noting that the preexponential factor is independent of temperature and that the heat of adsorption is identified with the depth of the surface potential.

For the high temperature regime an estimate for the desorption rate was extracted[31] from a Fokker-Planck equation which had been derived[30] from the master equation. Jack and Kreuzer[90-91] refined this estimate after they derived the phonon cascade Fokker-Planck equation,

$$\dot{n}(y,t) = \eta \frac{\partial}{\partial y} \left\{ F_5(\tanh^{-1}(y)/y) \left[\frac{k_B T}{2U_o} \frac{1}{y} \frac{\partial n(y,t)}{\partial y} - n(y,t) \right] \right\}, \tag{1.10}$$

where the variable y satisfies the relation $E = -U_o y^2$ and the function F_5 is defined by Eq. (4.11). The derivation of this equation will be presented in chapter 4 of this thesis. To calculate the isothermal desorption rate from Eq. (1.10) an ansatz for n(y,t) had to be assumed. Numerical studies showed that during the desorption process the adsorbate maintained an equilibrium distribution throughout the bound states except near the top of the potential well where, for high temperatures and gas-solid systems with a large number of bound states, the distribution was substantially depleted. Hence, for times long enough to allow transient effects to die away, the *ad hoc* ansatz

$$n(y,t) = \exp\,(t/t_d) \left[e^{y^2 \beta U_o} - 1 \right] \tag{1.11}$$

was used to find

$$\lambda = t_d^{-1} \approx 2\eta\beta U_o F_5(1)\, e^{-\beta U_o}. \qquad (1.12)$$

The factor $F_5(1)$ extends the validity of Eq. (1.12) to gas-solid systems which develop only a few shallow bound states, such as He/C or He/Ar, as well as systems exhibiting deep bound states and strong coupling between the gas and solid. It arises because of the Debye cutoff in the vibrational spectrum of the solid.

Both Eqs. (1.6) and (1.12) follow the Frenkel-Arrhenius parametrization (See Eq. (1.2).). Each of these equations has a heat of adsorption equal to the depth of the surface potential. This feature is a result of the approximations used to derive the desorption rate and is not a necessary consequence of either the Fokker-Planck equation (1.10) or the master equation (1.4). Indeed, both equations allow for a heat of adsorption which is weakly temperature dependent. Small changes in Q, however, can result in large changes in the desorption rate. The temperature dependence of the heat of adsorption will be discussed in chapter 6.

Where the two expressions for the desorption rate differ is through their prefactors. In the low temperature case the prefactor is independent of temperature in contrast to the high temperature case where the prefactor depends linearly on the temperature. An expression for the desorption rate which is valid for all temperatures should reduce to Eq. (1.6) in the low temperature limit and to Eq. (1.12) in the high temperature limit, as well as interpolate between these two expressions.

To obtain a better estimate of the desorption rate it is necessary to derive directly from the master equation the boundary conditions appropriate for desorption and then use them to self-consistently determine the desorption distribution and desorption rate. This is in contrast to the previous practice of simply assuming the form of the distribution function which satisfies a set of seemingly plausible but underived boundary conditions. This program will be carried out in chapters 5 and 6.

1.4 The Kramers Approach to Physisorption

Although there are numerous classical theories of physisorption[65 80 92-124] an approach utilizing the Kramers equation[63 119-124] or the master equation[115-118] are the most useful for studying physisorption. Before examining these stochastic models the purely deterministic models are reviewed.

As with the quantum theory the classical models start with Lennard-Jones[92]. In order to understand chemical bonding in a simple way Lennard-Jones modelled the bonding state of two molecules by a particle moving in a harmonic potential. When thermal agitation gave the harmonic oscillator enough energy to reach a critical value the bond was considered to have reached its breaking point. This yielded reasonable qualitative results. After some additional work by Slater[93], this model was modified by both Cabrera[94] and Zwanzig[95] in order to describe physisorption. They envisioned the solid as being represented by a one dimensional, semi infinite chain of mass points each connected to their nearest neighbours by a spring which was represented by a harmonic potential. The gas particle moves in a truncated harmonic potential which is attached to the free end of the chain. The resulting equations of motion formed a coupled system which could be solved exactly. From this solution a criterion for the trapping of the gas particle was obtained. This model has been subsequently analysed and built upon by numerous authors[96-110] and has evolved into a rather sophisticated problem in classical mechanics through the replacement of the truncated harmonic potential by the Morse potential[105 107] and the extension of the model to three dimensions[101 108]. The equations of motion at this more advanced stage only yield integral solutions which make expressions for the desorption rate[106 109] and the sticking coefficient[110] rather complicated.

In an effort to understand the mechanism behind the scattering of molecular beams off of solid surfaces, Logan and Stickney[111] put forward the hard cube model. This theory assumes that the impinging gas particle may only elastically scatter off of the flat surface of the solid. The portion of the surface involved in the collision with the gas particle is assumed to have a mass equal to the mass of a solid atom and to move only perpendicular to the surface with a Maxwellian velocity distribution. A collision with the surface will therefore

change only the perpendicular momentum component of the impinging gas particle. Qualitatively this model was in accord with experimental results and thus lends support to the one dimensional quantum models for mobile adsorbates. Because no surface potential exists in this model there can be no adsorption of the gas particles onto the solid surface.

An interesting heuristic approach was developed in Weinberg and Merill's[112] square well model. Assuming a square well surface potential they were able to derive conditions for trapping in terms of the accomodation coefficient. Using the experimentally determined values of the accomodation coefficient they were able to obtain values for the sticking coefficient which were in good agreement with the experimental results for the inert gases on tungsten.

In order to describe scattering more realistically and to study the adsorption process, Logan and Keck[113 114] introduced the soft cube model. It differs from the hard cube model by assuming a surface potential with an exponential repulsive part and a step attractive part. The collision site of the surface itself now moves in a harmonic potential attached to a rigid wall with an amplitude determined by the temperature of the solid. With this model the equations of motion can be solved exactly and an expression for the sticking coefficient which is guaranteed to never exceed one can be obtained.

The models discussed so far are all purely deterministic. Because exact solutions can be obtained only for very simple model potentials the results yield qualitative information only. The adjustable parameters which occur in these theories are often physically artificial and hence it is difficult to judge whether the values of these parameters needed to match experimental results are physically reasonable. If a more realistic potential, such as the Morse potential, is used then the solution of the equation of motion can be expressed only in integral form from which further information is difficult to extract. Conceptual difficulties also arise as to just when a particle has been adsorbed: an incoming gas particle may be adsorbed only to be desorbed and then readsorbed later. In order to get around such difficulties it is advantageous to use a stochastic model and to start from a kinetic equation such as the Kramers equation or the more fundamental master equation. The master equation will have the same form as in the quantum case; the only difference being that the transition rates are

derived from classical mechanics rather than quantum mechanics.

Pagni and Keck[115] have taken such an approach to physisorption: they used the soft cube model to derive transition rates for a master equation. These transition rates were found to be approximately Gaussian. From the master equation they were able to derive a diffusion equation with which they could study adsorption and desorption[116], sticking[117], and the energy distribution of desorbing adparticles[118]. Their results were in agreement with the experimental results for the heavier noble gases on metals. Part of the credit for this agreement with experiment is due to the derivation of a diffusion equation, from the master equation, which enabled the theory to include adparticle distributions which differed from equilibrium. It should be noted though that the correctness of the procedure used to derive the diffusion equation has been brought into question[31]. There will be comments on this matter in Chap. 5 of this thesis. One should also be aware that there are several parameters which were varied in order to bring about the agreement with experiment.

In an effort to obtain general properties for desorption kinetics Iche and Nozières[10] used a stochastic approach to discuss some of the problems of physisorption. They assumed that it was meaningful to describe the adsorbed states in terms of a wave packet which obeyed the classical equations of motion. This wave packet must not disperse too much over the course of one classical "round trip" in the potential well. All of their transition rates, sticking probabilities, and desorption rates are expressed in terms of this fundamental time unit. They gave a microscopic definition, in the form of an integral equation, for the sticking coefficient which was independent of the model used. To solve this equation the transition rates must be specified and hence the results are model dependent. They argue, however, that for deep potential wells the sticking probability may be expressed in terms of the desorption rate in such a way that it is always less than one. They also emphasize that the distribution adopted by the adsorbate during desorption is the equilibrium distribution except for a portion near the top of the potential. These ideas have been subsequently used extensively by Brenig and coworkers.

Rather than dealing with the details of a master equation or the integrals involving the transition rates in the Iche-Nozières approach one can still approach physisorption at the kinetic level by using the Kramers equation[65]. The one dimensional form of the Kramers equation is

$$\dot{n} = \frac{\partial U(z)}{\partial Z}\frac{\partial n}{\partial p} - \frac{p}{m}\frac{\partial n}{\partial Z} + \eta\frac{\partial}{\partial p}\left[pn + mk_B T\frac{\partial n}{\partial p}\right], \tag{1.13}$$

where $n=n(p,z,t)$ is the number of particles at time t and distance coordinate z with momentum p and mass m. The gas particle is moving in a surface potential $U(z)$ associated with the solid, which is at temperature T, and is subject to a frictional force which is proportional to η, the friction coefficient. The friction coefficient is phenomenological in nature and must be derived from microscopic theory.

Following the method of Schaich[73], Caroli *et al.*[119] have derived the Langevin equation which is equivalent to the Kramers equation for an adparticle classically coupled to the lattice vibrations of the solid. They explicitly evaluate the friction coefficient for a Morse potential and find that

$$\eta = 4\frac{m}{M}\omega_D\left[\frac{U_o}{\hbar\omega_D\sigma_o}\right]^4. \tag{1.14}$$

The Kramers equation can be solved for only a limited class of potentials[120]. For the remaining potentials, numerical methods[120-121] and approximation techniques[65,122] must be employed to extract desorption rates. The Kramers equation can be simplified somewhat when the limits of small or large friction are taken. The regime of small friction, which can be identified with weak coupling, is the one appropriate for physisorption. A concrete expression for this equation is realized only when the surface potential is specified. If a Morse potential

is chosen then the equation is

$$\dot{n}(y,t) = \eta \frac{\partial}{\partial y} \{(1-y)[\frac{k_B T}{2U_o} \frac{1}{y} \frac{\partial n(y,t)}{\partial y} - n(y,t)]\}, \tag{1.15}$$

where the energy of a particle trapped in the surface potential is

$$E = -U_o y^2 \tag{1.16}$$

There are some problems concerning the use of the Morse potential with the low friction Kramers equation, but for the moment they will be ignored; a thorough discussion of these problems will be presented in section 4.2 where it will be shown that under certain conditions the Kramers equation can be obtained from the Fokker-Planck equation.

In his original paper Kramers gave an integral expression for the desorption rate (It is referred to as the reaction rate in his paper.) which, when written in terms of the notation used in this thesis, is

$$\lambda \simeq \frac{\eta \exp(-U_o/k_B T)}{\int_0^1 dy \frac{y}{1-y} \exp(y^2 U_o/k_B T)}. \tag{1.17}$$

The divergent integral in (1.17) may be evaluated when altered, following Kramers, by ignoring the pole at $y=1$. This procedure yields

$$\lambda \simeq 2\eta\beta U_o e^{-\beta U_o}. \tag{1.18}$$

This expression is larger than Kramers' original estimate of the desorption rate by a factor of two, but nonetheless, it is the proper estimate of the desorption rate using Kramers method. Kramers realized this possibility, however, and issued the warning that his estimate of the desorption rate may be too small when applied to potentials with smooth activation barriers. This is certainly the case with the Morse potential. It is reassuring to note that in the limit

where the Kramers equation can be obtained from the phonon cascade Fokker-Planck equation the factor $F_s(1)$ reduces to one so that (1.12) reduces to (1.18).

To obtain a sounder estimate for the desorption rate from the Kramers equation it is necessary to follow the program mentioned at the end of the previous section.

The Kramers equation has also been used as a basis for a macroscopic theory of physisorption[123]. A set of hydrodynamic equations governing the physisoption system can be obtained by multiplying Eq. (1.13), by powers of the momentum p and then integrating over p. The resulting approximate desorption times are similar to those obtained by Kramers.

Another macroscopic approach to physisorption, based on Onsager's theory of nonequilibrium thermodynamics, has been presented by Müller and Brenig[124]. By identifying the forces and fluxes present in an adsorbate which can exchange energy with the solid substrate as well as energy and particles with the gas phase, they were able to present a pair of coupled equations governing the time evolution of the number of particles which are adsorbed and the total energy of the adsorbate. In this theory the particle and energy fluxes are related to the thermodynamic forces present through a set of kinetic coefficients. These kinetic coefficients were shown to be related to the desorption rate, sticking coefficient and accomodation coefficient. They were then evaluated by assuming that the adparticle could be represented as a classical particle moving in a truncated harmonic surface potential. Because Onsager's theory only holds for systems close to equilibrium these coefficients were in effect evaluated using the assumption that the adsorbate always has an equilibrium distribution. Although the resulting expressions for the kinetic coefficients are broad approximations this approach offers a general framework from which the boundary conditions for a hydrodynamic theory of a gas flowing past a solid surface might be formulated.

There is one last approach within the realm of classical mechanics which should be mentioned. As discussed earlier, if a realistic potential is used in a classical theory the equations of motion can at best be expressed in integral form. It is then difficult to extract expressions for the kinetic coefficients. By using the stochastic classical trajectory theory of Adelman and coworkers[125-127], Tully[128-131] has been able to obtain numerical results for the

various kinetic coefficients. Since the results obtained depend solely on the assumed properties of the gas solid interaction this method can be used to check the results of analytic theories and thus gain some insight into what are the important features of these theories. For instance, Leuthäusser[11] has used the work of Tully to determine the value of some of the free parameters in his theory.

In closing this section, in which so many different types of surface potentials have been mentioned, it seems fitting to comment on the theoretical form of the surface potential. Since it is impossible to invert scattering data to reveal a unique surface potential one must instead obtain a theoretical form for the potential and then see if it will reproduce the scattering data. There has been a great deal of work done on this subject. A convenient guide to this literature may be found in Ref. 3 where numerous review articles are listed and the various techniques used in this field are discussed. Suffice it to say that although it is well established that the van der Waals portion of the surface potential behaves as z^{-3} (Research still continues in this field[132-138].) it seems acceptable to use the Morse potential since it can yield bound state energies and transition rates which are in reasonable agreement with experimental work.

1.5 A Derivation of the Phenomenological Rate Equation

A few years ago there was a notable attempt by Brenig to derive the phenomenological rate equation from a discrete master equation (See Eq. (1.1).). In so doing, a microscopic expression for the sticking coefficient was obtained (See Eq. (1.30).). Unfortunately, this expression cannot guarantee a value less than one. It has been shown by Kreuzer and Gortel[3] that Brenig's expression for the sticking probability does indeed take on values greater than one. This implies that the principle of conservation of particles has been violated and thus renders Brenig's derivation untenable. It will be argued in chapter 3 that the origin of this defect lies in the assumptions made about the gas phase and can be remedied by treating the gas phase in a more realistic manner.

Since the initial stages of Brenig's work will be used later it is worthwhile to present an outline of Brenig's work. The discrete master equation (1.3) is an inhomogeneous first order differential system with respect to time, where the inhomogeneous term contains the distribution function of the gas phase. In other words the gas phase is an external source of particles to which the adsorbate distribution reacts. In order to solve this equation it is necessary to diagonalize the matrix formed by the transition rates. This is equivalent to finding the eigenvalues and eigenvectors of the following matrix,

$$W_{ji} - \sum_{i'=0}^{N-1} W_{i'j}\delta_{ji} - \sum_{k=-\infty}^{\infty} W_{kj}\delta_{ji} \quad . \tag{1.19}$$

Henceforth the summation limits will not be shown explicitly, it being understood that k denotes a continuum state while i and j denote bound states. It is possible to formally define left and right eigenvectors which, along with their associated eigenvalues, satisfy

$$\sum_j \tilde{e}_j^{(\nu)} \left\{ W_{ji} - \sum_{i'} W_{i'j}\delta_{ji} - \sum_k W_{kj}\delta_{ji} \right\} = \lambda_\nu \, \tilde{e}_i^{(\nu)} \quad , \tag{1.20}$$

and

$$\sum_i \left\{ W_{ji} - \sum_{i'} W_{i'j}\delta_{ji} - \sum_k W_{kj}\delta_{ji} \right\} e_i^{(\nu)} = \lambda_\nu \, \tilde{e}_j^{(\nu)} \quad , \tag{1.21}$$

respectively. These eigenvectors form the basis of a solution of Eq. (1.3) and have the usual properties of orthonormality and completeness (See App. A for a list of the properties of the eigenfunctions and ther eigenvalues.). The index ν ranges from 0 to N-1.

Using Eqs. (1.20) and (1.21) the discrete master equation may now be written as

$$\dot{n}_j(t) = \sum_{i=0}^{N-1} \sum_{\nu=0}^{N-1} \lambda_\nu \, e_j^{(\nu)} \tilde{e}^{(\nu)} \, n_i(t) + \sum_{k=-\infty}^{\infty} W_{jk} n_k(t) \quad , \tag{1.22}$$

which can readily be solved using the method of Laplace Transforms. The details of such a

calculation are to be found in App. B . The solution of Eq. (1.3) is then

$$n_j(t) = \sum_k e^{-\lambda_\nu t} \sum_i e_j^{(\nu)} \tilde{e}_i^{(\nu)} n_i(0)$$

$$+ \sum_\nu \sum_i \sum_k e^{-\lambda_\nu t} \int_0^t dt' e^{\lambda_\nu t'} e_j^{(\nu)} \tilde{e}^{(\nu)} W_{ik} n_k(t') \, . \qquad (1.23)$$

Because the eigenvalues form a sequence with a lower bound, the smallest eigenvalue determines the long time behaviour of the adparticle distribution. Assuming that this eigenvalue is much smaller than all of the other eigenvalues, the adparticle distribution function is then approximated as follows,

$$n_j(t) \approx \sum_i \sum_k e^{-\lambda_o t} \int_0^t dt' e^{\lambda_o t'} e_j^{(o)} e_j^{(o)} W_{ik} n_k(t') \, , \qquad (1.24)$$

where the initial distribution has been set equal to zero. This approximation implies that the gas phase can make transitions only into the distribution associated with the smallest eigenvalue.

The time dependent coverage is given by

$$\theta(t) = \frac{N_g}{N_s A} \sum_j n_j(t) \qquad (1.25)$$

and satisfies the following differential equation

$$\dot{\theta}(t) = \frac{N_g}{N_s A} \sum_i \sum_j \sum_k e_j^{(o)} \tilde{e}_i^{(o)} W_{ik} n_k(t) - \lambda_o \theta(t) \, , \qquad (1.26)$$

which has the same form as the phenomenological rate equation (1.1). The factor N_g is the number of gas particles in front of a surface with area A. This then leads to the identification

of the sticking coefficient as

$$S = \frac{(2\pi mk_BT)^{\frac{1}{2}}}{P} \frac{N_g}{A} \sum_i \sum_j \sum_k e_j^{(o)} \tilde{e}_i^{(o)} W_{ik} n_k^{eq} , \tag{1.27}$$

where, following Brenig, the equilibrium distribution

$$n_k^{eq} = \exp\ (-\hbar^2 k^2 / 2mk_BT) \tag{1.28}$$

for the gas phase has been assumed.

For a mobile adsorbate the following relation holds

$$\frac{k_BT}{h} = \frac{PA}{N_g(2\pi mk_BT)^{\frac{1}{2}}} = \sum_{k=0}^{\infty} \frac{\hbar k}{mL} \exp\ (-\hbar^2 k^2 / 2mk_BT) , \tag{1.29}$$

where L is the length of the container holding the gas (The volume of the container is therefore V=AL.). Use of this equation then yields Brenig's expression for the sticking coefficient

$$S = \frac{h}{k_BT} \sum_i \sum_j \sum_k e_j^{(o)} \tilde{e}_i^{(o)} W_{ik} n_k^{eq} . \tag{1.30}$$

Except for the presence of the eigenfunctions this expression for the sticking coefficient is identical to that given by Devonshire

$$S = \frac{h}{k_BT} \sum_i \sum_k W_{ik} n_k^{eq} . \tag{1.31}$$

Brenig has shown that the eigenfunctions ensure that the sticking coefficient goes to zero as the temperature goes to infinity. This is an improvement on the Devonshire result which predicts that the sticking coefficient will approach a constant value for large temperatures. Both of these expressions, however, can take on values greater than one. This is readily seen

by letting the transition rates become arbitrarily large which in turn forces the sticking coefficient to become arbitrarily large. It will be argued in chapter 3 that this is due to standard assumption that the gas phase maintains an equilibrium distribution in front of the surface of the solid regardless of the rate at which the gas phase is depleted by transitions from the continuum to the bound states.

Brivio and Grimley[139-140] have come across the same problem in their quantum mechanical work on the chemisorption of hydrogen on a metal surface. They proposed[140] the following definition for the sticking coefficient which is guaranteed not to exceed the value one,

$$S = \frac{R_{st}}{V_{coll} + R_{st}} , \tag{1.32}$$

where R_{st} is the rate at which gas particles with a given energy occupy the bound states and V_{coll} is the rate at which the gas particles collide with the surface. Using a model Hamiltonian, they give a microscopic expression for the sticking coefficient. It appears that they have yet to rigourously derive Eq. (1.32).

2. Macroscopic Equations for Physisorption

In this chapter some results of a study of physisorption kinetics on a macroscopic scale are presented[99]. The primary purpose for doing so is to introduce the friction coefficient. This coefficient characterizes how the adsorbate interacts with the solid. In particular, it governs the process of equilibration within the adsorbate. As will be shown in chapters 6 and 7, the friction coefficient is a naturally occurring component of the sticking coefficient and the desorption rate.

In the first section of this chapter a pair of macroscopic equations coupling the average adparticle energy and the fluctuations in the energy are developed. This coupling is typical of diffusive systems which are based on some form of Brownian motion. These equations are derived following the methods of van Kampen[141-143]. The derivations are done explicitly because these equations have not previously been derived for the case of a diffusive system. After these general equations have been derived the moments occurring in them are evaluated using the transition rates used in the phonon cascade model. Through the linearization of the moments occurring in the coupled equations a macroscopic law of friction is extracted and subsequently solved. This then leads to the identification of the friction coefficient as the characteristic time scale on which the adsorbate approaches equilibrium. It also provides an expression for the friction coefficient in terms of the microscopic parameters of the gas solid system. This analysis is only valid for an adsorbate eventually coming to an equilibrium state; it is not valid for the description of desorption since the latter is a purely nonequilibrium process which never comes to equilibrium.

In the second section a numerical study of an adsorbate approaching equilibrium with desorption processes included is presented. In this study it will be seen how well separated the time scales of equilibration and desorption are (Equilibration of the adsorbate within the surface potential is usually a much faster process than desorption is.). The buildup of nonequilibrium fluctuations is also illustrated.

2.1 The Macroscopic Law of Friction for Physisorption

To establish a macroscopic law of friction for an adsorbed gas particle it is necessary work in terms of the average energy per particle of the adsorbate

$$\bar{E}(t) = \langle E \rangle = \int_{-U_o}^{0} dE\, \tilde{\rho}(E) E \tilde{n}(E,t) \tag{2.1}$$

and its fluctuations (mean square deviations)

$$\sigma^2(t) = \langle E^2 \rangle - \langle E \rangle^2 = \int_{-U_o}^{0} dE\, \tilde{\rho}(E)(E - \langle E \rangle)^2 \tilde{n}(E,t). \tag{2.2}$$

It is assumed that the number of adparticles

$$N(t) = \int_{-U_o}^{0} dE\, \tilde{\rho}(E) \tilde{n}(E,t) \tag{2.3}$$

is held to a constant value of one. This is accomplished by suppressing the transitions between the bound states and the continuum states.

The equations of motion for these quantities are obtained from the continuous master equation (1.4) by multiplying the latter by the density of states, as well as by either the energy or the square of the energy, and then integrating over the bound state energies. The average energy then obeys the equation

$$\dot{\bar{E}}(t) = \langle \alpha_1(E) \rangle \ , \tag{2.4}$$

while the fluctuation in the energy obeys

$$\dot{\sigma}^2(t) = \langle \alpha_2(E) \rangle + 2 \left[\langle E \alpha_1(E) \rangle - \langle E \rangle \langle \alpha_1(E) \rangle \right] \ , \tag{2.5}$$

where the moments are defined as

$$\alpha_1(E) = \int_{-U_o}^{0} dE' \tilde{\rho}(E')(E'-E)^2 \tilde{W}(E',E) \tag{2.6}$$

and

$$\alpha_2(E) = \int_{-U_o}^{0} dE' \tilde{\rho}(E')(E'-E)^2 \tilde{W}(E',E) \ . \tag{2.7}$$

An expansion of the moments around the average energy then yields

$$\dot{\bar{E}} = \alpha_1(\bar{E}) + \tfrac{1}{2}\alpha_1''(E)\sigma^2 \ , \tag{2.8}$$

$$\dot{\sigma}^2 = \alpha_2(\bar{E}) + [\,2\alpha_1'(\bar{E}) + \tfrac{1}{2}\alpha_2''(\bar{E})]\sigma^2 \ , \tag{2.9}$$

where only the terms up to the first order in the fluctuations are kept. This pair of equations couples the average energy and its fluctuations into a closed set. Depending on the form of the moments this set of equations can be highly nonlinear.

The expressions for the moments are taken from App. D. They differ from the definitions (2.6) and (2.7) through their inclusion of bound state to continuum transitions. As a result they will be suspect in the region near the top of the surface potential. These moments may be approximated as follows,

$$\alpha_1(x) = 2\eta(1-x)\left(x - \frac{k_B T}{2U_o}\right) \ , \tag{2.10}$$

$$\alpha_2(x) = 4\eta U_o k_B T \ x \ (1-x) \ , \tag{2.11}$$

where

$$\bar{E} = -U_o(1-x)^2 \quad . \tag{2.12}$$

It will be seen shortly that the factor η is the friction coefficient. When substituted into the Eqs. (2.8) and (2.9), with the term α_3'' dropped, these moments yield.

$$\dot{x} = -\eta\left(x - \frac{k_B T}{2U_o}\right) + \frac{\eta}{8U_o^2}\left(1 - \frac{k_B T}{2U_o}\right)(1-x)^{-4}\,\sigma^2 \tag{2.13}$$

$$\dot{\sigma}^2 = 4\eta U_o k_B T\, x(1-x) - 2\eta\left(1 + \frac{k_B T}{2U_o} - 2x\right)(1-x)^{-1}\sigma^2 \tag{2.14}$$

which is the macroscopic law of friction. To the lowest order in the depth of the potential the equilibrium solution is

$$x^{eq} = \frac{k_B T}{2U_o} \tag{2.15}$$

$$\sigma^{2\,eq} = (k_B T)^2 \quad . \tag{2.16}$$

The system of equations, (2.13) and (2.14), is highly nonlinear and hence can be solved only through numerical methods. Before this is done it is worth noting that if the equations are linearized

$$\dot{x} = -\eta\left(x - \frac{k_B T}{2U_o}\right) \tag{2.17}$$

$$\dot{\sigma}^2 = 4\eta U_o k_B T\, x - 2\eta\sigma^2 \quad , \tag{2.18}$$

they have the following analytic solution

$$x(t) = \left[x(0) - \frac{k_B T}{U_o} \right] e^{-\eta t} + \frac{k_B T}{2U_o} \tag{2.19}$$

$$\sigma^2(t) = (k_B T)^2 (1 - e^{-2\eta t}) + 4U_o k_B T \left(x(0) - \frac{k_B T}{2U_o} \right) (e^{-\eta t} - e^{-2\eta t}) \ . \tag{2.20}$$

It is now apparent that the factor η is indeed the friction coefficient which governs the approach to the equilibrium state, Eqs. (2.15) and (2.16).

The numerical solution of equations (2.13) and (2.14) is shown in Fig. 1 as a phase portrait of the average energy and its fluctuations. The dotted and dashed lines define the set of points where the fluctuations and the average energy, respectively, are constant in time. These lines divide the space into domains which are characterized according to the signs of the time derivatives of the macroscopic variables. For instance in the upper right hand region the fluctuation in energy is always increasing as is the average energy.

The dashed and dotted lines intersect at two points: the point marked with an E is the equilibrium point and the point marked with an S is a saddle point. The significance of these points is illustrated by the trajectories of the macroscopic variables, denoted by the solid and dashed-dotted lines, which depend parametrically on time. These trajectories start, at time $t=0$, on the bottom axis and terminate either at point E or S as time t goes to infinity, or else on the right hand edge of the diagram. All trajectiories to the left of the dashed-dotted line asymptotically approach the equilibrium point as the time goes to infinity. The dashed-dotted line is the sole trajectory which approaches the saddle point S and delineates the domain of attraction of the equilibrium point; all trajectories to the right of this line exit the system altogether. The region to the right of the dashed-dotted line, which is within a thermal fluctuation of the top of the potential well, is therefore unstable. This instability is due to the use of the moments which include the bound to continuum transitions and hence is of no physical consequence.

In physical terms, the trajectories have the following interpretation. The adsorbate is initially prepared with a well defined energy. As time progresses the fluctuations in the average energy rapidly build up. Eventually the average energy of the system begins to decrease as the fluctuations allow the system to drift to lower energy levels. As the average energy of the system approaches its equilibrium value the fluctuations also decrease to their equilibrium value. It is apparent that for this system to come to its equilibrium state it is necessary for large nonequilibrium fluctuations to develop. In other words the fluctuations are as important as the macroscopic decay of the average energy.This behaviour is typical of a diffusive system.

2.2 A Numerical Study

In this section a numerical study of the time dependence of the macroscopic variables of the adsorbate is presented. The study is done for a Xe/W system and the results are obtained directly from the discrete master equation. The macroscopic variables studied are the total number of particles

$$N(t) = \sum_i n_i(t) \tag{2.21}$$

the average energy of the adsorbate

$$\bar{E} = \frac{E(t)}{N(t)} = \frac{\sum_i E_i n_i(t)}{N(t)} \tag{2.22}$$

and the fluctuations in the energy

$$\sigma^2 = \frac{\sum_i (E_i - E)^2 \, n_i(t)}{\sum_i n_i(t)} \tag{2.23}$$

In the first example an adsorbate is prepared in such a way that all of its constituent adparticles are in the sixteenth bound state of the surface potential. The solid as at 202.5°

Kelvin and the gas phase is arranged to be empty at all times. In otherwords, an isothermal desorption experiment is modelled. Since the bound state to bound state transition rates favour the emission of phonons the adparticles will descend into the potential well emitting nonequilibrium phonons into the solid (See the upper panel of Fig. 2 .). Large nonequilibrium fluctuations buildup and subsequently decay to thermal ones as the average energy approaches its equilibrium value (See the middle panel of Fig. 2 .). The relaxation time is given by η^{-1} which has a value of 5.3 times 10^{-13} seconds. Eventually the adsorbate desorbs according to a time scale which is about eight orders of magnitude larger than the equilibration time. This remarkable difference in time scales is readily apparent upon comparing the upper and lower panels of Fig. 2 .

A similar situation is considered in Fig. 3 where the adsorbate particles are all initially in the sixtieth bound state which is very close to the top of the potential well. The temperature of the solid is now 405° Kelvin. This situation leads to a large loss of adsorbate particles to the gas phase via the transient channels as is indicated by comparing the upper and lower panels. This loss of particles takes place on a time scale which is an order of magnitude smaller than or comparable to the equilibration time scale. The remaining adparticles eventually desorb after a time which is three orders of magnitude larger than the equilibration time. In Figs. 4 and 5 the evolution of the adparti.le distribution towards its equilibrium configuration is shown.

It should be stated that strictly speaking the adsorbate comes to a quasi-equilibrium and not full equilibrium as is implied by the text above. The distinction arises when the occupancy of the bound states near the potential well top are examined in detail. This will be done in chapter 6 where it will be shown that the these states are substantially depleted from their equilibrium value. This point is also discussed in Ref. 31. The distribution of adparticles is heavily weighted, according to the Boltzmann distribution, in favour of the particles being near the well bottom where an equilibrium distribution is maintained. Therefore, the average energy per particle and its fluctuations are, throughout the desorption process, virtually identical to their equilibrium values.

3. A Microscopic Theory of the Phenomenological Rate Equation

The phenomenological rate equation (1.1) is a macroscopic equation which describes desorption. As mentioned in chapter 1, it is the task of kinetic theory to derive this equation and its component kinetic coefficients from microscopic theory. In section 1.5 the attempt by Brenig to derive the phenomenological rate was presented and found to be unacceptable because the sticking coefficient could take on values greater than one. This unacceptable behaviour of the sticking coefficient is typical of quantum mechanical theories and can be traced to the manner in which the gas phase has been treated. It is usually assumed, unwittingly, that the gas phase can be treated as an infinite resevoir from which particles may be drawn for possible adsorption at an unlimited rate. If the the rate of adsorption, which is unconstrained according to the previous assumptons, is then divided by the thermal flux of particles which are actually arriving at the surface it is quite possible to obtain a value of the sticking coefficient which is greater than one. In effect, particles are being created and hence unitarity, in the physical sense of the word, has been violated. Only a unitary sticking coefficient can guarantee a value less than one. To rectify this problem the gas phase must be treated in a more realistic manner.

The main objective of this chapter is to derive the phenomenological rate equation and to obtain a plausible expression for a unitary sticking coefficient. The approach taken here differs from previous derivations through its treatment of the gas phase. Special attention will be paid to the rate at which particles can be supplied to the solid surface for possible adsorption in the hope that the unitarity of the sticking coefficient will be preserved.

3.1 Derivation of the Phenomenological Rate Equation

To derive the phenomenological rate equation from microscopic theory the time evolution of the adsorbate distribution function and its dependence on the gas phase distribution must be determined.

By starting from the discrete master equation (1.3) for the adsorbate distribution function, Brenig has shown rigourously that the adsorbate distribution function obeys the

following equation

$$n_i(t) = \sum_j \sum_\nu e_i^{(\nu)} \tilde{e}^{(\nu)} n_j(0) e^{-\lambda_\nu t} + \sum_\nu \sum_j \sum_k e_i^{(\nu)} \tilde{e}_j^{(\nu)} W_{jk} e^{-\lambda_\nu t} \int_0^t dt' e^{\lambda_k t} n_k(t') \quad . \tag{3.1}$$

The definitions and properties of the eigenvectors and eigenvalues are listed in Appendix A. A detailed derivation of Eq. (3.1) from Eq. (1.3) is given in section 1.5. As may be seen from Eq. (3.1), an expression for the gas phase distribution function must be inserted into (3.1) in order to determine the adsorbate distribution function. Brenig has assumed that the Boltzmann distribution is an appropriate ansatz to insert into Eq. (3.1). Doing so, as well as keeping only the $\nu=0$ terms, eventually yields the following expression for the sticking coefficient

$$S = \sum_i \sum_j \sum_k e_i \tilde{e}_j W_{jk} n_k^{eq} \quad , \tag{3.2}$$

where $e = e^{(0)}$, $\tilde{e} = \tilde{e}^{(0)}$. This expression goes to zero as the temperature approaches infinity and hence is an improvement on the expression, Eq. (1.31), derived by Lennard-Jones and Devonshire. Kreuzer and Gortel have shown, however, that the equilibrium ansatz leads to a nonunitary sticking coefficient. The reason for this failure is discussed in the introductory paragraphs of this chapter. As mentioned above this situation can be corrected by assuming, or better yet, deriving a physically more realistic expression for the gas phase distribution function.

The derivation of an expression for the gas phase distribution starts with the discrete rate equation for the gas phase

$$\dot{n}_k(t) = \sum_i \left\{ W_{ki} n_i(t) - W_{ik} n_k(t) \right\} + \frac{\hbar k}{mL} \left[n_k^{eq} - n_k(t) \right] \quad . \tag{3.3}$$

Remember that L is the length of the chamber containing the gas. Note that both the phonon mediated and the collision-induced transitions between the continuum states of the gas phase

have been omitted. Considering the gas pressures and densities studied experimentally these are reasonable assumptions to make. The last two terms of Eq. (3.3) are source and sink terms. The first of the two represents a thermal flux of gas particles which is directed into the vacuum chamber toward the solid surface. This stream of particles has a Maxwell-Boltzmann distribution, i.e.

$$n_k^{eq} = \exp\left(-\frac{\hbar^2 k^2}{2mk_B T}\right) . \tag{3.4}$$

The rate at which a particle enters the chamber is given by the velocity of the particle divided by the length of the chamber. The sink term in (3.3) represents the rate at which particles leave the chamber after they have scattered off of the solid surface.

Equation (3.3) may be solved through the use of Laplace transforms to yield

$$n_k(t) = n_k(0)e^{-\mu_k t} + \frac{n_k^{eq}}{\mu_k}\frac{\hbar k}{mL}\left(1 - e^{-\mu_k t}\right)$$

$$+\sum_i W_{ki} e^{-\mu_k t}\int_0^t dt' e^{\mu_k t} n_i(t') , \tag{3.5}$$

where

$$\mu_k = \frac{\hbar k}{mL} + \sum_i W_{ik} . \tag{3.6}$$

In Eq. (3.5) the initial values of the $n_k(t)$ have been set equal to zero. Physically this means that the vacuum chamber starts the experiment in an empty state. See Appendix B of this thesis for details of this calculation.

The μ_k, which are of the order of L^{-1}, are the time scales on which the individual gas phase states, with wavevector k, evolve when there is no adsorbate present. The adsorbate evolves on the time scale λ_0^{-1} which is much faster than the time scale of the gas phase states.

For the most part, the individual gas phase states evolve slowly in time while the adsorbate reacts very quickly to any changes in the gas phase. The only component of the gas phase which changes quickly is the term which is coupled directly to the adsorbates states. The adsorbate distribution function may then be taken outside of the integral in (3.5) thus allowing the integral to be evaluated. Equation (3.5) then becomes

$$n_k(t) = \left[\frac{n_k^{eq}}{\mu_k} \frac{\hbar k}{mL} + \frac{\sum_i W_{ki}}{\mu_k} n_i(t) \right] \left(1 - e^{-\mu_k t} \right) . \tag{3.7}$$

The terms on the RHS of Eq. (3.7) contain the same exponential time dependence. Because the time scale of these terms is so slow when compared to the time scales of the adsorbate, the exponential terms may be regarded as being constant. This constant can then be absorbed into the unnormalized distribution function for the gas phase. Therefore, a plausible expression for the gas phase distribution function, which is to be inserted into expression (3.1) for the adsorbate, is

$$n_k(t) = \left[\frac{n_k^{eq}}{\mu_k} \frac{\hbar k}{mL} + \frac{\sum_i W_{ki}}{\mu_k} n_i(t) \right] . \tag{3.8}$$

Through the use of the property of detailed balance and Eq. (3.6) it can be shown that if the Boltzmann distribution is assumed for the adsorbate in Eq. (3.8), then the gas phase states also assume the Boltzmann distribution. This ensures that the adsorbate and the gas phase approach equilibrium in tandem.

Inserting the above expression into Eq. (3.1) yields

$$n_i(t) = \sum_\nu \sum_j \sum_k e_i^{(\nu)} e_j^{(\nu)} W_{jk} e^{-\lambda_\nu t} \int_0^t dt' \frac{e^{\lambda_\nu t'}}{\mu_k} \left[n_k^{eq} \frac{\hbar k}{mL} + \sum_i W_{ki} n_i(t') \right] , \tag{3.9}$$

where it has been assumed that initially there are no particles in the adsorbate states. The first term on the RHS may be integrated immediately, so that after some algebra (3.9) becomes

$$n_i(t) = \sum_k \sum_j \sum_\nu e_i^{(\nu)} \tilde{e}_j^{(\nu)} W_{jk} \frac{\hbar k}{mL} \frac{n_k^{eq}}{\mu_k} \frac{1}{\lambda_o} \left(1 - e^{-\lambda_o t}\right)$$

$$+ \sum_{i'} \sum_k \sum_j \sum_\nu e_i^{(\nu)} \tilde{e}_j^{(\nu)} W_{jk} \frac{1}{\mu_k} W_{ki'} e^{-\lambda_o t} \int_0^t dt' e^{\lambda_o t'} n_{i'}(t') \ . \qquad (3.10)$$

By assumption, the eigenvalue λ_0 is much smaller than all of the other eigenvalues. Since the transient effects are to be neglected, all of the eigenvalues other than the smallest are dropped. Equation (3.10) then becomes

$$n_i(t) = e_i \sum_j \sum_k \tilde{e}_j W_{jk} \frac{\hbar k}{mL} \frac{n_k^{eq}}{\mu_k} \frac{1}{\lambda_o} \left(1 - e^{-\lambda_o t}\right)$$

$$+ e_i \sum_{i'} \sum_j \sum_k \tilde{e}_j W_{jk} \frac{1}{\mu_k} W_{ki'} e^{-\lambda_o t} \int_0^t dt' e^{\lambda_o t'} n_{i'}(t') \ . \qquad (3.11)$$

It is apparent from the structure of Eq. (3.11) that it has a solution of the form

$$n_i(t) = e_i \, n(t) \ . \qquad (3.12)$$

The substitution of (3.12) into (3.11) results in an integral equation,

$$n(t) = \frac{1}{\lambda_o} \left(1 - e^{-\lambda_o t}\right) \sum_j \sum_k \tilde{e}_j W_{jk} \frac{\hbar k}{mL} \frac{n_k^{eq}}{\mu_k}$$

$$+ \sum_i \sum_j \sum_k \tilde{e}_j W_{jk} \frac{1}{\mu_k} W_{ki} e_i e^{-\lambda_o t} \int_0^t dt' e^{\lambda_o t'} n(t') \ , \qquad (3.13)$$

which may be solved using Laplace transforms. One then finds the following expression for

the adsorbate distribution function

$$n_i(t) = \frac{\left[\sum_j \sum_k \tilde{e}_j W_{jk} \frac{\hbar k}{mL} \frac{n_k^{eq}}{\mu_k}\right]}{\lambda_o(1-R)} \left[1 - e^{-\lambda_o(1-R)t}\right], \tag{3.14}$$

where

$$R = \frac{1}{\lambda_o} \sum_j \sum_k \tilde{e}_j W_{jk} \frac{1}{\mu_k} W_{ki} e_i \ . \tag{3.15}$$

By multiplying (3.14) by the factors appropriate for a mobile adsorbate[3] and summing over the index i an expression for the time dependent coverage is obtained

$$\Theta(t) = \frac{k_B T}{h} \frac{S}{\lambda_o(1-R)} \left[1 - e^{-\lambda_o(1-R)t}\right], \tag{3.16}$$

where

$$S = \frac{h}{k_B T} \sum_i \sum_j \sum_k e_i \tilde{e}_j W_{jk} \frac{n_k^{eq}}{\mu_k} \frac{\hbar k}{mL} \ . \tag{3.17}$$

A differentiation of Eq. (3.17) finally yields

$$\dot{\Theta}(t) = \frac{k_B T}{h} S - \lambda_o(1-R)\, \Theta(t) \ , \tag{3.18}$$

which has the same form as the phenomenological rate equation (1.1). This finally allows for the identification of the sticking coefficient as S, as is defined by Eq. (3.15).

As may be seen from Eq. (3.15) the adsorbate has an exponential time dependence which decays with an effective desorption rate of

$$\tilde{\lambda}_o = \lambda_o(1-R) = \lambda_o \left[1 - \frac{1}{\lambda_o} \sum_i \sum_j \sum_k \tilde{e}_j W_{jk} \frac{1}{\mu_k} W_{ki} e_i\right] \ . \tag{3.19}$$

This effective desorption rate can be thought of as a renormalized desorption rate where transitions from a bound state to a continuum state and back again have been taken into account. Because of the approximation leading to Eq. (3.7) higher order processes, i.e. multiple scatterings from the bound states to the continuum states and back again, have been dropped.

The properties of the sticking coefficient will be discussed in the next section. In particular, the property of unitarity will be discussed. In section 3.3 the effective desorption rate will be discussed further.

3.2 The Sticking Coefficient

In the previous section an expression for the sticking coefficient was derived. The derivation was general in the sense that the results are independent of what the transition rates are. In order to calculate the temperature dependence of the sticking coefficient a microscopic model of the gas-solid interaction must be specified so that the transition rates can be determined. Before embarking on this venture it will be worthwhile to study the structure of the sticking coefficient and see under what conditions it is unitary.

The definition of the sticking coefficient, Eq. (3.17), can be reworked into the following form

$$S = \frac{1}{\left[\sum_k \frac{\pi k}{mL}\, n_k^{eq}\right]} \left\{ \sum_k \frac{\pi k}{mL}\, n_k^{eq} \left[\frac{\sum_i \sum_j e_j \tilde{e}_j W_{jk}}{\frac{\pi k}{mL} + \sum_i W_{ik}} \right] \right\} . \qquad (3.20)$$

It is now apparent that the sticking coefficient is a weighted average of the terms inside the square brackets. The average is weighted with respect to the thermal flux. If the individual terms inside the square brackets are all less than or equal to one then the weighted average, and hence the sticking coefficient, will be less than or equal to one. More precisely, if it can

be shown that

$$\sum_j W_{jk} > \sum_j \sum_i e_i \tilde{e}_j W_{jk} \quad , \tag{3.21}$$

for all k, then the sticking coefficient is guaranteed to be less than or equal to one. Unfortunately, it appears that condition (3.21) cannot be proved in general. It may indeed be possible to concoct a set of transition rates which would violate (3.21), but such a set would probably be unphysical. It will be seen in chapter 6 that in practice the above condition is always satisfied in the temperature regimes of practical interest.

A unitary sticking coefficient would be obtained if the function μ_k (See Eq. (3.6)) could be modified as follows

$$\mu_k = \frac{\dot{n}_k}{mL} + \sum_i W_{ik} = \frac{\dot{n}_k}{mL} + \sum_i \sum_j \sum_\nu e_i^{(\nu)} e_j^{(\nu)} W_{jk}$$

$$= \frac{\dot{n}_k}{mL} + \sum_i \sum_j e_i \tilde{e}_j W_{jk} \quad , \tag{3.22}$$

where the completeness relation for the eigenvectors has been used. The definition of the sticking coefficient then becomes

$$S = \frac{1}{\left[\sum_k \frac{\dot{n}_k}{mL} n_k^{eq}\right]} \left\{ \sum_k \frac{\dot{n}_k}{mL} n_k^{eq} \left[\frac{\sum_i \sum_j e_i \tilde{e}_j W_{jk}}{\frac{\dot{n}_k}{mL} + \sum_i \sum_j e_i \tilde{e}_j W_{jk}} \right] \right\} \quad , \tag{3.23}$$

which, considering the discussion of the prceeding paragraph is obviously unitary.

There are grounds for making the approximation (3.22). Remember that to arrive at Eq. (3.11) it was necessary to drop all terms where $\kappa \neq 0$. This effectively eliminates all transitions from the transient distribution to the gas phase continuum states and vice versa. One then argues that on physical grounds this is tantamount to saying that the gas phase exchanges particles only with the nontransient mode of the adsorbate and hence, right from

the start, i.e. Eq. (3.8), the damping factor μ_k of the gas phase should have been approximated according to Eq. (3.22). If this is not done and the gas particles are allowed to adsorb via all possible channels while the adsorbed particles are restricted to desorption via the nontransient mode, then it seems possible that particle conservation will be violated thus destroying the desired property of unitarity. It may well be that this is why Eq. (3.20) cannot be proven to satisfy the unitarity property.

Although the above arguments are physically appealing they are difficult to justify mathematically. The only mathematically rigourous way of following the above argument would be to alter the transition rates in the rate equation (3.3) so that Eq. (3.22) became an exact statement rather than an approximate one. In order to remain on safe mathematical grounds, further work on the sticking coefficient will be based on Eq. (3.20).

The terms inside the square brackets of Eq. (3.20) can be loosely interpreted as the ratio of the rate at which particles are absorbed from a continuum state of wavevector k to the rate at which particles are removed from the same continuum state through the processes of adsorption and escape from the vacuum chamber itself. The structure of this ratio lends itself to a further approximation of the sticking coefficient. Often the transition rates are sharply peaked around neighboring energy states (See fig. 4.1). Since only the continuum to bound state transition rates occur in the definition of the sticking coefficient, the major contributions to S will come from the indices which correspond to the low energy continuum states and the high energy bound states. It therefore seems reasonable to average each of the terms separately and thus approximate the sticking coefficient as follows

$$S \approx \frac{L \frac{k_B T}{h} \sum_k \sum_i \sum_j e_i \tilde{e}_j W_{jk} n_k^{eq_{k^{-1}}}}{\left[1 + \frac{k_B T}{h} L \sum_i \sum_k W_{ik} n_k^{eq_{k^{-1}}}\right]} \tag{3.24}$$

The above approximation for the sticking coefficient can be shown to be unitary as follows. Using the completeness property of the eigenvectors, the sum occurring in the

denominator may be written as

$$\sum_i \sum_k W_{ik} n_k^{eq} = \sum_k \sum_i \sum_j \sum_\nu e_i^{(\nu)} \tilde{e}_j^{(\nu)} W_{jk} n_k^{eq}$$

$$= \sum_k \sum_i \sum_j e_i \tilde{e}_j W_{jk} n_k^{eq} + \sum_k \sum_i \sum_j \sum_{\nu \neq 0} e_i^{(\nu)} \tilde{e}_j^{(\nu)} W_{jk} n_k^{eq} \quad . \quad (3.25)$$

The second term in the last line of Eq. (3.25) can be manipulated using the properties of the eigenfunctions (See App. A) to yield

$$\sum_\nu \sum_i \sum_j e_i^{(\nu)} \tilde{e}_j^{(\nu)} W_{jk} n_k^{eq} = \left(\sum_i e_i^{(\nu)} \right) \left(\sum_k \sum_j W_{kj} n_j^{eq} e_j^{(\nu)} \right)$$

$$= \lambda_\nu \left(\sum_i e_i^{(\nu)} \right) \left(\sum_j \tilde{e}_j^{(\nu)} n_j^{eq} \right)$$

$$= \lambda_\nu \left(\sum_i e_i^{(\nu)} \right)^2 \left(\sum_j n_j^{eq} \right) > 0 \quad . \quad (3.26)$$

Therefore,

$$\sum_i \sum_k W_{jk} n_k^{eq} > \sum_k \sum_i \sum_j e_i \tilde{e}_j W_{jk} n_k^{eq} \quad , \quad (3.27)$$

from which it may be concluded that the denominator in Eq. (3.24) is larger than the numerator. The approximate expression (3.24) for the sticking coefficient is therefore unitary.

The form of Eq. (3.24) has an appealing physical interpretation. It is easy to see from Eq. (3.24) that when the transition rates are very large the value of S will be in the vicinity of one or less. Physically, the gas particles are adsorbed almost as soon as they arrive in the vacuum chamber. If the transition rates are very small then the thermal velocity term in

the denominator will dominate and S will take on very small values. In otherwords most of the gas particles leave the vacuum chamber before they can be adsorbed.

This approximate sticking coefficient bears some resemblence to a couple of microscopic expressions that others have derived. Brenig's expression for the sticking coefficient, Eq. (3.2), can be obtained if the sum occurring in the denominator is omitted. This structure ensures that the low and high temperature behaviour, where the sticking coefficient goes to zero, is the same as Brenig's expression. The approximate sticking coefficient, given by Eq. (3.24), is therefore expected to rise to some maximum value less than one and then decrease slowly to zero as the temperature goes to infinity. One can view Eq. (3.24) as a modification of Brenig's result to take into account the finite rate at which gas particles can arrive at the surface.

Brivio and Grimley[140] have proposed a unitary sticking coefficient (1.32) which has the same form as Eq. (3.22). Their definition, however, is only a proposal which has yet to be proven. There is a difference between expressions (3.22) and (1.32): Eq. (3.22) contains different summation terms in the denominator and numerator while in Eq. (1.32) the corresponding terms are identical. Brivio and Grimley have estimated their sticking coefficient using a model Hamiltonian. Unfortunately, it does not seem to have the desired property of going to zero as the temperature goes to infinity. This problem is probably a consequence of the specific model Hamiltonian that they used.

Before proceeding to the discussion of the effective desorption rate some comments about the eigenvectors are in order. The combination

$$g_j = \tilde{e}_j \sum_i e_i \qquad (3.28)$$

occurs in the definition of the sticking coefficient (3.15) and the expression for the adsorbate distribution function through (3.14). It can be shown that (3.28) is the nontransient distribution function for an adsorbate which is undergoing ideal desorption, that is, desorption where the transitions from the continuum into the bound states have been suppressed. The

approximation of dropping all of the $\kappa \neq 0$ terms to arrive at Eq. (3.11) intentionally selects this distribution because the phenomenological rate equation is a macroscopic entity which describes the long time behaviour of the adsorbate. The inclusion of this distribution in the definition of S is important because, as Brenig has shown, it is responsible for the sticking coefficient going to zero as the temperature goes to infinity.

3.3 The Effective Desorption Rate and Readsorption Coefficient

The effective desorption rate can be expressed in terms of the ideal desorption rate and a correction term which takes into account the possibility of an adparticle readsorbing after it has desorbed. This correction term (3.15), which will be denoted the readsorption coefficient, may be rewritten as

$$R = \frac{1}{\left[\sum_j \sum_k g_j W_{kj} n_j^{eq}\right]} \left\{ \sum_j \sum_k W_{kj} n_j^{eq} g_j \left[\frac{\sum_i g_i W_{ik}}{\frac{\hbar k}{mL} + \sum_i W_{ik}} \right] \right\} . \qquad (3.29)$$

The readsorption coefficient (3.29), like the sticking coefficient, is expressed as a weighted average of the ratio of the adsorption rate to the total rate of depletion of the gas phase. In this case, however, the average is weighted with respect to the desorption flux.

As with the sticking coefficient, unitarity cannot be proven rigourously unless the same approximation leading to (3.24) is made. The readsorption coefficient then becomes

$$R = \frac{\sum_k \sum_i \sum_j k^{-1} g_i W_{ik} W_{kj} g_i n_j^{eq}}{\left[\frac{\hbar}{mL} \sum_k \sum_j W_{kj} g_j n_j^{eq} + \sum_i \sum_j \sum_k W_{ik} k^{-1} W_{kj} g_j n_j^{eq} \right]} . \qquad (3.30)$$

Arguments similar to those found after Eq. (3.24) will show that Eq. (3.30) is also unitary.

It is expected that the readsorption coefficient will be equal to one when the sticking coefficient is equal to one. In physical terms this is because in a gas-solid system with a sticking coefficient of one the gas particles cannot escape from the surface because as soon as they desorb they are immediately readsorbed. The effective desorption rate would then be equal to zero which, by virtue of Eq. (3.19), requires that the readsorption coefficient be

equal to one. It is also expected that the readsorption coefficient will be significant when the sticking coefficient is close to one. This will cause a substantial decrease in the adsorption and desorption rates. Because of the presence of the desorption distribution, Eq. (3.28), in Eq. (3.30) the readsorption coefficient will also go to zero as the temperature goes to infinity.

Keeping the above discussion in mind, as well as the arguments leading to the approximation of the sticking coefficient by Eq. (3.24), it is tempting to approximate the readsorption coefficient by setting it equal to the sticking coefficient. This approximation is checked in chapter 7. The phenomenological rate equation then becomes

$$\dot{\Theta}(t) = \left[\frac{k_B T}{h} + \lambda_o \Theta(t)\right] S - \lambda_o \Theta(t) \ . \tag{3.31}$$

To fully justify the above approximation would require an extensive investigation which is beyond the scope of this thesis. For the time being a good rule of thumb is that for gas-solid systems which have a small sticking coefficient, the effective desorption rate is, for all intents and purposes, equal to the isothermal (ideal) desorption rate which is usually calculated. For systems with a sticking coefficient close to one, which is often the case for systems with a large number of bound state, the desorption rate may be sustantially reduced. The level of this reduction is roughly determined by the multiplicative factor (1-S).

It appears that there are no other theories of physisorption kinetics which attempt to include the readsorption process. The possibility of these effects being important was, however, noted by Holloway *et al.*[101].The fact that such a coefficient has not been presented before is presumably due to the standard practice of assuming that the gas phase has a constant (steady state) distribution.

To calculate the effective desorption rate the ideal desorption rate must be known. As mentioned in passing, ideal desorption refers to the model situation where an adsorbate is desorbing into a perfect vacuum, i.e. one which remains evacuated at all times. In terms of the master equation this amounts to suppressing the continuum to bound state transitions and setting the continuum state occupations equal to zero. The desorption rate for this situation is

called the ideal desorption rate and is determined by finding the smallest eigenvalue which satisfies Eqs. (1.20) and (1.21). Hence, the solution of the ideal desorption problem provides the information necessary to calculate the sticking coefficient, the readsorption coefficient, and the effective desorption rate.

The next three chapters will be devoted to the solution of the ideal desorption problem. Three chapters are needed because the mathematical machinery to solve this problem must first be developed. After an approximate solution is obtained the sticking coefficient will be calculated analytically and compared to the numerical results. The readsorption coefficient will also be evaluated numerically.

4. The Phonon Cascade Fokker-Planck Equation

In the previous chapter the phenomenological rate equation (3.18) for physisorption was derived from microscopic theory. To obtain an explicit expression for the sticking coefficient and the effective desorption rate it is necessary to solve the ideal desorption problem. In particular, the ideal desorption rate, i.e. the smallest eigenvalue, and its corresponding eigenfunctions must be calculated. Once these quantities have been obtained the various summations involving the transition rates between the continuum states of the gas phase and the bound states of the adsorbate may be performed. This procedure can be carried out numerically but it is desirable to do it analytically as well; only then will the dependence of the sticking coefficient and the effective desorption rate on the dynamic parameters of the gas-solid system be seen explicitly. This program would also enable gas-solid systems with a large number of bound states to be studied (There is a computational limit to the rate equation approach due to the need for matrix diagonalization in the determination of the smallest eigenvalue.).

To analytically calculate the smallest eigenvalue and its corresponding eigenvector from the discrete master equation (1.3) is a hopeless task. In order to overcome this difficulty it is necessary to approximate the rate equation as a continuous master which may then be converted into a Fokker-Planck equation which is at least amenable to an approximate solution.

The primary goal of this chapter will therefore be to derive, from the continuous master equation (1.4),what will be called the phonon cascade Fokker-Planck equation, or Fokker-Planck equation for short. In order to solve this equation it will be necessary to derive boundary conditions, appropriate to the process of ideal desorption, from the master equation. This will be done in the next chapter. The actual solution of the phonon cascade Fokker-Planck equation, both approximately and numerically, will be done in chapter 6.

In order to derive the required Fokker-Planck Equation it is necessary to perform a Kramers-Moyal expansion of the master equation and then truncate it according to van Kampen's large parameter scheme. The boundary condition for ideal desorption is also derived

within van Kampen's large parameter scheme[141-143]. As will be seen, this procedure is of interest in its own right because it is an application of van Kampen's ideas to a complicated physical system; van Kampen's large parameter expansion is not a purely academic excercise, it is of tremendous practical importance.

After deriving the phonon cascade Fokker-Planck equation it will be shown that, under certain conditions, the low friction version of Kramers' equation can be obtained from the phonon cascade Fokker-Planck equation. This will then allow the friction coefficient to be identified and expressed in terms of the microscopic parameters which characterize the gas-solid system. This expression is then compared with the friction coefficient obtained from linear response theory. In addition, the conditions of coincidence of classical mechanics and quantum mechanics at the kinetic level will then become apparent (Remember that the Kramers equation is classical in origin while the phonon cascade Fokker-Planck equation is based on quantum mechanics.). And finally, some general properties of the phonon cascade Fokker-Planck equation will be discussed.

4.1 Derivation of the Phonon Cascade Fokker-Planck Equation

The starting point for the derivation of the phonon cascade Fokker-Planck equation is the continuous master equation (1.4). Since only the behaviour of the adsorbate is of interest in this section it will be understood that the variable E takes on only negative values while E' may take on both positive and negative values.Jack and Kreuzer[91] found it convenient to introduce the dimensionless energy variable $\epsilon = E/U_o$ into Eq. (1.4) to get

$$\dot{n}(\varepsilon,t) = \int_{-1}^{\infty} d\varepsilon' \rho(\varepsilon') W(\varepsilon,\varepsilon') n(\varepsilon',t) - \int_{-1}^{\infty} d\varepsilon' \rho(\varepsilon') W(\varepsilon',\varepsilon) n(\varepsilon,t) \quad , \qquad (4.1)$$

where $\rho(\epsilon') = \sigma_o / 2(|-\epsilon'|)$, $\tilde{W}(E,E') = W(\epsilon,\epsilon')$, and $\tilde{n}(E,t) = n(\epsilon,t)$.

One look at the full expression for the transition rates given in App. C should convince the reader that an exact analytic solution of Eq. (4.1) is quite impossible. It is possible, however, to use Eq. (4.1) to obtain an estimate of the desorption rate in the low

temperature regime (See Eq. (1.6).).

In order to proceed, the master equation must be converted into a Fokker-Planck equation via a Kramers-Moyal expansion. This is usually a straightforward procedure. In the case of the continuous master equation for physisorption the Kramers-Moyal expansion is more complicated due to the presence of the finite lower limit in the integrations. Because of this complication the expansion will explicitly be done below.

First, the master equation must be multiplied by an arbitrary test function $\tau(\epsilon)$ and the density of states factor $\rho(\epsilon)$, and then integrated with respect to ϵ from -1 to ∞. This yields the following equation,

$$\int_{-1}^{\infty} d\varepsilon \rho(\varepsilon)\tau(\varepsilon)\dot{n}(\varepsilon,t) = \int_{-1}^{\infty} d\varepsilon \rho(\varepsilon) \int_{-1}^{\infty} d\varepsilon' \rho(\varepsilon')\tau(\varepsilon')W(\varepsilon',\varepsilon)n(\varepsilon,t)$$

$$- \int_{-1}^{\infty} d\varepsilon \rho(\varepsilon)\tau(\varepsilon) \int_{-1}^{\infty} d\varepsilon' \rho(\varepsilon')W(\varepsilon',\varepsilon)n(\varepsilon,t) \quad . \tag{4.2}$$

The test function, and all of its derivatives, are assumed to be well behaved throughout the range of integration and to also have the property of going to zero as their arguments go to infinity. With this in mind it is possible to expand the test function, which occurs in the first set of integrals, in a Taylor series around the point $\epsilon'=e$, i.e.

$$\tau(\varepsilon') = \sum_{k=0}^{\infty} \frac{1}{k!} \tau^{(k)}(\varepsilon) \, (\varepsilon' - \varepsilon)^k \quad . \tag{4.3}$$

The substitution of this expression into the first set of integrals on the RHS of Eq. (4.2) then yields

$$\int_{-1}^{\infty} d\varepsilon \tau(\varepsilon)\rho(\varepsilon)\dot{n}(\varepsilon,t) = \sum_{k=1}^{\infty} \int_{-1}^{\infty} d\varepsilon \tau^{(k)}(\varepsilon) \frac{(-1)^k}{k!} \rho(\varepsilon)\alpha_k(\varepsilon)n(\varepsilon,t) \quad , \tag{4.4}$$

where the moments are defined as

$$\alpha_k(\varepsilon) = \int_{-1}^{\infty} d\varepsilon' \rho(\varepsilon')(\varepsilon'-\varepsilon)^k W(\varepsilon',\varepsilon) \quad . \tag{4.5}$$

A series of integration by parts then gives

$$\int_{-1}^{\infty} d\varepsilon \tau(\varepsilon)\rho(\varepsilon)\dot{n}(\varepsilon,t) = \int_{-1}^{\infty} d\varepsilon \tau(\varepsilon)\left\{\sum_{k=1}^{\infty} \frac{(-1)^k}{k!}\frac{\partial^k}{\partial\varepsilon^k}\left[\rho(\varepsilon)\alpha_k(\varepsilon)n(\varepsilon,t)\right]\right\}$$

$$-\left\{\sum_{k=0}^{\infty}\tau^{(m)}(\varepsilon)\sum_{k=m+1}^{\infty}\frac{(-1)^k}{k!}\left(\frac{\partial}{\partial\varepsilon}\right)^{k-m-1}\left[\rho(\varepsilon)\alpha_k(\varepsilon)n(\varepsilon,t)\right]\right\}_{\varepsilon=-1} \quad . \tag{4.6}$$

Since a result independent of the test function is desired it is necessary to require that the sums over the index k, in the second term of the RHS of Eq. (4.6), must vanish for each value of m. The moments must therefore satisfy the following auxiliary conditions at the bottom of the potential well ($\epsilon = -1$),

$$\sum_{k=m+1}^{\infty}\frac{(-1)^k}{k!}\left(\frac{\partial}{\partial\varepsilon}\right)^{k+m-1}\left(\rho(\varepsilon)\alpha_k(\varepsilon)n(\varepsilon,t)\right)_{\varepsilon=-1} = 0 \quad , \tag{4.7}$$

for each value of m. Any approximate form of the moments must also abide by the restrictions of Eq. (4.7). A similar situation has been considered by van Kampen and Oppenheim[144].

With the terms at the well bottom now eliminated it is possible to use the following standard argument. Since the test function is arbitrary the integrands of the LHS and RHS of Eq. (4.6) must be equal, i.e.

$$\rho(\varepsilon)\dot{n}(\varepsilon,t) = \sum_{k=1}^{\infty}\frac{(-1)^k}{k!}\frac{\partial^k}{\partial\varepsilon^k}\left[\rho(\varepsilon)\alpha_k(\varepsilon)n(\varepsilon,t)\right] \quad . \tag{4.8}$$

The master equation (4.1) has been converted into an infinite series of differential operators. This is the standard result of a Kramers-Moyal expansion, except that in this case the moments occurring in the expansion are subject to the auxiliary conditions (4.7).

Typically, one then proceeds in the derivation of a Fokker-Planck equation by simply truncating the infinite series (4.8) at the k=2 term. It has been argued by van Kampen[141-143] that this step is not justified unless the moments can be made to depend inversely on a dimensionless large parameter characteristic of the system under study. Futhermore, this inverse dependence must obey a power law with the power given by the index of the moment so that the higher order moments contribute little.

It is not possible to know, a priori, what this large parameter should be; it will vary with each problem. Instead, one must appeal to one's physical insight to make an educated guess. Sometimes the choice is obvious, such as the ratio of the of the mass of a heavy Brownian particle and the mass of the lighter bath particle in the case of Brownian motion. Oftentimes, however, one must examine the structure of the transition rates for clues.

For the case under study here, there are two possible candidates. One is the ratio of the potential well depth to the thermal energy of the adparticles and the other is the dimensionless parameter σ_o. The former option is acceptable only at low temperatures. The latter, however, is independent of temperature and is proportional to the size of the system. An examination of the transition rates in App. C reveals that the rates decay exponentially with the parameter σ_o via the gamma functions. This can be seen quite dramatically in Figs. 6 and 7 . For systems with a large number of bound states it appears that σ_o is the best choice. Because the transition rates decay exponentially with σ_o it seems possible that it might also be a suitable large parameter for gas-solid systems with only a few bound states.

Regarding σ_o as the required large parameter, the first two moments may be calculated (See App. D.) and are

$$\alpha_1(\varepsilon) = \frac{5\eta k_B T}{U_o \sqrt{-\varepsilon}} \left[\frac{1}{1+\varepsilon} - \frac{\tanh^{-1}(\sqrt{-\varepsilon})}{\sqrt{-\varepsilon}} \right] F_6\left(\tanh^{-1}(\sqrt{-\varepsilon})/\sqrt{-\varepsilon}\right)$$

$$-2\eta\sqrt{-\varepsilon}\; F_5\left(\tanh^{-1}(\sqrt{-\varepsilon})/\sqrt{-\varepsilon}\right) + O(\sigma_o^{-6}) \;, \qquad (4.9)$$

and

$$\alpha_2(\varepsilon) = \frac{4\eta k_B T}{U_o}\sqrt{-\varepsilon}\; F_5\left(\tanh^{-1}(\sqrt{-\varepsilon})/\sqrt{-\varepsilon}\right) + O(\sigma_o^{-6}) \;, \tag{4.10}$$

where

$$F_n(s) = s^{-n}\left\{1 - \exp\left(-\sigma_o\hbar\omega_D s/U_o\right)\sum_{k=0}^{n-1}\frac{s^k}{k!}\left(\frac{\sigma_o\hbar\omega_D}{U_o}\right)^k\right\} , \tag{4.11}$$

and

$$\eta = 36\,\pi\omega_D\,\frac{m}{M}\left(\frac{U_o}{\hbar\omega_D\sigma_o}\right)^4 \tag{4.12}$$

In Eq. (4.12) M is the mass of a constituent particle (unit cell) of the solid. As seen in the second chapter, η is the friction coefficient. It must be noted that $\eta \sim \sigma_*^{-4}$ and hence α_1 and α_2 are of the order σ_*^{-4}. All higher order moments are of the order σ_*^{-6} and hence are much smaller than the first two moments. It may then be concluded that the parameter σ_* is indeed the large parameter required by van Kampen for the truncation of the Kramers-Moyal expansion.

It has been shown by Pawula[145] that if the Kramers-Moyal expansion is truncated it must be done so at either the k=1 or k=2 term. If this is not done then the positivity of the adparticle disribution function cannot be guaranteed. The truncation of the Kramers-Moyal expansion at the k=2 term is equivalent to keeping only terms of the order σ_*^{-4}. Thus, only the leading order terms of the two moments are required. To keep higher order terms of the moments, or to use the exact expression for the moments would be improper. These approximate moments must still satisfy the auxiliary conditions.

Because only the k=1,2 terms in the Krames-Moyal expansion are kept, only the first two auxiliary conditions remain, namely

$$\frac{1}{2}\left[\frac{\partial}{\partial\varepsilon}\left(\rho(\varepsilon)\alpha_2(\varepsilon)n(\varepsilon,t)\right)\right]_{\varepsilon=-1} = \left[\rho(\varepsilon)\alpha_1(\varepsilon)n(\varepsilon,t)\right]_{\varepsilon=-1} , \tag{4.13}$$

and

$$\frac{1}{2}\left[\rho(\varepsilon)\alpha_2(\varepsilon)n(\varepsilon,t)\right]_{\varepsilon=-1} = 0 . \tag{4.14}$$

Through a bit of elementary calculus and algebra it may be shown that, up to the order σ_*^{-4}, the moments satisfy the following relation

$$\rho(\varepsilon)\alpha_1(\varepsilon) = -\frac{U_o}{2k_BT}\rho(\varepsilon)\alpha_2(\varepsilon) + \frac{1}{2}\frac{\partial}{\partial\varepsilon}\left(\rho(\varepsilon)\alpha_2(\varepsilon)\right) . \tag{4.15}$$

Through the use of Eq. (4.15), the auxiliary condition (4.13) may then be written as

$$\left[\frac{1}{2}\rho(\varepsilon)\alpha_2(\varepsilon)\left(\frac{\partial n(\varepsilon,t)}{\partial\varepsilon} + \frac{U_o}{k_BT}n(\varepsilon,t)\right)\right]_{\varepsilon=-1} = 0 . \tag{4.16}$$

A reexamination of Eq. (4.10) will show that, up to the order σ_*^{-4}, the second moment is equal to zero at the well bottom. The approximate expressions for the moments therefore satisfy the auxiliary conditions provided the distribution function n(e,t) and its derivative are finite at the well bottom. With the auxiliary conditions satisfied the derivation may proceed.

Inserting Eqs. (4.9) and (4.10) into Eq. (4.8) and keeping terms up to the order σ_*^{-4} finally yields the phonon cascade Fokker-Planck equation,

$$\dot{n}(\varepsilon,t) = 2\eta\sqrt{-\varepsilon}\,\frac{\partial}{\partial\varepsilon}\left\{F_5\left(\tanh^{-1}(\sqrt{-\varepsilon})/\sqrt{-\varepsilon}\right)\left[\frac{k_BT}{U_o}\frac{\partial n(\varepsilon,t)}{\partial\varepsilon} + n(\varepsilon,t)\right]\right\} , \tag{4.17}$$

where Eqs. (4.15) and (4.10) have been used. Note that as the number of bound states goes to infinity Eq. (4.17) becomes an exact result.

By making the variable change

$$y^2 = -\varepsilon \tag{4.18}$$

Eq. (4.17) may be transformed into

$$\dot{n}(y,t) = \eta \frac{\partial}{\partial y}\left\{ F_5\left(\tanh^{-1}(y)/y\right) \left[\frac{k_B T}{2U_o} \frac{1}{y} \frac{\partial n(y,t)}{\partial y} - n(y,t)\right]\right\} . \tag{4.19}$$

It will be seen later that the auxiliary condition (4.16) is equivalent to requiring that the adparticle current in energy space be zero at the bottom of the potential well. Hence, the potential well bottom may be regarded as a perfectly reflecting boundary.

As it stands now, the Fokker-Planck equations, (4.17) and (4.19), are not analytic at the well bottom due to the presence of the function $\tanh^{-1}(y)$ in the function F_5. This unphysical feature is an artifact of the approximations used to evaluate the moments (See App. D.). To dispose of this spurious result the function F_5 is approximated as follows.

First, the exponential terms (See Eq. (4.11)) are replaced by a constant equal to their value at the well top ($y=0$). The remaining terms are then expanded in a Taylor series around $y=0$. Keeping only the first few terms in the series yields

$$F_5 = \left(\tanh^{-1}(y)/y\right) \approx F_5(1)\left(1-y^2\right)\left(1- \frac{2}{3}y^2\right) . \tag{4.20}$$

Note that because the approximate expression for F_5, Eq. (4.20), is equal to zero at the well bottom ($y=1$) the auxiliary conditions are still satisfied.

The substitution of (4.20) into (4.19) gives

$$\dot{n}(y,t) = \eta F_5(1) \frac{\partial}{\partial y}\left\{ \left(1-y^2\right)\left(1- \frac{2}{3}y^2\right) \left[\frac{k_B T}{2U_0} \frac{1}{y} \frac{\partial n(y,t)}{\partial t} - n(y,t)\right]\right\} . \tag{4.21}$$

The phonon cascade Fokker-Planck equation is now analytic throughout the range of interest and hence is amenable to the standard mathematical techniques used to study partial differential equations[146-147]. Before embarking on a discussion of the properties of Eq. (4.21),

the connection between the phonon cascade Fokker-Planck equation and the low friction version of Kramers' equation (1.15) will be presented.

4.2 Connection with the Kramers Equation

As mentioned in section 1.4, one of the most commonly used equations for studying kinetic processes is the Kramers equation, whose one dimensional form is

$$\dot{n}(z,p,t) = \frac{\partial U(z)}{\partial Z}\frac{\partial n}{\partial p} - \frac{p}{m}\frac{\partial n}{\partial Z} + \eta \frac{\partial}{\partial p}\left[pn + mk_B T \frac{\partial n}{\partial p}\right], \qquad (4.22)$$

where $n=n(z,p,t)$, and p is the momentum of the particle. Kramers derived this equation by assuming that the particle trapped in the potential $U(z)$ was coupled to a thermal bath at temperature T and hence could be regarded as executing Brownian motion in phase space. Usually Eq.(4.22) is used to calculate the rate of escape of the particle from the potential well. The escape rate typically follows the Frenkel-Arrhenius law for thermally activated processes.

Originally developed to study the kinetics of chemical reaction rates, the Kramers equation has since found application in a number of other fields of which physisorption is one. For studying physisorption the low friction version of Kramers' equation has been of the most use. To derive this version of his equation, Kramers argued that for many successive oscillations the particle orbits in phase space are within the thermal fluctuations in z and p of each other. Therefore, for all practical purposes, the particle orbits can assumed to be closed. In otherwords, the particle losses very little energy to the frictional force. This assumption allowed Kramers to average Eq. (4.22) over an orbit in phase space to obtain an equation which can formally be expressed in terms of action and angle variables. These variables, and hence the equation itself, can be determined only after the potential $U(z)$ has been specified. For a Morse potential the low friction Kramers equation is

$$\dot{n}(y,t) = \eta \frac{\partial}{\partial y}\left\{(1-y)\left[\frac{k_B T}{2U_o}\frac{1}{y}\frac{\partial n(y,t)}{\partial y} - n(y,t)\right]\right\} \qquad (4.23)$$

and is valid only when the low friction condition

$$n < \frac{2\gamma k_B T}{\sqrt{2mU_o}} \tag{4.24}$$

is satisfied.

It should be noted that Eq. (4.23) may not be correct for the energy states near the top of the potential i.e. near $y=0$. In this region, the time of oscillation of a classial particle becomes arbitrarily large so that, no matter how weakly the particle and thermal bath are coupled, the frictional force will cause the particle's trajectory in phase space to deviate from the desired closed orbit within a few oscillations. With the idea of closed orbits no longer meaningful in this region, Kramers' derivation breaks down.

It is of considerable interest to determine under what conditions the low friction Kramers equation can be obtained from the phonon cascade Fokker-Planck equation. In so doing information concerning the passage from the quantum to the classical domain will be obtained.

To show the connection between the Kramers and Fokker-Planck equations it is necessary to approximate F_s in a different manner. The function F_s is approximately linear throughout most of the potential well. Only in the region near the top of the potential well ($y=0$) does the linear character of F_s change. It therefore seems plausible to approximate the function as a straight line. Because F_s obviously deviates from linearity near the well top ($y=0$), there is then some question as to what the numerical value of the slope should be. Since the following discussion will concentrate on the qualitative aspects of performing such an approximation rather than the quantitative details, the slope of the line will be set equal to -1 for the ease of discussion. Hence, the following approximation is made

$$F_s\left(\tanh^{-1}(y)/y\right) \approx \left(1-y\right) . \tag{4.25}$$

When the above approximation is inserted into Eq. (4.19) the low friction case of the Kramers equation (4.23) results.

The approximation used above is a reasonable one when y is not too close to zero and when

$$\sigma_o \hbar\omega_D >> U_o \qquad (4.26)$$

The latter condition is equivalent to requiring that the time scale of the phonon bath is much faster than that of the adparticle motion. Although Eq. (4.26) was derived as a restriction on the friction coefficient, it may also be taken as a condition on the allowed values of the temperature. As such, it defines the high temperature regime in which the low friction Kramers equation is valid. It should be noted that the Fokker-Planck equation has no such temperature restriction.

For values of y close to zero Eq. (4.25) is a poor approximation; it cannot even qualitatively reproduce F_s in this region. This failure indicates that the low friction Kramers equation is indeed not valid for the higher energy states of the Morse potential. Therefore, the low friction Kramers equation for a Morse potential can accurately only describe the kinetics of the adparticles deeply bound in the surface potential.

With the coincidence of the Fokker-Planck and Kramers equation shown the parameter η may safely be identified as the friction coefficient. Hence Eq. (4.12) defines the friction coefficient, a macroscopic quantity, in terms of the microscopic parameters of the gas-solid system. This is an important result because the friction coefficient governs the equilibration process of the adsorbate, i.e. it determines the time scale on which fluctuations in the energy of the adsorbate decay.

The expression (4.12) is, up to a factor 9π, the same as the expression (1.14) obtained by Caroli *et al.*[119] from their microscopic model of physisorption based on classical mechanics. The discrepency of a constant factor between the two results is suspected to be due to the approximations used by Caroli *et al.* in their calculation. More specifically, their result

is valid only to the lowest order of the mass ratio (M/m), with m much greater than M, whereas the phonon cascade result is valid to the lowest order in σ_o^{-1} independent of the mass ratio and consistent with the large parameter expansion of van Kampen. The use of the mass ratio as an expansion parameter is dictated by the implicit use of linear response theory in the derivation of the Kramers equation. Since the derivation of the Kramers equation[73] requires that the mass ratio be small in order to linearize the microscopic equations of motion, this implies that the discrepency noted above is due to the use of linear response theory. Further study is needed before a definitive statement can be made but this result raises serious questions concerning the validity of linear response theory; van Kampen[141] has critisized linear response theory on the grounds that the linearization of the equations of motion at the microscopic level is valid for times in the transient regime but not for times in the kinetic regime. In seems from the considerations above that the use of linear response theory forces the use of an expansion parameter which may yield poor approximations. It is nonetheless heartening to find that the dependence of the friction coefficient on the parameters of the gas-solid system is the same in both the classical and quantum mechanical approaches.

The friction coefficient has also been calculated by d'Agliano *et al.*[72]. By comparing the results of Pagni and Keck's work[115] on the soft cube model with the Kramers equation, they were able to estimate, to the lowest order in the mass ratio m/M where M is much greater than m, the following estimate for the friction coefficient

$$\eta = 16 \frac{m}{M} \frac{U_o}{\hbar\sigma_o} \tag{4.27}$$

This expression differs from the phonon cascade result by a factor of $9\pi^5 U_o^3/2(\hbar\sigma_o\omega_D)^3$, which, by virtue of Eq. (4.26) is small. This then indicates that the linear response result (4.27) is much larger than either the phonon cascade result (4.12) or the classical result (1.14). This large discrepency is in part due to the absence of the characteristic frequency of the solid (The Debye frequency for instance.) in the expression. One might expect this on the grounds that in the limit of a very light adparticle the solid lattice might appear to be

essentially rigid.

In summary, the Kramers equation may be obtained from the phonon cascade Fokker-Planck equation when: the surface potential has a large number of bound states, the time scale of the phonon reservoir is much faster than the time scale of the adparticles, and the gas-solid system is at a high temperature (See Eq. (4.24).). When these conditions are not satisfied the phonon cascade Fokker-Planck equation must take precedence. Also, since the transition rates used to obtain the phonon cascade Fokker-Planck equation only involve one phonon processes, it may be concluded that it is not necessary to have a multitude of coherent quantum processes to pass from the quantum to the classical realm: a series of incoherent one quantum processes will suffice.

4.3 Properties of the Phonon Cascade Fokker-Planck Equation

Perhaps the single most important property of the phonon cascade Fokker-Planck equation, in all of its forms, is that it has the Boltzmann distribution as its equilibrium solution. Because the master equation (4.1) has this property it would be very suspicious if the Fokker-Planck equation did not. For the discussion that follows it is convenient to make use of this property and define a reduced distribution function in the following manner,

$$g(y,\tau) = n(y,t)\, e^{-y^2 \beta U_o}, \tag{4.28}$$

where the dimensionless time

$$\tau = \frac{\eta F_5(1) k_B T}{2U_o}\, t \tag{4.29}$$

has been introduced. It is readily seen that if the adsorbate is in its equilibrium state, i.e. the Boltzmann distribution, then the reduced distribution function equals unity up to a normalization factor. Deviations of $g(y,\tau)$ from unity indicate deviations from equilibrium. In the remainder of this work $g(y,\tau)$ will often be referred to as the distribution function.

The insertion of Eq. (4.28) into Eq.(4.21) converts the Fokker-Planck equation into

$$e^{y^2\beta U_o}\frac{\partial g(y,\tau)}{\partial \tau} = \frac{\partial}{\partial y}\left\{\left(1-y^2\right)\left(1-\frac{2}{3}y^2\right)\frac{e^{y^2\beta U_o}}{y}\frac{\partial g(y,\tau)}{\partial y}\right\} . \qquad (4.30)$$

This equation is clearly amenable to the separation of variables technique. Bearing in mind that the distribution function must decay in time, Eq. (4.30) therefore has a solution of the form

$$g(y,\tau) = \sum_{n=0}^{\infty} a_n e^{-\lambda_n \tau} g_n(y) \qquad (4.31)$$

where the eigenfunctions $g_n(y)$ and their associated eigenvalues λ_n satisfy

$$\frac{\partial}{\partial y}\left\{\left(1-y^2\right)\left(1-\frac{2}{3}y^2\right)\frac{e^{y^2\beta U_o}}{y}\frac{\partial g(y)}{\partial y}\right\} = \lambda_n e^{y^2\beta U_o} g_n(y) = 0 . \qquad (4.32)$$

The solution of Eq. (4.32), subject to a set of homogeneous boundary conditions, constitutes a Sturm-Liouville problem[146-147]. With the exception of the Lamé equation[147], which has four singular points, the solvable differential equations of the Sturm-Liouville type which lead to the special functions of mathematical physics never have more than three singular points. The equation above has five regular singularities ($y=0,\pm 1,\pm 3/2$) and an irregular singularity at infinity. Therefore, an exact solution of Eq. (4.32), and hence Eq. (4.30), seems impossible. Fortunately, the range of physical interest, $0=y=1$, has regular singular points only at the boundary points so that the general properties of Sturm-Liouville theory may still be used.

The eigenfunctions, which are solutions of Eq. (4.30), form a complete orthogonal

set with respect to their weight function, $\exp(y^2U_o/k_BT)$, i.e.

$$\frac{\int_0^1 dy g_n(y)g_m(y)e^{y^2\beta U_o}}{\int_0^1 dy\,[g_n(y)]^2\,e^{y^2\beta U_o}} = \delta_{nm} \tag{4.33}$$

Their associated eigenvalues form an ordered sequence, λ_0, λ_1, λ_2,...,etc. . For the desorption process, which is actually specified through the boundary conditions, the lowest eigenvalue, which is positive definite, is identified as the desorption rate. All higher order eigenvalues describe the transient evolution of the distribution function. In the long time limit these transient effects may be ignored and the solution to the Fokker-Planck equation may be approximated as follows,

$$g(y,\tau) \approx a_o g_o(y) e^{-\lambda_o \tau} . \tag{4.34}$$

The expansion coefficient a_0 may be determined only when the initial condition is specified.

The approximate solution to the Fokker-Planck equation (4.30) can therefore be expressed entirely in terms of the smallest eigenfunction and its associated eigenvalue. These quantities must be determined in an approximate fashion. Sturm-Liouville theory does provide a variational method for determining the smallest eigenvalue, but this proceedure requires that the general form of the eigenfunction be known. There are other methods for obtaining an approximate expression for the eigenfunction but they, as well as the variational method, require that the boundary conditions be specified. The required boundary conditions will be derived in the next chapter.

5. Boundary Conditions for Ideal Desorption

By itself the phonon casacde Fokker-Planck equation contains no information about the desorption process: it can describe the kinetics of adparticles inside the potential well but it makes no statements about how the adparticles leave the potential. Information about whether particles are desorbing or adsorbing and the manner in which they do so is contained in the boundary conditions which the solutions (the adparticle distribution function) of the Fokker-Planck equation must satisfy. Hence, to calculate the ideal desorption time and determine the corresponding distribution function from the phonon cascade Fokker-Planck equation the boundary conditions for the reduced adparticle distribution function must be known. The boundary conditions in energy space, at both the potential well top and bottom, must be specified, as well as the temporal boundary conditions, i.e. the initial condition and the long time behaviour.

When an integral equation is converted to a differential equation it will also yield boundary conditions to go along with it. Some of the boundary conditions for ideal desorption must then be extracted from the master equation appropriate for ideal desorption. Before deriving these conditions it is worthwhile to physically describe the process of ideal desorption once again.

At the start of the process of ideal desorption the continuum states and the adsorbate states are assumed to be in thermal equilibrium so that their relative occupancies obey the Boltzmann distribution. Now imagine that the gas phase is instantaneously emptied and remains that way for the duration of the process. This means that as soon as an adparticle desorbs it is removed from the system. The adsorbate, which was in an equilibrium state, starts to empty into the continuum states. Once an adparticle desorbs it can never return because the continuum to bound state transitions have been suppressed and it is immediately swept out of the system. Having started in equilibrium the adsorbate distribution function evolves into a form which is characteristic of the desorption process (Because the gas phase is always empty and the adsorbate is not, there is a possibility of their being a discontinuity in the distribution function at the top of the potential well.) As time proceeds to infinity this

distribution exponentially decays according to the ideal desorption rate.

5.1 Temporal Boundary Conditions

From the preceeding discussion it is obvious that the solution to the Fokker-Planck equation must go to zero as time goes to infinity. This feature has already been incorporated into the general form of the solution (See Eq. (4.31)).

Since the adsorbate starts from an equilibrium distribution, the reduced distribution function must satisfy the following initial condition,

$$g(y,\tau=0) = 1 \ . \tag{5.1}$$

From this condition the expansion coefficient a_o occuring in the approximate solution (4.34) can be determined as follows.

Imposing (5.1) on the expression (4.31) yields

$$\sum_{n=0}^{\infty} a_n g_n(y) = 1 \tag{5.2}$$

By employing the orthogonality of the g(y) one readily obtains

$$a_o = \frac{\int_0^1 dy \, [g_o(y)]^2 \, e^{y^2 \beta U_o}}{\int_0^1 dy g_o(y) \, e^{y^2 \beta U_o}} \tag{5.3}$$

so that the approximate solution of the Fokker-Planck equation, (4.30), becomes

$$g(y,\tau) \approx \frac{\int_0^1 dx \, [g_o(x)]^2 \, e^{y^2 \beta U_o}}{\int_0^1 dx g_o(x) \, e^{y^2 \beta U_o}} g_o(y) \, e^{-\lambda_o \tau} \ . \tag{5.4}$$

5.2 Use of the Auxiliary Conditions

In deriving the Fokker-Planck equation it was found that a pair of auxiliary conditions, Eqs. (4.13) and (4.14)), had to be satisfied to ensure that the presence of the potential well bottom did not affect the validity of the Fokker-Planck equation. In physical terms these conditions required that the adparticle current must be zero at the bottom of the potential well (See Eq. (4.16)). These conditions were found to be always satisfied as long as the distribution function and its derivative were finite at the bottom of the potential well. These conditions will serve as boundary conditions on the reduced adparticle distribution function at the bottom of the potential ($y=1$). Boundary conditions such as these serve to eliminate unphysical solutions which diverge.

5.3 The Radiative Boundary Condition

The boundary condition at the top of the potential well contains the most information about the desorption process itself and must be derived from the continuous master equation appropriate for ideal desorption, i.e.

$$\frac{\partial n(\varepsilon,t)}{\partial t} = \int_{-1}^{0} d\varepsilon'\rho(\varepsilon')W(\varepsilon,\varepsilon')n(\varepsilon',t) - \int_{-1}^{0} d\varepsilon'\rho(\varepsilon')W(\varepsilon',\varepsilon)n(\varepsilon,t)$$

$$- \int_{0}^{\infty} d\varepsilon'\rho(\varepsilon')W(\varepsilon',\varepsilon)n(\varepsilon,t) \quad . \tag{5.5}$$

Note that the continuum to bound state transitions have been suppressed. It is more convenient to work with the reduced adparticle distribution function which, in energy space, is defined as

$$f(\varepsilon,t) = n(\varepsilon,t)\, e^{\varepsilon\beta U_o} \tag{5.6}$$

where T is either the solid temperature T_s, or the gas temperature T_g, depending on whether ε

is negative or positive respectively. The substitution of the distribution (5.6) into Eqs. (5.5) and (4.17) yields

$$e^{-\varepsilon\beta U_o}\frac{\partial f(\varepsilon,t)}{\partial t} = \int_{-1}^{0} d\varepsilon'\rho(\varepsilon')W(\varepsilon,\varepsilon')\, e^{-\varepsilon'\beta U_o}\left[f(\varepsilon',t) - f(\varepsilon,t)\right]$$

$$-\int_{0}^{\infty} d\varepsilon'\rho(\varepsilon')W(\varepsilon',\varepsilon)\, e^{-\varepsilon\beta U_o} f(\varepsilon,t)\ , \tag{5.7}$$

and

$$e^{-\varepsilon\beta U_o}\frac{\partial f(\varepsilon,t)}{\partial t} =$$

$$\sqrt{-\varepsilon}\,\frac{2\eta}{\beta U_o}\frac{\partial}{\partial\varepsilon}\left\{F_5\left(\tanh^{-1}(\sqrt{-\varepsilon})/\sqrt{-\varepsilon}\right)\, e^{-\varepsilon\beta U_o}\frac{\partial f(\varepsilon,t)}{\partial\varepsilon}\right\}, \tag{5.8}$$

respectively.

The terms inside the curly brackets of Eq. (5.8) can be identified as the adparticle current in energy space.

Following Keck[149], the boundary condition at the top of the potential well ($\epsilon=0$) is derived by equating the adparticle current at the potential well top, as determined from Eq. (5.8), to the current calculated directly from the master equation (5.7). This is accomplished by multiplying Eqs. (5.7) and (5.8) by $\rho(\epsilon)$, integrating each equation with respect to the variable ϵ over the range -1 to 0, and then equating the results. This then yields the following equation

$$\frac{\eta\sigma_o}{\beta U_o}F_5(1)\left[\frac{\partial f(\varepsilon)}{\partial\varepsilon}\right]_{\varepsilon=0} = -\int_{-1}^{0} d\varepsilon\rho(\varepsilon)\int_{0}^{\infty} d\varepsilon'\rho(\varepsilon')W(\varepsilon',\varepsilon)\, e^{-\varepsilon'\beta U_o} f(\varepsilon')\ , \tag{5.9}$$

where the time argument has been omitted for convenience.

Since the transition rates are sharply peaked near $\epsilon = \epsilon'$ the double integral on the RHS of Eq. (5.9) will receive its main contribution from the region near $\epsilon = \epsilon' = 0$. It is therefore possible to expand $f(\epsilon)$ in a Taylor series, for ϵ less than zero around the point $\epsilon = 0$. In the case of ideal desorption $f(\epsilon) = 0$ for positive energies so that unless the distribution function goes to zero as the energy approaches zero from the negative side there will be a discontinuity in $f(\epsilon)$ at $\epsilon = 0$. Hence, the value of $f(0)$ is set as the average of the limiting values of $f(\epsilon)$ as ϵ approaches zero from both the positive and negative sides. The Taylor series is then

$$f(\varepsilon') = \frac{1}{2} f(0^-) + \varepsilon' \left[\frac{\partial f(\varepsilon)}{\partial \varepsilon}\right]_{\varepsilon=0^-} + \frac{(\varepsilon')^2}{2} \left[\frac{\partial^2 f(\varepsilon)}{\partial \varepsilon^2}\right]_{\varepsilon=0^-} + \cdots \qquad (5.10)$$

for ϵ' less than or equal to zero. The substitution of (5.10) into the RHS of (5.9) yields,

$$\frac{\sigma_o \eta}{\beta U_o} F_5(1) \left[\frac{\partial f(\varepsilon)}{\partial \varepsilon}\right]_{\varepsilon=0^-} =$$

$$- \frac{f(0^-)}{2} \int_{-1}^{0} d\varepsilon' \rho(\varepsilon') \int_{0}^{\infty} d\varepsilon \rho(\varepsilon) W(\varepsilon, \varepsilon') \, e^{-\varepsilon' \beta U_o}$$

$$- \left[\frac{\partial f(\varepsilon)}{\partial \varepsilon}\right]_{\varepsilon=0^-} \int_{-1}^{0} d\varepsilon' \rho(\varepsilon') \int_{0}^{\infty} d\varepsilon \rho(\varepsilon) W(\varepsilon, \varepsilon') \varepsilon' \, e^{-\varepsilon' \beta U_o}. \qquad (5.11)$$

The integrals occurring in Eq. (5.11) are evaluated in Appendix D. After evaluating the above integrals and keeping only the lowest powers of σ_o^{-1}, in accordance with van Kampen's large parameter expansion[141-143], one obtains the radiative boundary condition

$$\left.\frac{\partial f}{\partial \varepsilon}\right|_{\varepsilon=0} = - \frac{\sigma_o}{4} \frac{F_4(1)}{F_5(1)} f(0) \, , \qquad (5.12)$$

or,

$$\left[\frac{1}{y}\frac{\partial g}{\partial y}\right]_{y=0} = \frac{\sigma_o}{2}\frac{F_4(1)}{F_5(1)}\,g(0)\ , \tag{5.13}$$

when written in terms of the function $g(y,\tau)$. Equation (5.12) has been checked for a Xe/W system and is in good agreement with with numerical results obtained directly from the discrete master equation (1.3).

In the limit given by Eq. (4.30), the equations (5.12) and (5.13) reduce to

$$\frac{\partial f}{\partial \varepsilon}\bigg|_{\varepsilon=0} = -\frac{\sigma_o}{4}\,f(0)\ , \tag{5.14}$$

and

$$\left[\frac{1}{y}\frac{\partial g}{\partial y}\right]_{y=0} = +\frac{\sigma_o}{2}\,g(0)\ , \tag{5.15}$$

respectively.

As σ_o goes to infinity the classical limit is reached and the radiative boundary condition reduces to the case of a purely absorbing boundary, i.e.

$$f(0) = g(0) = 0 \tag{5.16}$$

provided the derivatives in (5.15) remain finite. This is the boundary condition which is usually assumed when one attempts to extract a desorption rate from the Kramers equation. It is now apparent that if absorbing boundary conditions are used the resulting desorption rate will be valid only in the classical regime.

It is interesting to note that the radiative boundary condition, (5.12) and (5.13), is independent of temperature. This is not the case for the radiative boundary condition derived by Keck[149] and susequently used by Pagni and Keck[115-116] in their version of the soft cube

model for physisorption.

If Keck's general expression for the radiative boundary condition is used for the phonon cascade model then the boundary condition becomes

$$\frac{\partial f}{\partial \varepsilon}\Big|_{\varepsilon=0} \approx \frac{U_o}{k_B T} f(0) \qquad (5.17)$$

This relation implies that as the temperature decreases the deviations from equilibrium increase when in fact the opposite must be true. The discrepency between Eqs. (5.14) and (5.17) can be traced back to Keck's assumption that the function $R(\epsilon,\epsilon')=W(\epsilon,\epsilon')\exp(-\epsilon' U_o/k_B T)$ can be expanded as a Taylor series in $\bar{\epsilon}=(\epsilon+\epsilon')/2$. In the phonon cascade model $R(\epsilon,\epsilon')$ contains a factor $\exp(-\bar{\epsilon} U_o/k_B T)$ which, for low temperatures, cannot safely be approximated by the first two terms of a Taylor series. See Ref. 31 for further comments on the comparison of Pagni and Keck's approach to physisorption and the phonon cascade model.

It should be emphasized that Eqs. (5.12-15) have been derived within the framework of van Kampen's large parameter expansion. Only boundary conditions derived within this framework can be consistent with the phonon cascade Fokker-Planck equation.

6. Ideal Desorption Rate and Distribution Function

Now that the boundary conditions for ideal desorption have been specified it is possible to derive analytic expressions for the ideal desorption rate and distrbution function from the phonon cascade Fokker-Planck equation. As discussed in section 4.3, an exact solution of the Fokker-Planck equation does not seem possible. Hence, approximate analytic expressions must suffice. Because approximate expressions for the desorption rate and the distribution function will be obtained care must be taken to ensure that these expressions are obtained in a self consistent manner.

An immediate consequence of the radiative boundary condition is that $\lambda=0$ is not an acceptable eigenvalue for the ideal desorption process because its associated function, $g(y)=1$, does not satisfy Eq. (5.13). Therefore, the smallest contributing eigenvalue will be positive definite and proportional to the ideal desorption rate, i.e.

$$\lambda_o = \frac{2U_o}{\eta k_B T \; F_5(1)} \; t_d^{-1} \quad , \tag{6.1}$$

provided that all the other eigenvalues are much larger than the smallest one, as has been assumed.

It was also mentioned in Section 4.3, that a variational method may be used to determine the smallest eigenvalue and its corresponding eigenfunction. This proceedure works, however, only when one has some idea of the general form of the eigenfunction. For this reason a method based on an expansion of the $g_o(y)$ in powers of the λ_o is used first. The resulting expression for g_o provides the basis of a postulated form of the trial eigenfunction to be used in the variational method. Once these expressions are obtained they will be compared to the exact numerical results obtained from the master equation.

6.1 Small Eigenvalue Expansion

A few years ago Zatsepin[122] presented a perturbation technique for extracting the isothermal desorption rate from the Kramers equation (The conditions that Zatsepin assumed for the isothermal desorption process makes it identical to the ideal desorption problem.). This method relies on the eigenvalue λ_0 being very small so that it may be used as an expansion parameter in a functional series expansion of the eigenfunction $g_0(y)$. In the case of the Kramers equation the smallest eigenvalue is approximately

$$\lambda_o \approx (2\beta U_o)^2 e^{-\beta U_o} . \tag{6.2}$$

This indicates that λ_0 is a suitable expansion parameter at low temperatures. The method must fail, however, at higher temperatures where λ_0 is if the order of one. Similarly, this method will work best for gas-solid systems with deep surface potentials. To apply this method to the Fokker-Planck equation one assumes that the eigenfunction $g_0(y)$ may be expanded as a power series in λ_0 as follows,

$$g_o(y) = 1 + \sum_{k=1}^{\infty} \frac{(-\lambda_o)^k}{k!} h_k(y) . \tag{6.3}$$

Because the function $g_0(y)$ is unnormalized it is permissable to require that it equal one at the well bottom ($y=1$). Note that if $\lambda_0=0$ the equilibrium solution is recovered. This feature has been built into the expansion because it is anticipated that near the bottom of the potential well the adsorbate will be very close to the equilibrium distribution throughout the desorption process. Of course this behaviour is not expected near the top of the well.

The functions $h_k(y)$ are determined by inserting (6.3) into Eq. (4.32) and then equating coefficients of equal powers of λ_0. This procedure yields the following recursion

relation,

$$\frac{\partial}{\partial y}\left\{(1-y^2)\left(1-\frac{2}{3}y^2\right)\frac{e^{y^2\beta U_o}}{y}\frac{\partial h_k(y)}{\partial y}\right\} = k h_{k-1}(y)\, e^{y^2\beta U_o} \tag{6.4}$$

where $h_o(y)=1$. This equation may be inverted by integrating twice to arrive at,

$$h_k(y) = k\int_y^1 ds\, \frac{se^{-s\beta U_o}}{(1-s^2)\left(1-\frac{2}{3}s^2\right)}\int_s^1 dr\, h_{k-1}(r)\, e^{r^2\beta U_o}, \tag{6.5}$$

where the condition $g_o(1)=1$, and the requirement that the derivative of $g_o(y)$ be finite at $y=1$, have been used to determine the constants of integration. In terms of the recursion functions these conditions are $h_k(1)=0$, and the requirement that the derivative of the $h_k(y)$ be finite at $y=1$, respectively. Since $h_o(y)=1$ the function $h_1(y)$ is then

$$h_1(y) = \int_y^1 ds\, \frac{se^{-s^2\beta U_o}}{(1-s^2)\left(1-\frac{2}{3}s^2\right)}\int_s^1 dr\, e^{r^2\beta U_o} \tag{6.6}$$

$$\approx (\beta U_o)^{-2}\, e^{(1-y^2)\beta U_o} \tag{6.7}$$

The asymptotic expression for Dawson's integral[150] and the assumption that U_o/k_BT is much larger than one has been used to estimate the the integrals in Eq. (6.6). Note that the approximate form (6.7) violates the condition that $h_1(1)=0$ and so is valid at those temperatures for which $\lambda_o(k_BT/2U_o)^2$ is much less than one so as to ensure that $g_o(1)$ is close to one (See Eq. (6.8) below).

By keeping only the first power of λ_o in Eq. (6.3) the eigenfunction may be written as

$$g_o(y) \approx 1 - \lambda_o h_1(y) . \tag{6.8}$$

By requiring that (6.8) satisfy the radiative boundary condition (5.13) a simple algebraic equation for λ_0 is obtained. The solution of this equation is

$$\lambda_o \simeq \sigma_o F_4(1) \left\{ 2F_5(1) \int_0^1 dr\, e^{r^2\beta U_o} + \sigma_o F_4(1) \int_0^1 ds \frac{se^{-s^2\beta U_o}}{(1-s^2)(1-\frac{2}{3}s^2)} \int_s^1 dr\, e^{r^2\beta U_o} \right\}^{-1} \tag{6.9}$$

$$\simeq \frac{4\sigma_o F_4(1)\,(\beta U_o)^2}{\sigma_o F_4(1) + 4F_5(1)\,\beta U_o} e^{-\beta U_o}, \tag{6.10}$$

where once again the integrals were approximated using the asymptotic expressions for Dawson's integral. The details of this calculation and the one leading to Eq. (6.7) may be found in Appendix E. Therfore the ideal desorption rate (See Eq. (6.1)) is,

$$t_d^{-1} \simeq \frac{2\eta\sigma_o F_4(1) F_5(1) \beta U_o}{\left[\sigma_o F_4(1) + 4F_5(1)\,\beta U_o\right]} e^{-\beta U_o}. \tag{6.11}$$

The ideal desorption rate given above follows the Frenkel-Arrhenius parametrization (See Eq. (1.2)) with $Q=U_0$. The prefactor, however, has a more complicated structure than has previously been encountered. This richer structure allows Eq. (6.11) to interpolate between the low and high temperature regimes; for high temperatures Eq. (6.11) reduces to Eq. (1.12) and for low temperatures it reduces to

$$t_d^{-1} = \frac{1}{2}\eta\sigma_o F_4(1) e^{-\beta U_o}, \tag{6.12}$$

which, except for the factor $F_4(1)$, is the same as Eq. (1.6). The factor $F_4(1)$ will come out of Kreuzer and Teshima's calculation when it is redone with more precision.

It is worth noting that when condition (4.26) holds the factors $F_4(1)$ and $F_5(1)$ are close to unity so that the desorption rate takes on the simple form

$$t_d^{-1} \approx \frac{2\eta\sigma_o\beta U_o}{\left[\sigma_o + 4\beta U_o\right]} e^{-\beta U_o} . \tag{6.13}$$

The reduced distribution function, which, within the approximation (4.34), decays according to the ideal desorption rate, has a time-independent factor of $g(y)=a_0 g_0(y)$. To the lowest order in λ_0 it is

$$g(y) = a_o g_o(y) \approx 1 + \lambda_o \frac{\int_0^1 ds\, h_1(s)\, e^{s^2\beta U_o}}{\int_0^1 ds\, e^{s^2\beta U_o}} - \lambda_o h_1(y) , \tag{6.14}$$

where Eqs. (6.8) and (5.3) have been used. The eigenvalue λ_0 is of course given by Eq. (6.9). After approximating the integrals above, Eq. (6.14) becomes

$$g(y) \approx 1 - \frac{\sigma_o F_4(1)}{\left[\tau_o F_4(1) + 4F_5(1)\, \beta U_o\right]} e^{-y^2\beta U_o} , \tag{6.15}$$

where terms of the order $\exp(-U_o/k_BT)$ have been dropped.

The behaviour of the distribution function, as given by Eq. (6.15), differs in the low and high tempurature regimes. As the tempurature approaches zero the distribution function approaches unity. In other words the adsorbate approaches the equilibrium distribution. This is the temperature regime in which the perturbation theory for the master equation is valid. For high temperatures, Eq. (6.15) reduces to the *ad hoc* ansatz (1.11) previously used to calculate the desorption rate from the Fokker-Planck equation. Again this is consistent with the behaviour of the desorption rate, i.e. Eq. (6.11) reduces to (1.18) in this limit.

It is worth noting that when condition (4.26) holds then the reduced distribution

function (6.15) reduces to

$$g(y) \approx 1 - \frac{\sigma_o e^{-\beta U_o y^2}}{(\sigma_o + 4\beta U_o)} . \tag{6.16}$$

The small eigenvalue method used above may also be used to extract the ideal desorption time and reduced distribution function from the Kramers equation (4.23) with the absorbing boundary condition (5.16). The calculation is almost identical to that done for the Fokker-Planck equation and so only the final results are reported.

The ideal desorption rate and the reduced distribution function may be written in terms of the function

$$h_1(y) = \int_y^1 ds \frac{s}{1-s} e^{-s^2\beta U_o} \int_s^1 dr\, e^{r^2\beta U_o} \tag{6.17}$$

as follows,

$$t_d^{-1} \approx \frac{\eta}{2\beta U_o h_1(o)} \tag{6.18}$$

$$\approx 2\eta\beta U_o e^{-\beta U_o} , \tag{6.19}$$

and

$$g(y) \approx 1 - \frac{h_1(y)}{h_1(o)} \tag{6.20}$$

$$\approx 1 - e^{-y^2\beta U_o} . \tag{6.21}$$

Expressions (6.19) and (6.21) were obtained by once again using the asymptotic expression

for Dawson's integral.

It is readily seen that the expressions for the ideal desorption rate derived via the small eigenvalue expansion (6.19) and Kramers' method (1.12) are identical. The underlying integral expressions, however, are different. The small eigenvalue integral expression, (6.18) with (6.17), is mathematically well defined in contrast to the Kramers integral expression, Eq. (1.17), which is divergent. The classical expression for the desorption rate, Eq. (1.18), now has a solid basis and is definitely larger than the original estimate of Kramers by a factor of two for the case of the Morse potential.

In the small eigenvalue expansion method one assumes that λ_0 is much less than one. This is not necessarily the case at elevated temperatures, even for systems that satisfy condition (4.26). This method nonetheless still provides insight into the general form of the distribution function. This information can be used to develop more accurate methods of dealing with the Fokker-Planck equation. One such method is reported in the next subsection.

6.2 Variational Method

Since the desorption rate is proportional to the lowest eigenvalue, λ_0, it is possible to use a variational method to obtain an estimate of the desorption rate. From the Calculus of Variations it is known that the eigenfunction associated with the smallest eigenvalue minimizes the functional

$$\Lambda[g] = \frac{\int_0^1 dy \ (1-y^2)\left(1-\frac{2}{3}y^2\right) \frac{1}{y}\left[\frac{\partial g}{\partial y}\right]^2 e^{-y^2\beta U_0} + \frac{\sigma_0}{2}\frac{F_4(1)}{F_5(1)}\left[g(0)\right]^2}{\int_0^1 dy\,[g]^2\, e^{-y^2\beta U_0}} \tag{6.22}$$

to the value of the smallest eigenvalue, i.e. $\lambda_0 = \Lambda[g=g_0(y)]$. Bearing in mind the results of the small eigenvalue expansion it seems reasonable to assume that the lowest eigenfunction has the form

$$g(a,b;y) = 1 - ae^{-y^2 b\beta U_0} \tag{6.23}$$

where a and b are parameters. After imposing the radiative boundary condition (5.13) on the trial function g(a,b;y), the parameter c may be eliminated in favour of the parameter a so that (6.23) becomes,

$$g(b;y) = 1 - \frac{\sigma_o F_4(1)\, e^{-b\beta U_o}}{\left(\sigma_o F_4(1) + 4F_5(1)\, b\beta U_o\right)} \quad . \tag{6.24}$$

Already the trial function has taken on much of the same structure as the previously obtained expressions (Eq. (6.8) with Eqs. (6.7) and (6.10). The assumed exponential dependence is necessary because of the presence of a similar factor in the Fokker-Planck equation. The preexponential factor, which is responsible for the crossover between the low and high temperature regimes, originates solely from the radiative boundary condition.

An estimate for λ_o may be obtained by inserting Eq. (6.24) into Eq. (6.22) and then minimizing Λ with respect to b. Unfortunately the resulting equation is only solvable through numerical means. The values of b thus determined can be inserted back into (6.24) to yield an approximate expression for the eigenfunction $g_o(y)$. The desorption distribution is finally obtained when the expressions for the eigenfunction $g_o(y)$ is inserted into Eq. (5.3) to determine a_o.

6.3 Numerical Comparison

To start this section the various expressions for the desorption distribution, Eqs. (6.14) and (6.15) will be compared with the results obtained directly from a diagonalization of the discrete master equation. After this a similar comparison will done for the heat of adsorption and the prefactor occuring in the Frenkel-Arrhenius parametrization of the desorption rate.

In Figs. 8 and 9 the distribution of adparticles within the bound states of the Morse surface potential according to various expressions and temperatures are displayed. The dotted lines are the exact results obtained from the diagonalization of the discrete master equation for desorption, Eq. (1.3). As mentioned on previous occasions, the exact distribution is

greatly depleted from the equilibrium distribution near the top of the potential well (y=0) while an equilibrium distribution is maintained near the bottom of the potential well (y=1). At the top of the potential the distribution has a parabolic character as is required by the radiative boundary condition, Eq. (5.13). By comparing Figs. 8 and 9 it may be seen that as the number of bound states is increased the depletion in the immediate vicinity of the top of the potential also increases, however, the region which suffers the depletion grows smaller. This latter feature is a consequence of the radiative boundary condition (5.13) which requires that as the number of bound states increases so must the parabolic curvature of the distribution. As the temperature inceases the magnitude of the depletion, as well as the extent to which it penetrates into the well, increases. Conversely, as the temperature decreases the adparticle distribution approaches the equilibrium distribution. Only at very high temperatures, 810° K., is the equilibrium at the well bottom disturbed for the Xe/W system. The Ar/Ag system, however, shows disruption of the equilibrium distribution at the well bottom at the much lower temperature of 225° K. This difference arises from two sources. First, the Debye temperature of silver (225° K.) is approximately half of the Debye temperature of tungsten (405° K.), which, when coupled with the fact that the Xe-W surface potential is six times deeper than the Ar/Ag surface potential, reveals that there are, accoring to the Bose-Einstein distribution, a larger number of high energy phonons available for transitions to higher bound states in the Ar/Ag system than there are in the Xe/W system. Secondly, there are three times the number of bound states in the Xe/W system than in the Ar/Ag system. The net effect of these differences is to effectively insulate the distribution of particles in the low lying bound states of the Xe/W system from the influence of the gas phase vacuum until high temperatures are reached.

When these high temperatures are reached the distribution at the bottom of the potential takes on values which are larger than the equilibrium distribution. This somewhat odd behaviour is difficult to interpret physically. It might reflect the relative inefficiency of the bound state to bound state transitions at the bottom of the potential when compared to

scales might lead to an excess of particles in the lower bound states after the transients have died away. One should not interpret this excess as meaning that the adparticles are actually congregating at the bottom of the potential. Once the desorption process starts the number of particles in a given bound state is always less than the number which initially occupied that state.

The dashed and dashed-dotted lines are the results of the integral expressions obtained from the variational and small eigenvalue methods respectively. It is readily seen that they both describe the exact results rather well, except at high temperatures, where the variational method does a better job than the small eigenvalue expansion method. This is especially noticable for the Ar/Ag system. The relatively poor description by the small eigenvalue method at this elevated temperature can be traced to the breakdown of the assumption that the eigenvalue is small: it is in fact larger than one at this temperature. With this in mind, it is amazing that the result is as reasonable as it is. At more moderate temperatures the variational and small eigenvalue methods yield almost identical results. This coincidence is presumably due to the patterning of the variational procedure trial function on the results of the small eigenvalue method. Notice that both of these methods also yield a distribution which exceeds the equilibrium distribution at low temperatures in agreement with the exact theory. Mathematically speaking, this excess is due to the expansion coefficient a_0 exceeding the value of one. Unfortunately this fact sheds little, if any, light on the physical origin of this feature.

In Figs. 10 and 11 the prefactor of the desorption rate and the heat of adsorption, for the exact numerical results and the various integral expressions, are plotted for the Xe/W and Ar/Ag systems. The exact results are again indicated by the dotted lines, while the solid and the dashed-dotted lines display the results of the variational and small eigenvalue methods respectively. Once again there is good agreement between the two approximation techniques and the exact results except in the case of the small eigenvalue method at high temperature.

The results for the prefactor and the heat of adsorption at extremely low temperatures are not shown because they are experimentally inaccessible; the corresponding desorption times

the prefactor levelling off to a constant value in accord with Eq. (6.13).

Perhaps the most interesting feature of these graphs is the correlated decrease in the heat of adsorption and the prefactor as the temperature increases. This degree of correlation is such that for high temperatures the prefactor and the heat of adsorption pass through a minimum at what appears to be the same temperature. For the Xe/W system this minimum would occur around 900°K and is of little experimental interest. The Ar/Ag system, however, passes through its minimum around 225°K which might be experimentally observable. This decrease is on the order of 20 per cent. This is a substantial amount when it is considered that the desorption rate depends exponentially on the heat of adsorption. A decrease in the heat of adsorption yields an increase in the desorption rate but this effect is partially compensated for by the concomitant decrease in the preexponential factor. These results therefore indicate the existance of a compensation effect in the desorption rate. It should be noted that this effect is purely kinetic in origin; it has nothing to do with the any physical changes in the nature of the gas-solid interaction. This effect should therefore be present in any system which exhibits stochastic behaviour similar to Brownian motion.

The systems studied so far both have a large number of bound states. It is interesting to see if the theory developed can give good results for systems with a small number of bound states. In Fig. 12 the scaled desorption rate, for a He/LiF system, is plotted as a function of the inverse temperature. The exact results are denoted by the dotted line, the variational results are given by the solid line, the small eigenvalue results are given by the dashed-dotted line, and the dashed line denotes the curve defined analytically by Eq. (6.11). The agreement with the exact results is quite good considering that there are only four bound states in the He/LiF system. Even the analytic result gives, at its worst, agreement within a factor of two. The distribution function is not examined because it would contain only four points for the exact numerical results and thus would not provide an adequate basis for comparison.

The exact numerical results are described rather well in both a qualitative and a quantitative fashion for small and large systems alike. It therefore seems reasonable to use the

(6.10) in any further analytic work on the sticking coefficient or the readsorption coefficient. If necessary the heat of adsorption can be allowed to vary with temperature rather than being set equal to the depth of the potential well.

7. Preliminary Results for the Kinetic Coefficients

In the previous chapter it was concluded that the distribution function could be approximated by a fairly simple analytic expression (6.10). With this expression in hand it is possible to derive an analytic expression for the sticking coefficient. The reason for doing this is to see how the sticking coefficient depends on the temperature of the solid and gas as well as how it depends on the friction coefficient and the other parameters which characterize the gas-solid system. After this is done the expression will be compared with the exact results obtained from the discrete master equation.

The readsorption coefficient is also examined, but only numerically.

7.1 An Algebraic Expression for the Sticking Coefficient

Before proceeding some comments on the nature of Eq. (6.10) must be made. The approximation (6.10) is never larger than one. This then guarantees that the sticking coefficient (3.20) never exceeds one as well. The exact distribution does not have this feature. At high enough temperatures the exact distribution is larger than one for bound states near the bottom of the potential well. It was because of the possibility of this occurrence that it was not possible to state that Eq. (3.20) was unitary. It so happens that the exact distribution exceeds one only at high temperatures where the transition rates are usually less than the thermal escape rate from the chamber. This means that in practice the sticking coefficient never exceeds the value one. It therefore seems acceptable to use Eq. (6.10) in the definition of the sticking coefficient without worrying about it qualitatively changing the end result.

To use expression (6.10) it is necessary to first pass to the continuum limit with Eq. (3.20)

$$S = \frac{1}{\left[\int_0^\infty d\varepsilon\, e^{-\varepsilon\beta U_o}\right]} \int_0^\infty d\varepsilon\, e^{-\varepsilon\beta U_o} \left\{ \frac{\frac{\sigma_o}{2}\int_{-1}^{0} d\varepsilon' \frac{1}{\sqrt{-\varepsilon'}}\, g(\varepsilon')W(\varepsilon',\varepsilon)}{\frac{1}{4}\sqrt{\frac{2U_o\varepsilon}{m}} + \frac{\sigma_o}{2}\int_{-1}^{0} d\varepsilon' \frac{1}{\sqrt{-\varepsilon'}}\, W(\varepsilon',\varepsilon)} \right\} \quad (7.1)$$

those in chapter 3, the numerator and denominator are integrated separately to yield

$$S = \frac{\frac{\sigma_o}{2}\int_{-1}^{0} d\varepsilon' \frac{1}{\sqrt{-\varepsilon'}} f(\varepsilon')W(\varepsilon',\varepsilon)\, e^{-\varepsilon\beta U_o}}{\left[\frac{1}{L}\sqrt{\frac{2U_o\varepsilon}{m}}\int_{0}^{\infty} d\varepsilon\, e^{-\varepsilon\beta U_o} + \frac{\sigma_o}{2}\int_{-1}^{0} d\varepsilon' \int_{0}^{\infty} d\varepsilon \frac{1}{\sqrt{\varepsilon'}} W(\varepsilon',\varepsilon)\, e^{-\varepsilon'\beta U_o}\right]} \quad (7.2)$$

These separate double integrals can be evaluated approximately to the lowest order in σ_o. The details of such a calculation are somewhat involved and so they have been relegated to App. F. The resulting expression for the sticking coefficient is

$$S = \frac{S_0 - S_1}{1 + S_0} \quad (7.3)$$

where

$$S_0 = \frac{\eta h\sigma_o^2}{8U_o}\left(\frac{T_S}{T_g}\right) F_4\left(1 + \frac{U_o}{2\sigma_o k_B}\left(\frac{1}{T_g} - \frac{1}{T_S}\right)\right), \quad (7.4)$$

and

$$S_1 = \left(\frac{\eta h T_S}{8U_o T_g}\right)\frac{\sigma_o^3 F_4(1) F_4\left(1 + \frac{U_o}{2\sigma_o k_B T_g}\right)}{\left[\sigma_o F_4(1) + 4F_5(1) U_o/k_B T_S\right]}. \quad (7.5)$$

The temperature of the gas and the solid need not be the same and hence they are denoted by the appropriate subscript. For the purposes of this thesis only the case where the temperatures are equal will be studied. After setting the temperatures equal the sticking coefficient becomes

$$S = \frac{\eta h\sigma_o^2}{8U_o}\,\frac{\left[1 - \frac{\sigma_o^3 F_4(1) F_4\left(1 + U_o/2\sigma_o k_B T\right)}{\left[\sigma_o F_4(1) + F_5(1) U_o/k_B T_S\right]}\right]}{\left[1 + \frac{\eta h\sigma_o^2}{\ldots}\right]} \quad (7.6)$$

$$S \simeq \eta h \sigma_o^2 \frac{\left\{1 - \left[\frac{\sigma_o}{\sigma_o + 4U_o\beta}\right]\left[\frac{2\sigma_o}{2\sigma_o + \beta U_o}\right]\right\}^4}{\left[8U_o + \eta h \sigma_o^2\right]} \quad . \tag{7.7}$$

From this expression it can readily be seen that in the low temperature limit the sticking coefficient approaches its maximum value which is not necessarily one. As the temperature increases the value of S decreases, eventually going to zero as the inverse of the temperature. Qualitatively, this agrees with the experimental findings although the extreme low temperature region is difficult to achieve numerically.

The terms in the numerator guarantee that the sticking coefficient goes to zero as the temperature goes to infinity. The origin of these terms can be traced to the presence of the distribution function inside the integrals of (7.2). As the temperature goes to infinity the adparticle distribution at the top of the potential goes to zero (See Figs. 6.1 and 6.2). This indicates that the particles which adsorb into the upper bound states of the potential only reside there for times comparable to the time scale of the transients and so quickly rejoin the gas phase. The cause of this effect is presumably the near equality of the probability of a phonon being created or destroyed at high temperatures.

The analytic approximation for the alternative definition of the sticking coefficient, Eq. (3.23), can easily be obtained by simply replacing the second term of the denominator with the numerator. This proceedure yields

$$S \simeq \frac{\eta h \sigma_o^2}{8U_o} \frac{\left[1 - \left(\frac{\sigma_o}{\sigma_o + 4\beta U_o}\right)\left(\frac{2\sigma_o}{2S_o + \beta U_o}\right)^4\right]}{\left[1 + \frac{\eta h \sigma_o^2}{8U_o}\left[1 - \left(\frac{\sigma_o}{\sigma_o + 4\beta U_o}\right)\left(\frac{2\sigma_o}{2\sigma + \beta U_o}\right)^4\right]\right]} \quad . \tag{7.8}$$

As with the original discrete definitions, Eqs. (3.20) and (3.23), the approximate expressions (7.7) and (7.8) will differ for moderate to high temperatures when the number of bound

7.2 Numerical Comparison

Before discussing the comparison of the analytic and exact numerical results, a comparison of the sticking coefficient defined by Eq. (3.20) to that defined by Brenig's formula, Eq. (1.30), is made in Fig. 13 . The values of the parameters for the model He/Ar system studied are the same as those chosen by Kreuzer and Gortel to illustrate the violation of unitarity by Brenig's expression. It is readily seen that the definition for S proposed in this thesis, Eq. (3.20), does not take on values greater than one. The expression for S consistent with the Devonshire theory, Eq. (1.31), is also presented in order to illustrate that it does not go to zero at high temperatures but rather goes to a constant value larger than one. It should be noted that the exact numerical results shown in fig. 13 drop precipitously to zero as the temperature goes to zero. The analytic result, which is not shown in fig. 13, does not go to zero as the temperature goes to zero: it approaches a finite nonzero value. This is a result of the approximations used. From fig. 13 it is apparent that the sticking coefficient does not exceed the value one. It remains to be seen, however, whether the values of S defined by Eq. (3.20) are consistent with the experimental results.

For He gas at 290° Kelvin adsorbing on solid Xe at 3.4° Kelvin, Lee[151] has measured a value of 0.37 for the sticking probability. By choosing Morse potential parameters which reproduce the heat of adsorption measured by Lee, values for S were obtained which varied from .32, for a system with ten bound states, to .47, for a system with six bound states. These values are in the correct range. By adjusting the number of bound states of the Morse potential it should be possible to reproduce the experimental value exactly. Lee's value of the heat of adsorption has an experimental error associated with it thus allowing for an even larger latitude of freedom in choosing the Morse parameters.

Sinvani *et al.*[152] have done some low temperature experiments for He adsorbing on Sapphire. The temperature of the Sapphire substate was 3.6° Kelvin while the gas had a temperature ranging from 10-20° Kelvin. For surface coverages ranging from 0 to .7 the sticking coefficient was found to have a constant value greater than .66 but substantially less

Unfortunately, the heat of adsorption for the helium on sapphire system was not measured so that a direct comparison is not possible.

Before trying to fit the Morse parameters to these data points it is desirable to constrain the possible values of the parameters by experimentally measuring the number of bound states. In the meantime it seems safe to claim that small systems can be described fairly well.

In Figs. 14 and 15 the sticking coefficient defined by Eq. (3.20) as well as by the analytic formula (7.6) are plotted, along with the readsorption coefficient, for the Xe/W system. At low temperatures the values of S are in the region of one. The system with 80 bound states, Fig. 15, comes very close to one but falls just short at a value of about .98 at its maximum. Since the value of S is so close to one at low temperatures, this system seems to exhibit classical behaviour. One would then expect that the system shown in Fig. 14, which has a larger number of bound states than the system shown in fig. 15, would also have a low temperature value close to one. This is not the case; the maximum value of S actually decreases. It seems that the classical results are obtained when there are a large number of bound states due to the well being very deep.

The experimental values of S for the Xe/W system at low coverage vary according to the situation. Ehrlich[153] gives a value of .4 for Xe at 300° Kelvin adsorbing on polycrystalline tungsten at 81° Kelvin. Dresser *et al.*[154] measured a value of .5 at 104° K for the W(111) surface. Yates and Erikson[155] repeated this measurement at 120° K and obtained a value close to one. It is difficult to reconcile these two results. Wang and Gomer have since examined the W(110) and W(100) surfaces at 62° K and 65° K respectively. For the former case the the gas temperature was 105° K and yielded a value of .85 for the sticking coefficient. In the latter case the gas temperature ranged from 110-300° K and yielded values from 0.95-0.9 for the sticking coefficient. Both of the Figs. 14 and 15 presented seem to be consistent with the overall picture given by the experimental data. A definitive statement would require a clarification of some of the experimental data and a more direct comparison of the theoretical expression with the experimental results.

The analytic expression for the sticking coefficient is also plotted in Figs. 14 and 15. For low temperatures the analytic expression underestimates the value of the sticking coefficient while at higher temperatures the sticking coefficient is overestimated. The analytic expression can reproduce only the qualitative behaviour of the sticking coefficient.

In Figs. 14 and 15 the readsorption coefficient has been plotted along with the sticking coefficient. At low temperatures the readsorption coefficient and the sticking coefficient are almost identical but as the temperature increases the latter decreases more rapidly than the former. The speculation in chapter 3 that these two coefficients might be approximately equal is therefore warranted only for low temperatures. It is readily apparent that the readsorption coefficient is not a negligible factor; in the case of the Xe/W system with 80 bound states the readsorption coefficient reduces the desorption rate by a factor of 20 at low temperatures. If the number of bound states are increased this effect will decrease. To extract this coefficient from the experiments may well involve a reinterpretation of the experimental results.

For contrast one more graph (Fig. 16) of a large system (Ar/Ag) is presented. At low temperatures the maximum value of S around 0.5 . It is interesting to note that in this system the low temperature maximum is rather prominent. This feature doesn't show up in the low temperature behaviour of the analytic expression. Presumably higher order terms would have to be included to recover this feature. This system has the same number of bound states as the Xe/W system shown in Fig. 15 but doesn't exhibit the same degree of classical behaviour. This is presumably because the Ar/Ag has a relatively shallow potential. Once again it is seen that the readsorption coefficient is not a negligible factor.

On the whole these preliminary results look very promising. Particularly pleasing is the ability to describe large and small systems alike.

8. Summary and Conclusions

In the introduction a program calling for the derivation of the phenomenological rate equation from kinetic theory was presented. A natural consequence of this program is the development of microscopic expressions for the kinetic coefficients, i.e. the desorption rate, the sticking coefficient, and the readsorption coefficient, which occur in the phenomenological equation. It is also desirable to evaluate, both numerically and analytically, these coefficients. In this thesis this program has been largely carried out. In so doing a variety of mathematical techniques were used. In particular van Kampen's large parameter expansion was heavily used.

In order to catalogue the accomplishments of this thesis the results will be summarized chapter by chapter.

In chapter two a set of macroscopic equations was derived for a study of the adsorbate as a whole. The equations were derived explicitly to ensure that all of the terms required for a diffusive process would be included. This set of equations coupled the average energy of the adsorbate and the fluctuations in the energy. Both of these equations were needed because in a physisorbed system the fluctuations of a macroscopic variable are as important as the the macroscopic variable itself. From the study of this system of equations it was determined that the adsorbate evolves on a time scale determined by the friction coefficient. This leads to a macroscopic law of friction for physisorption. Also presented in this chapter was a numerical study of the adsorbate energy, its fluctuations, and the number of particles in the adsorbate during desorption. This gave a graphic illustration of the separation of time scales during desorption. From this study it was conclude that the adsorbate maintained a quasi-equilibrium during the process of desorption.

The third chapter was devoted to the the derivation of the phenomenological rate equation from a master equation. It was found that the rate equation had to be modified through the introduction of a new kinetic coefficient dubbed the readsorption coefficient. This coefficient takes into account the possibility that a desorbing particle will readsorb. Microscopic definitions of this and the other coefficients were obtained. In particular a couple

of definitions for the sticking coefficient were put forward of which one is guaranteed to never exceed the value one. This definition has never been given before and so solves a long standing problem in physisorption kinetics. The derivation of these quantities and the phenomenological rate equation was general in the sense that the transition rates were never specified. The remainder of the thesis was devoted to the evaluation of the sticking coefficient and the desorption rate, and to a lesser extent, the readsorption coefficient.

The first step towards the determination of these coefficients was taken when, starting from the phonon cascade model of physisorption, the master equation was converted into a Fokker-Planck equation using van Kampen's large parameter expansion. To do so meant that the large parameter had to be identified for a complicated physical system, something that has probably never been accomplished before. The large parameter was found to be the Morse parameter σ, which is a measure of the number of bound states.The extraction of the Fokker-Planck equation was complicated by the presence of the potential well bottom. It was found that the effect of this boundary could be ignored if the moments of the Kramers-Moyal expansion satisfied a set of auxiliary conditions. These conditions were later found to be equivalent to requiring that the adparticle current be zero at the bottom of the potential, implying that the bottom of the potential could be regarded as a perfectly reflecting boundary in energy space. The equation resulting from this procedure was dubbed the phonon cascade Fokker-Planck equation.

Contact with classical theories was made when it was shown that the Kramers equation could be obtained through an approximation of the phonon cascade Fokker-Planck equation. This approximation was found to be valid for energies within the surface potential which were not too close to the escape energy, thus implying that the Kramers equation can describe the kinetics of equilibration within the surface potential but cannot accurately describe the desorption process. There are additional conditions which must must be satisfied to obtain the Kramers equation: the surface potential must have a large number of bound states, the gas-solid system must be at a high temperature, and the time scale of the phonon reservoir must be much faster than the time scale of the adparticle. This latter condition is

implicit when the master equati approach is used. This derivation of the low friction Kramers equation removes the restriction that the adparticle must be much heavier than the solid atoms used in the derivation of the Kramers equation by Caroli *et al.*[119], although it is technically only valid for the case of a particle moving in a Morse potential.

Having made the connection with the Kramers equation, the friction coefficient was identified and expressed in terms of the microscopic parameters which characterize the gas-solid system. This expression was found to differ by a factor of 9π from that obtained by Caroli *et al.*[119] within the framework of classical mechanics and linear response theory. It was argued that this discrepency may well be due to the use of linear response theory and hence raises questions concerning the validity of linear response theory.

In order to proceed with the evaluation of the kinetic coefficients the ideal desorption rate and distribution function had to be extracted from the phonon cascade Fokker-Planck equation. This could only be done after the boundary conditions had been derived in chapter five. The interesting feature here was the extraction of a radiative boundary condition from the master equation within the framework of van Kampen's large parameter scheme. This was in contrast to the often used absorbing boundary condition. The radiative boundary condition was found to be independent of temperature. Thus, any temperature effects which enter the desorption rate are determined solely by the Fokker-Planck equation.

With the boundary conditions in hand the ideal desorption rate and distribution function are calculated in chapter six. This was done both analytically and numerically. The analytic work yielded a reasonably simple expression for the desorption distribution and rate which compare favourably with the exact numerical results. The exact numerical results for the desorption rate match the experimental results quite well. In addition, the analytic desorption rate was found to be valid for both the low and high temperature regimes. A numerical examination of the heat of adsorption and the preexponential revealed a temperature dependent compensation effect with regard to the desorption rate. This effect is purely kinetic in origin and has nothing to do with the interaction between the gas particle and the solid possibly being temperature dependent. It is probably common to all systems which

exhibit behaviour similar to Brownian motion.

The analytic expressions for the desorption rate and its associated distribution were used in chapter seven to obtain an analytic expression for the sticking coefficient. The sticking coefficient was also calculated numerically and graphed as a function of temperature. The results seemed to be in agreement with experimental values and, as required, never gave values greater than one. The readsorption coefficient was also evaluated numerically and was found to alter the desorption rate significantly in the Xe/W system. A careful reexamination of the existing experimental work seems to be in order.

The program for the phenomenological rate equation has been largely completed. There is still the outstanding question of which definition for the sticking coefficient is the correct one, Eq. (3.20) or Eq. (3.23). By making use of Tully's[128 130] computer results for the energy dependent sticking coefficient it may be possible to choose between these two definitions. Of course more work in comparing the theoretical results with the experimental results for various other gas-solid systems can be done. The important point is that the overall structure of the theory is sound and that the preliminary results appear to be in agreement with the experimental values. The theory presented provides a coherent view from which experimental work can be interpreted and systematically analysed.

Once the coefficients have been thoroughly examined it may be possible to build upon the theory by incorporating the influence of the adparticles upon each other, i.e. go beyond the low coverage limit, and thus obtain kinetic coefficients which depend on the coverage as well as the temperature. One could also attempt to modify the theory to include a more realistic model of the solid surface and see how the kinetic coefficients change with varying surface conditions.

Besides advancing a general frame work for physisorption kinetics this thesis also sheds light on the nature of the equilibration process within the surface potential. It is anticipated that these results will be useful for studying chemisorption with a physisorption precursor state. The general framework may even be a suitable basis for a theory of chemisorption and catalysis. The methods used here may also be useful in approaching

photodesorption kinetics entirely analytically.

In this thesis a solution to the problem of the violation of unitarity by the sticking coefficient has been put forward. This approach might also be applicable to a similar problem with the accomodation coefficient. This quantity, which is a measure of the efficiency with which a gas particle can thermalize with a solid surface, is defined as the ratio of the energy lost by a gas to the solid divided by the amount that would have been lost by the gas if it had perfectly thermalized with the solid surface. Physical intuition says that this ratio should have a value of one or less. At this point in time there are no theories which guarantee this property. It seems likely that the general framework and methods of this thesis will be able to solve this problem as well. This, however, will not be a trivial extension of the work done here since the the energy can be exchanged through conductive (collisions) and convective (adsorption and desorption) processes. Should this problem be solved one would then be in a position to address the problem of the nature of boundary conditions for the flow of a dilute gas past the surface of a solid and hence make a contribution to the field of aerodynamics.

As can be imagined from the discussion above, physisorption kinetics has some fascinating problems that are still unsolved.

FIGURE 1. Phase portrait of the macroscopic equations of physisorption: analysis of Eqs. (2.13) and (2.14). The phase space is divided into characteristic regions by the dashed curve $\dot{x}=0$ and the dotted curve $\dot{\sigma}^2=0$. To the right of the dotted curve lies the region where the fluctuations in the adparticle energy grow in time, $\dot{\sigma}^2>0$, while to the right of the dotted curve lies the region where the fluctuations decay in time, $\dot{\sigma}^2<0$. The dashed curve divides the space in a similar manner: the region where the average adparticle energy decreases in time, $\dot{x}=0$, lies below the curve and the region of increasing average energy lies above the curve. The two points where the dashed and dotted curves cross are marked by the letters E and S indicating the equilibrium point and saddle point respectively. The dashed-dotted curve delineates the right hand limit of the domain of attraction of the point E. The four solid curves are phase trajectories calculated from Eqs. (2.13) and (2.14).

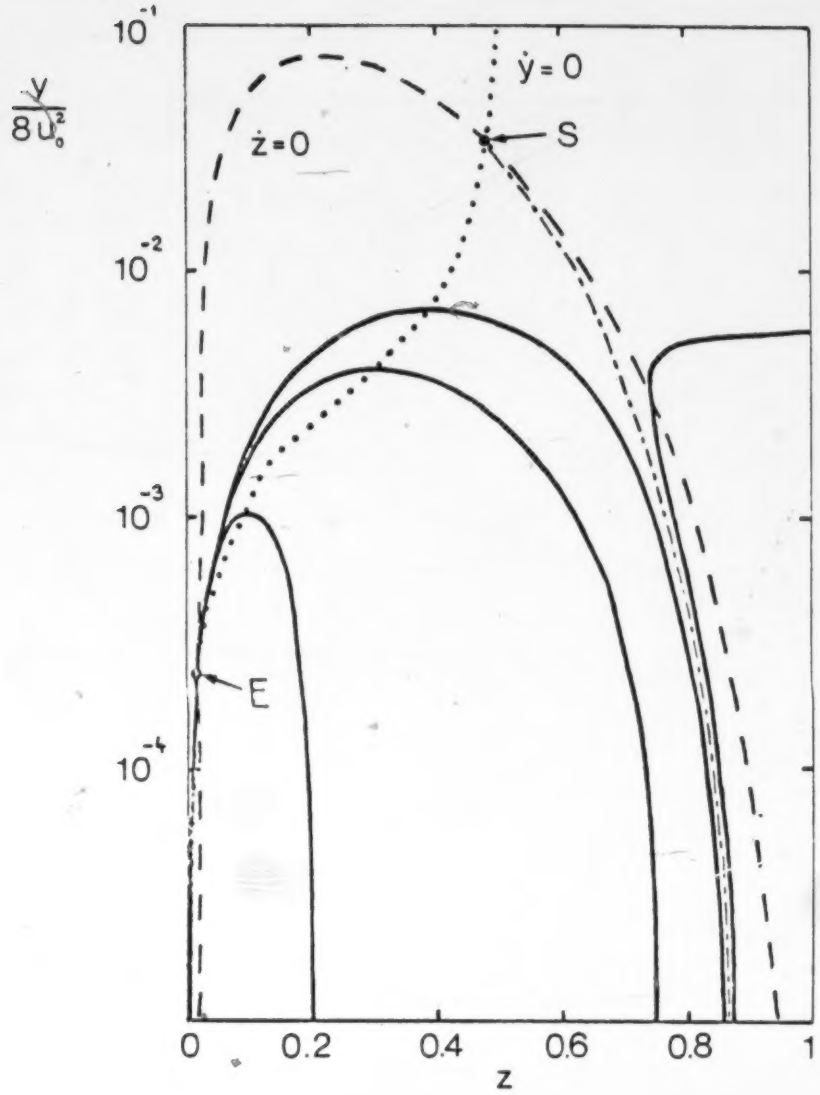
$\frac{V}{8u_o^2}$
10^{-1}
10^{-2}
10^{-3}
10^{-4}
$\dot{y}=0$
$\dot{z}=0$
S
E
0
0.2
0.4
0.6
0.8
1
z

FIGURE 2. The time evolution of a particle initially put into the sixteenth energy level of a surface Morse potential with eighty bound states is followed in three panels; upper panel: dimensionless average energy $\epsilon = E/\hbar\omega_D$ (See Eq. (2.22)); centre panel: fluctuations in the dimensionless average energy $\sigma^2 = \sigma^2/(\hbar\omega_D)^2$ (See Eq. (2.23)); lower panel: normalized occupation probability, Eq. (2.21), as functions of $\log_{10}(\eta t)$. The solid curves are from both the discrete rate equation (1.3) and the macroscopic equations (2.13) and (2.14). The parameters used are typical of a Xe/W system: $u_* = (U_*/\hbar\omega_D) = 11.56$, $(m/M) = 0.714$, $\sigma_* = 79.76$, and $\omega_D = 5.3 \times 10^{12}\ s^{-1}$. The system is at $T = 202.5°K$, so that $\delta = (\hbar\omega_D/k_B T) = 2$.

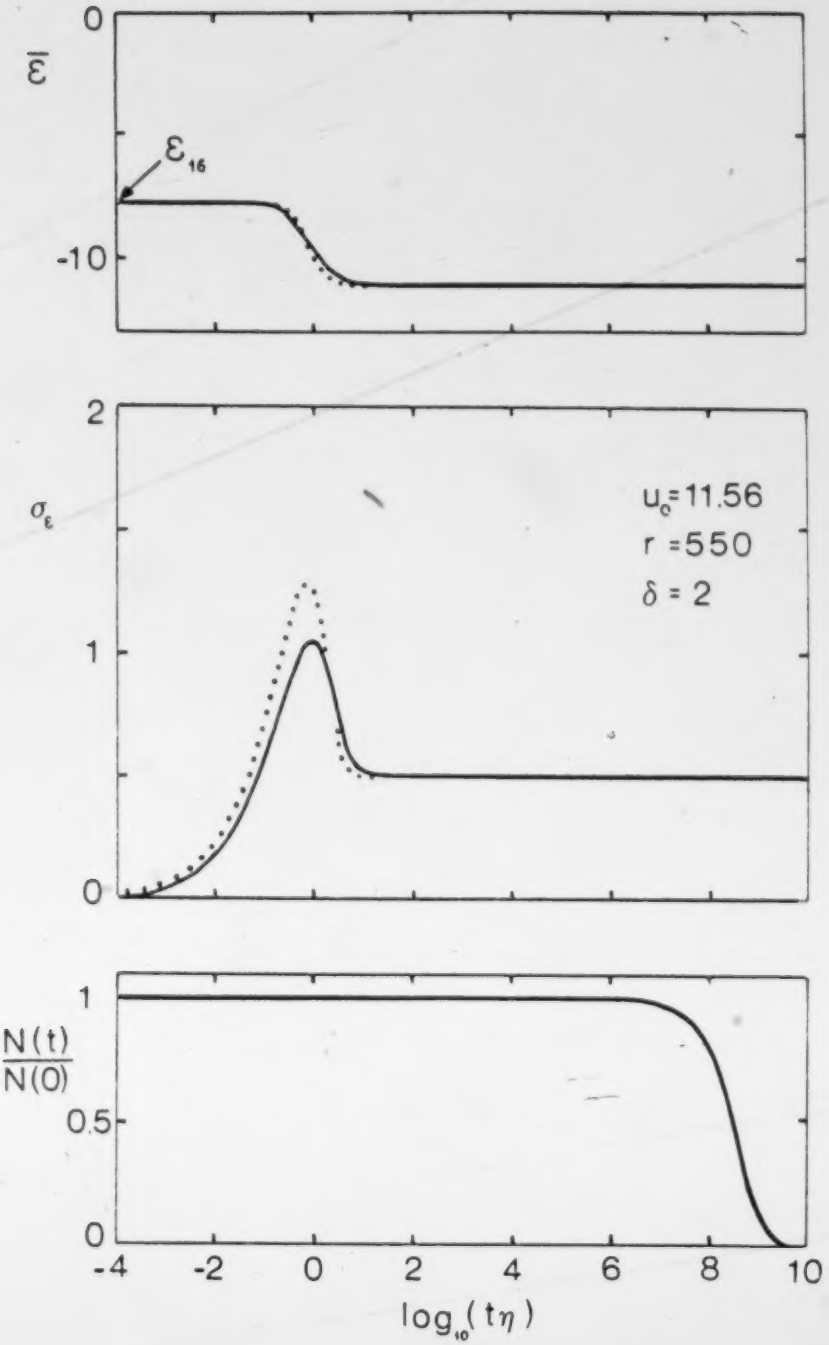
0
$\bar{\varepsilon}$
ε_{16}
-10
2
σ_ε
u_e=11.56
r =550
δ = 2
1
0
1
N(t)
N(0)
0.5
0
-4
-2
0
2
4
6
8
10
$\log_{10}(t\eta)$

FIGURE 3. The same as Fig. 2 but with a particle injected into the sixtieth bound state of the surface potential at a temperature of 405°K. .

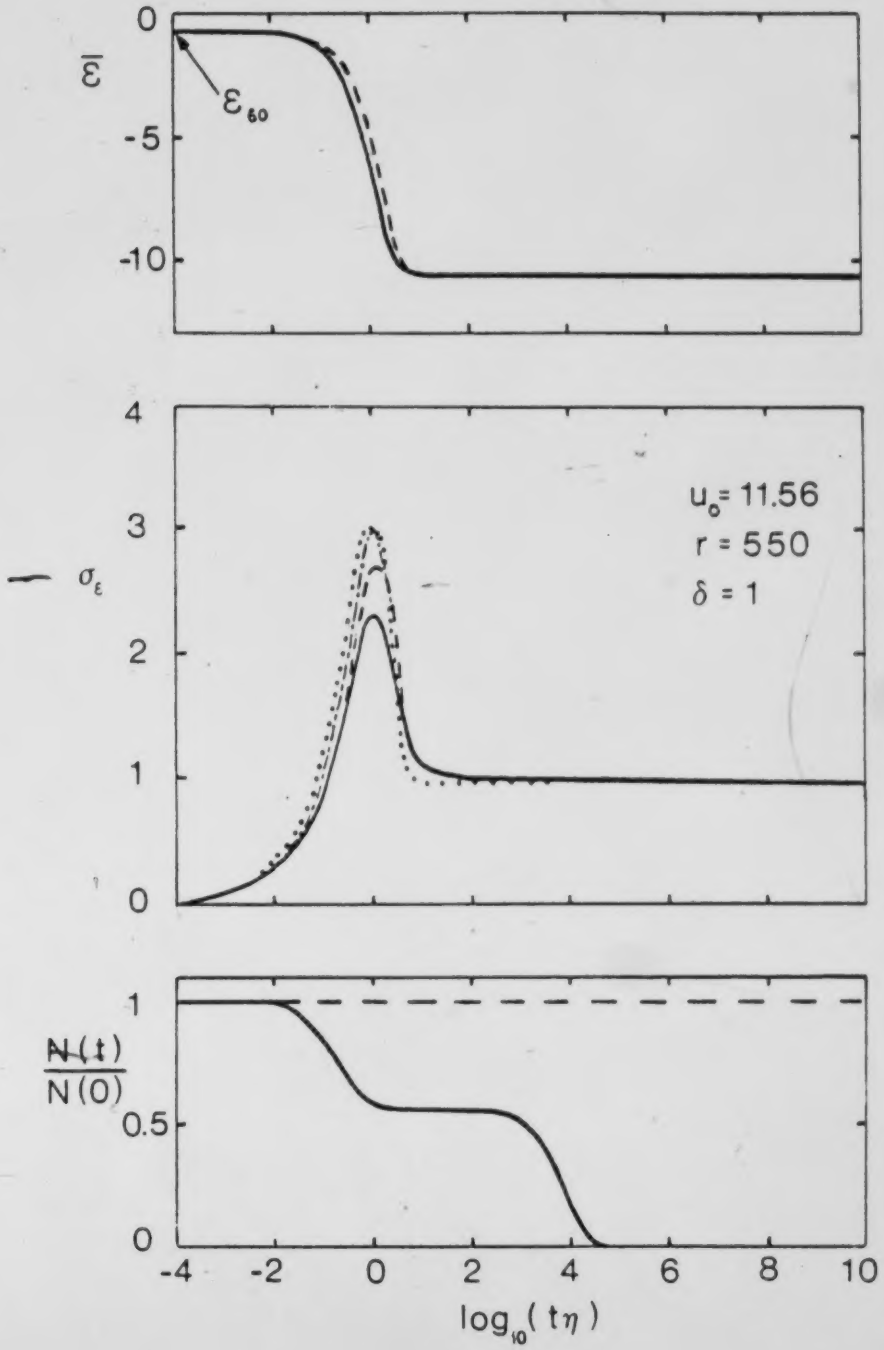
0
-5
-10
$\bar{\varepsilon}$
ε_{60}
4
3
2
1
0
σ_ε
$u_o = 11.56$
$r = 550$
$\delta = 1$
1
0.5
0
$\frac{N(t)}{N(0)}$
-4
-2
0
2
4
6
8
10
$\log_{10}(t\eta)$

FIGURE 4. The time evolution of a particle initially put into the sixteenth energy level of a surface Morse potential with eighty bound states. The index i denotes the bound state number. The vertical height of the figure is proportional to the probability of the particle occupting state i at time t. The temperature of the system is 405°K. .

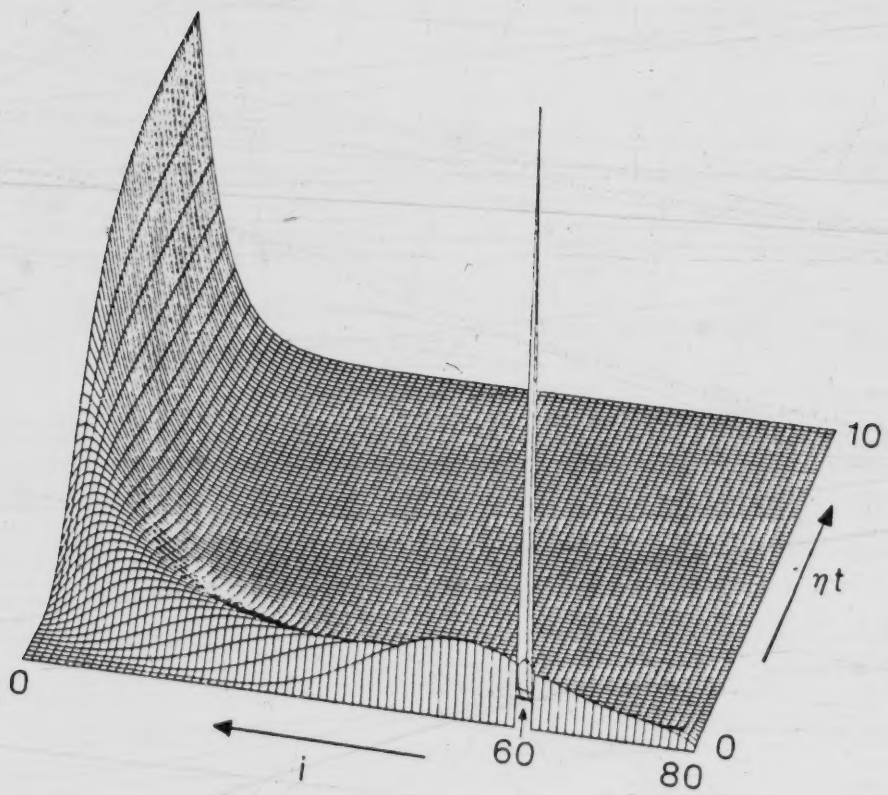
10
ηt
0
i
60
0
80

FIGURE 5. The same as Fig. 4 but with a logarithmic time scale.

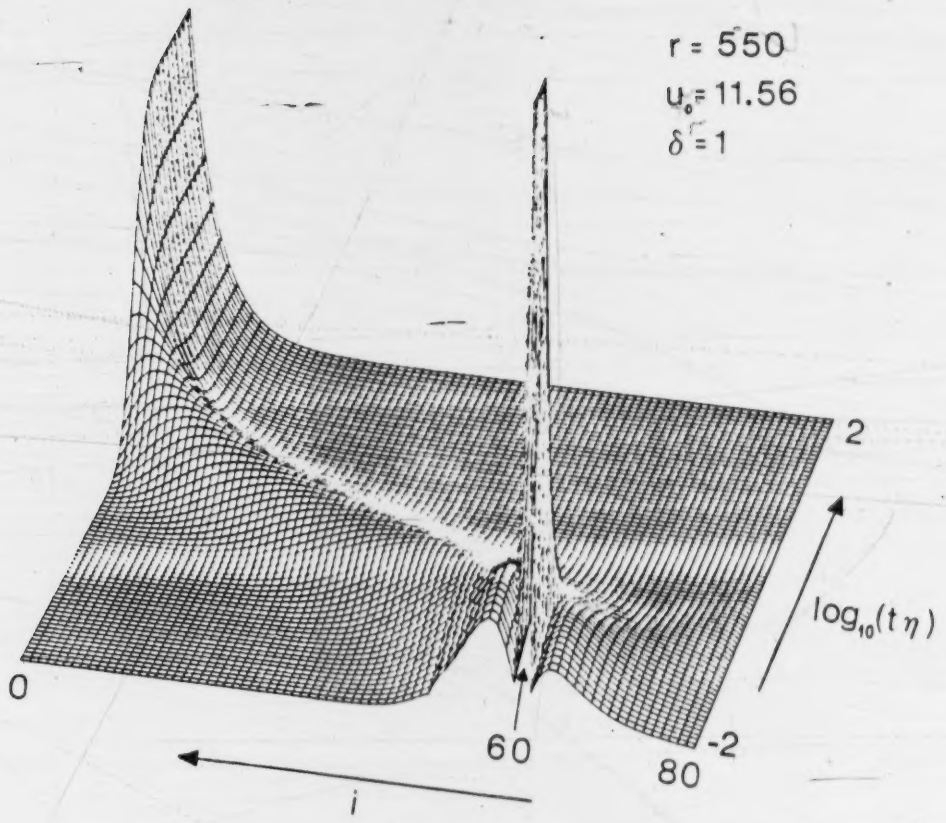
r = 550
u_0 = 11.56
δ = 1
2
$\log_{10}(t\,\eta)$
-2
0
60
80
i

FIGURE 6. The transition rates W(e,e'), where $e = \epsilon U_o/\hbar\omega_D$, for the phonon cascade model. The values of the parameters are appropriate for a Xe/W system: $\sigma_o = 239.67$, $u_o = U_o/\hbar\omega_D = 11.56$, $m/M = 0.714$, and $\omega_D = 5.302 \times 10^{13}\ s^{-1}$.

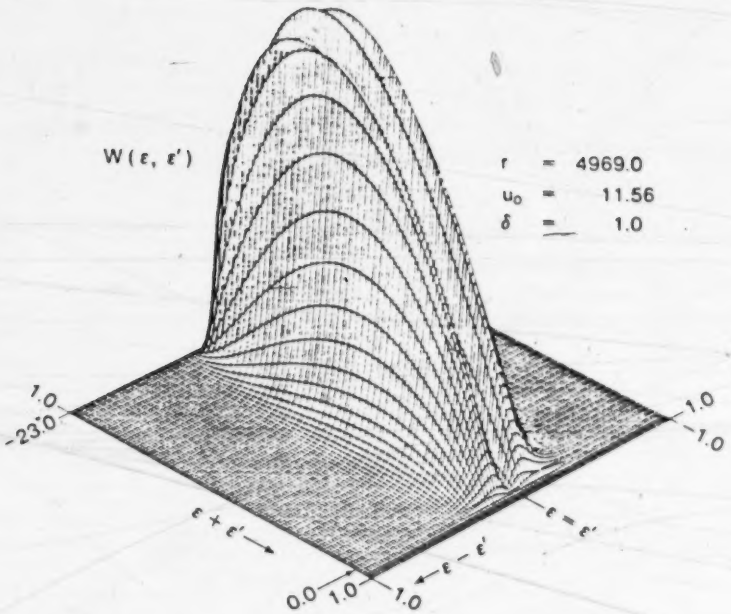
W(ε, ε')
r = 4969.0
u₀ = 11.56
δ = 1.0
1.0
-23.0
ε + ε'
0.0
1.0
1.0
ε - ε'
ε = ε'
1.0
1.0

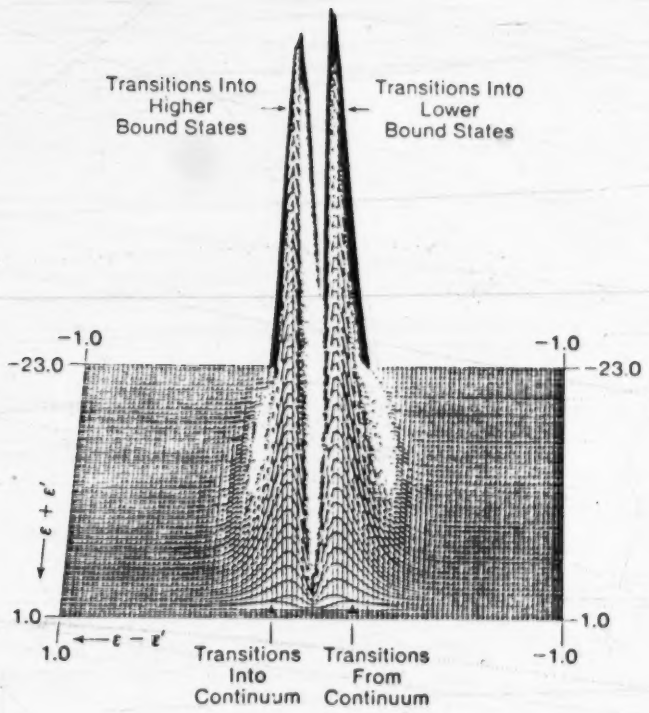
Transitions Into Higher Bound States
Transitions Into Lower Bound States
-1.0
-23.0
-1.0
-23.0
ε + ε'
1.0
1.0
1.0
ε - ε'
-1.0
Transitions Into Continuum
Transitions From Continuum

FIGURE 7. The section of Fig. 6 near the origin $e=e'=0$ is shown.

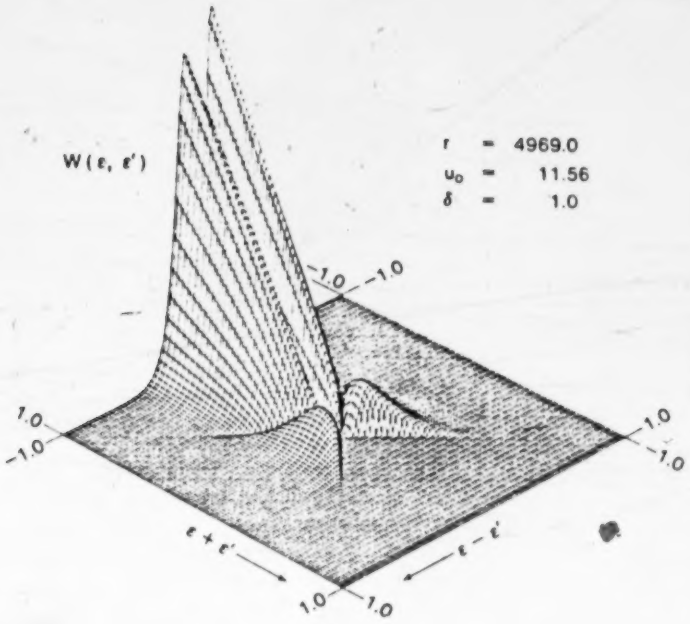
W(ε, ε')
r = 4969.0
u₀ = 11.56
δ = 1.0
-1.0
-1.0
1.0
-1.0
1.0
-1.0
ε + ε'
ε - ε'
1.0
1.0

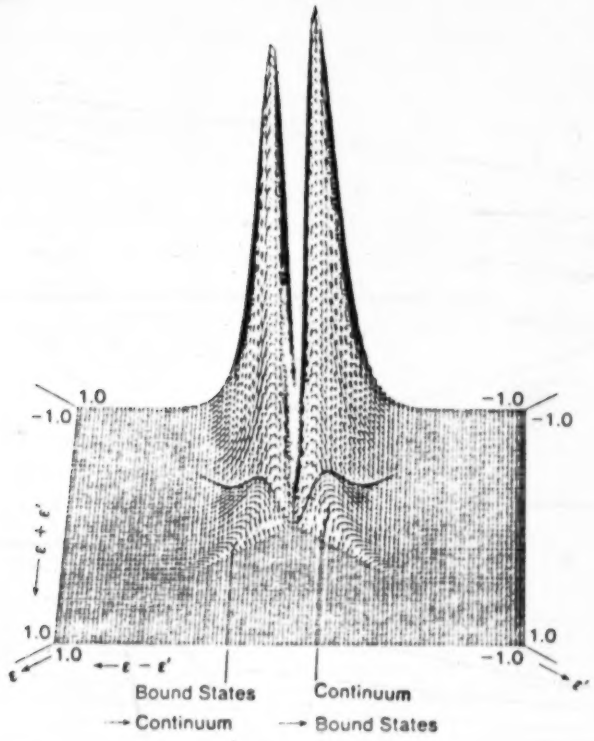
1.0
-1.0
-1.0
1.0
ε + ε'
1.0
1.0
ε
ε - ε'
-1.0
1.0
ε'
Bound States
Continuum
Continuum
Bound States

FIGURE 8. The reduced distribution function for a particle inside a Morse potential is shown. The dotted curve is calculated directly from the discrete rate equation (1.3); the solid curve is calculated using the variational method (6.24); and the dashed curve is obtained from the small eigenvalue expansion method (6.14). The parameters used are appropriate for a Xe/W system with 240 bound states. The Debye temperature is $T_D = 405°K$. . When $T/T_D = 0.5, 1$ the dashed curve lies on top of the solid curve.

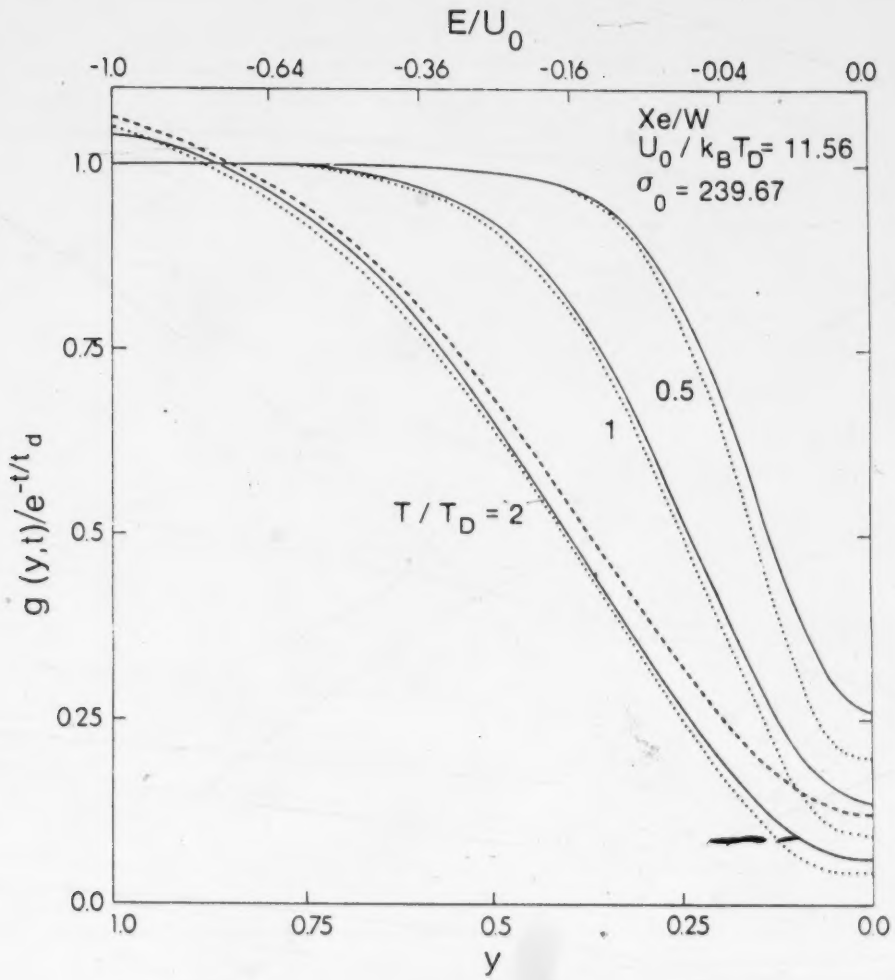
E/U0
-1.0
-0.64
-0.36
-0.16
-0.04
0.0
Xe/W
U0 / kB TD= 11.56
σ0 = 239.67
1.0
0.75
0.5
0.25
0.0
g (y,t)/e-t/td
0.5
1
T / TD = 2
1.0
0.75
0.5
0.25
0.0
y

FIGURE 9. The reduced distribution function for a Ar/Ag system. The same as Fig. 8 but for a Ar/Ag system with a Debye temperature of 225°K. .

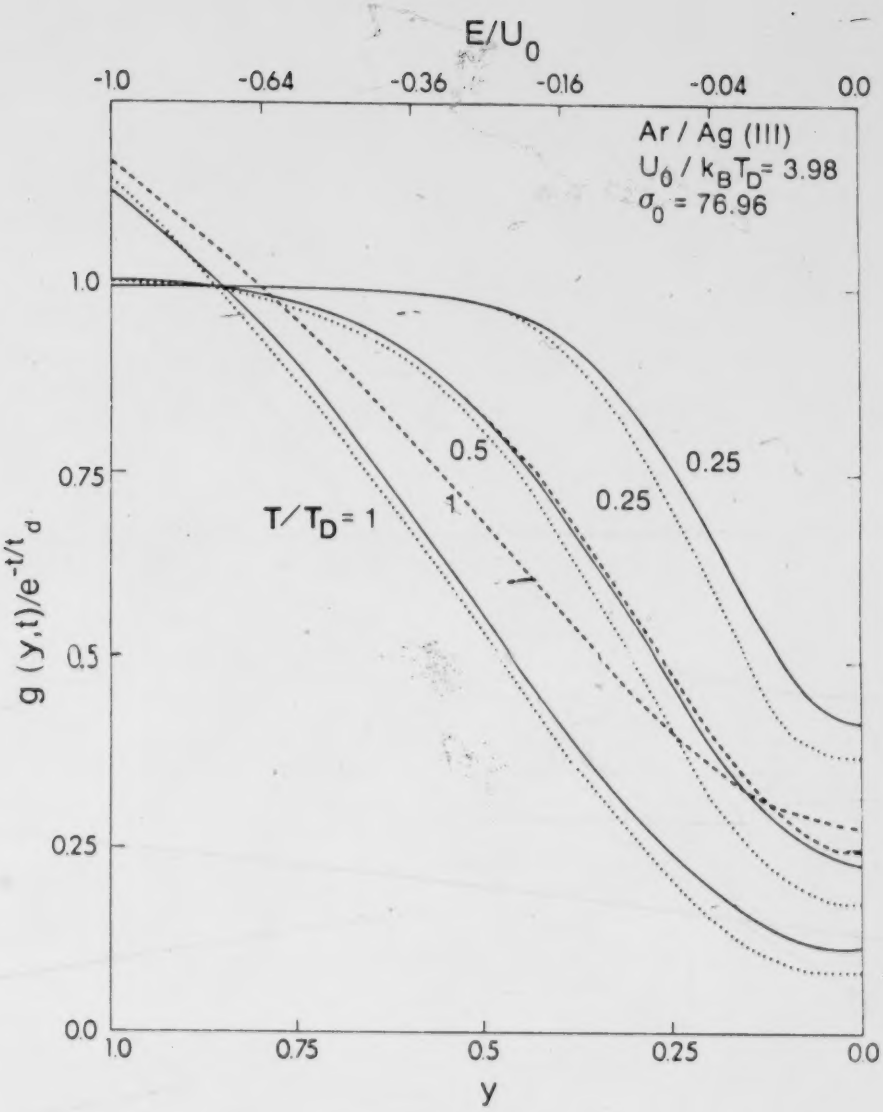
E/U0
-1.0
-0.64
-0.36
-0.16
-0.04
0.0
Ar / Ag (111)
U0 / kB TD = 3.98
σ0 = 76.96
1.0
0.75
0.5
0.25
0.0
g (y,t)/e-t/td
T/TD = 1
0.5
1
0.25
0.25
1.0
0.75
0.5
0.25
0.0
y

FIGURE 10. The scaled prefactor and heat of adsorption, for a Xe/W system, as functions of inverse temperature. The dotted curves are obtained from the discrete rate equation (1.3). The solid curve is obtained from the variational method (6.22). The dashed curve is obtained from the small eigenvalue expansion (6.9). By comparing the upper and lower panels it may be seen that the minima in the prefactor and heat of adsorption occur at the same temperature. This feature signals the existence of a compensation effect.

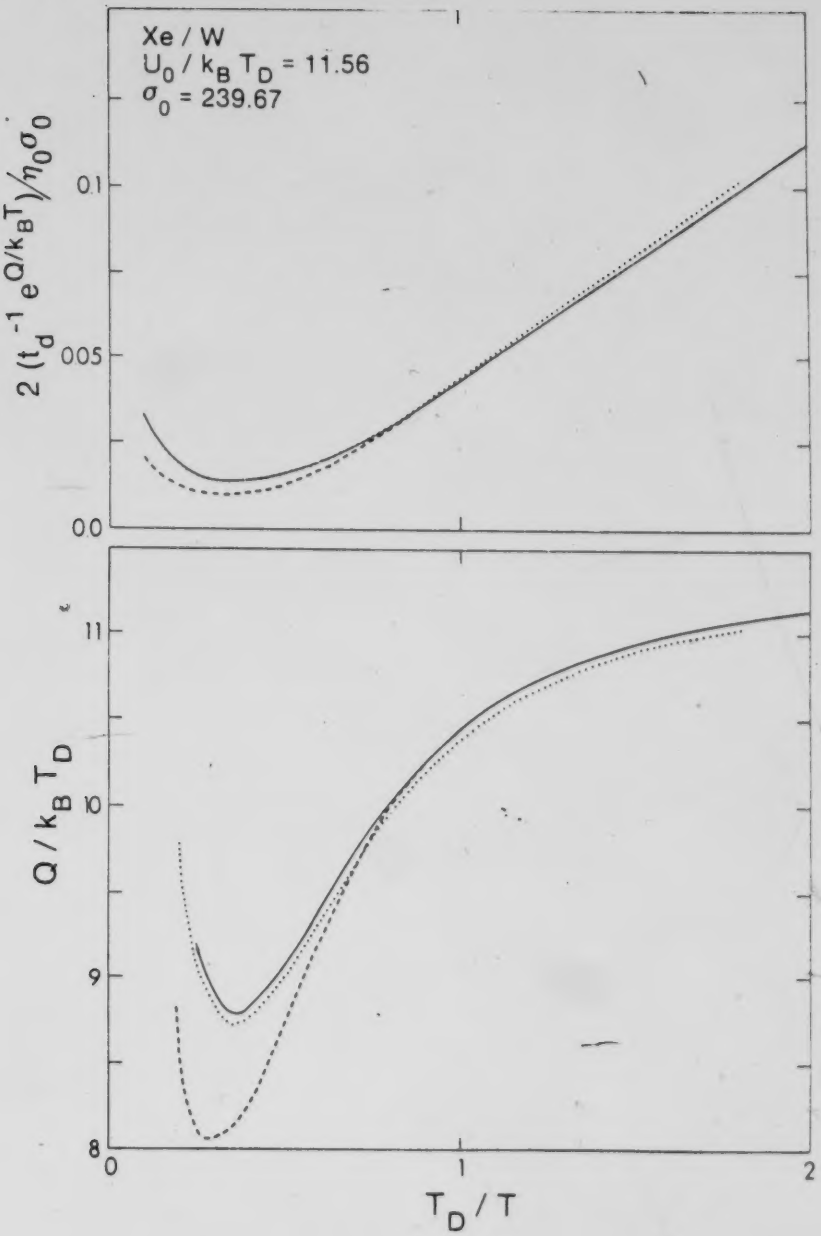
Xe / W
$U_0 / k_B T_D = 11.56$
$\sigma_0 = 239.67$
$2 (t_d^{-1} e^{Q/k_B T}) / \eta_0 \sigma_0$
0.0
0.05
0.1
$Q / k_B T_D$
8
9
10
11
0
1
2
T_D / T

FIGURE 11. The scaled prefactor and heat of adsorption, for an Ar/Ag system, as a function of inverse temperature. The nomenclature is the same as in Fig. 10 .

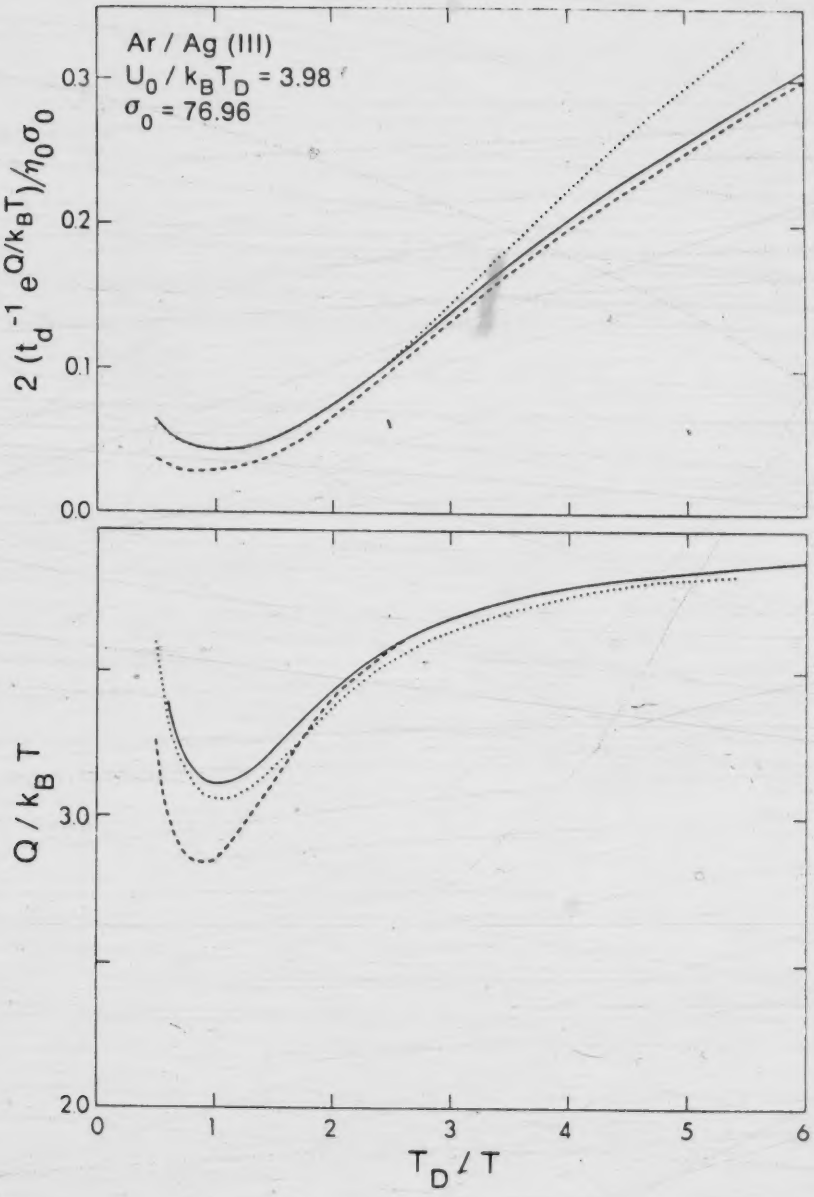
Ar / Ag (111)
$U_0 / k_B T_D = 3.98$
$\sigma_0 = 76.96$
$2 (t_d^{-1} e^{Q/k_B T}) / \eta_0 \sigma_0$
0.0
0.1
0.2
0.3
$Q / k_B T$
2.0
3.0
0
1
2
3
4
5
6
T_D / T

FIGURE 12. The scaled desorption rate vs. inverse temperature for a He/LiF system. The dotted line is the exact result obtained from the discrete master equation (1.3). The heavy solid line denotes the variational method results (6.22). The dashed lines are the small eigenvalue results (6.9). The light solid line is the approximate analytic result (6.10). The Debye temperature is 730°K. .

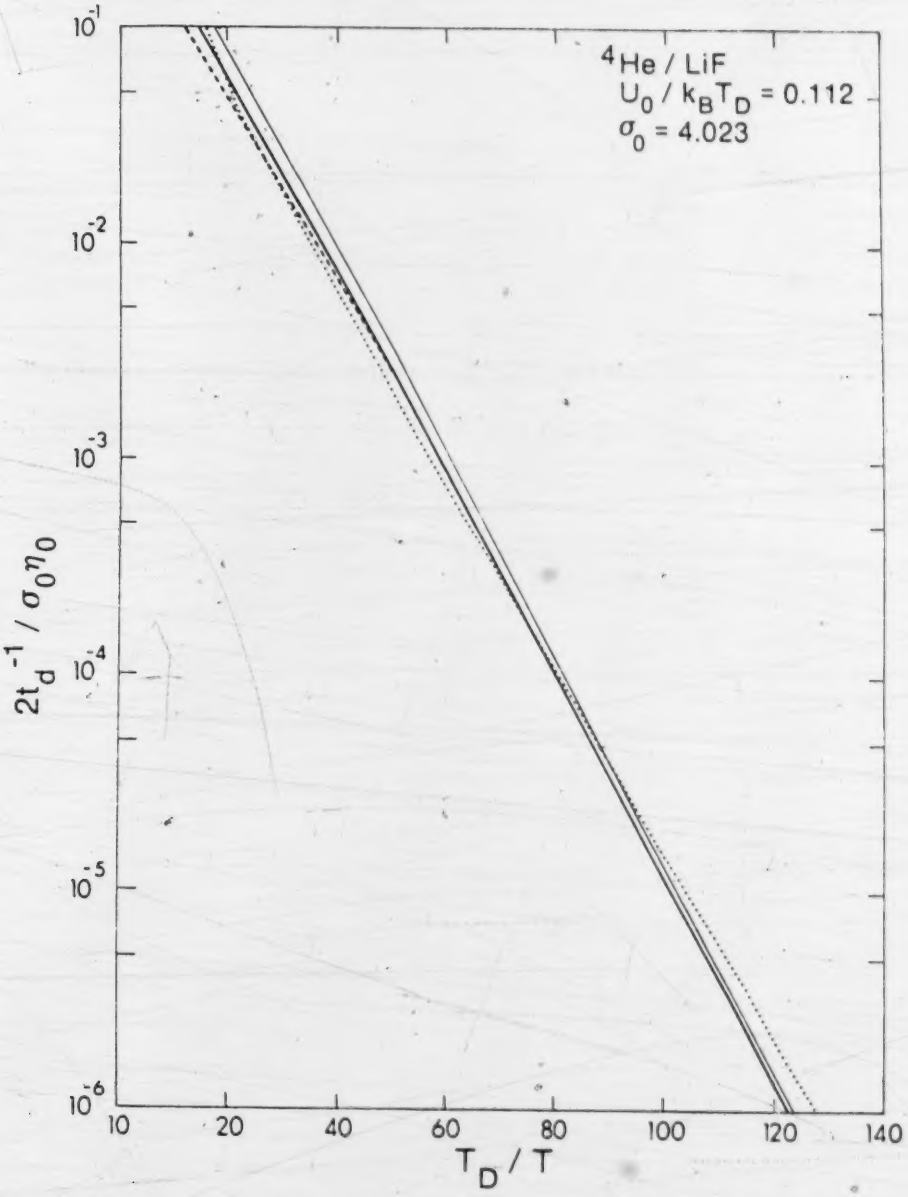
^{4}He / LiF
$U_0 / k_B T_D = 0.112$
$\sigma_0 = 4.023$
$2t_d^{-1} / \sigma_0 \eta_0$
T_D / T
10^{-1}
10^{-2}
10^{-3}
10^{-4}
10^{-5}
10^{-6}
10
20
40
60
80
100
120
140

FIGURE 13. The sticking coefficient as a function of temperature for Devonshire's (D) expression (1.31), Brenig's (B) expression (1.30), and the expression (3.20) proposed in this thesis (S).

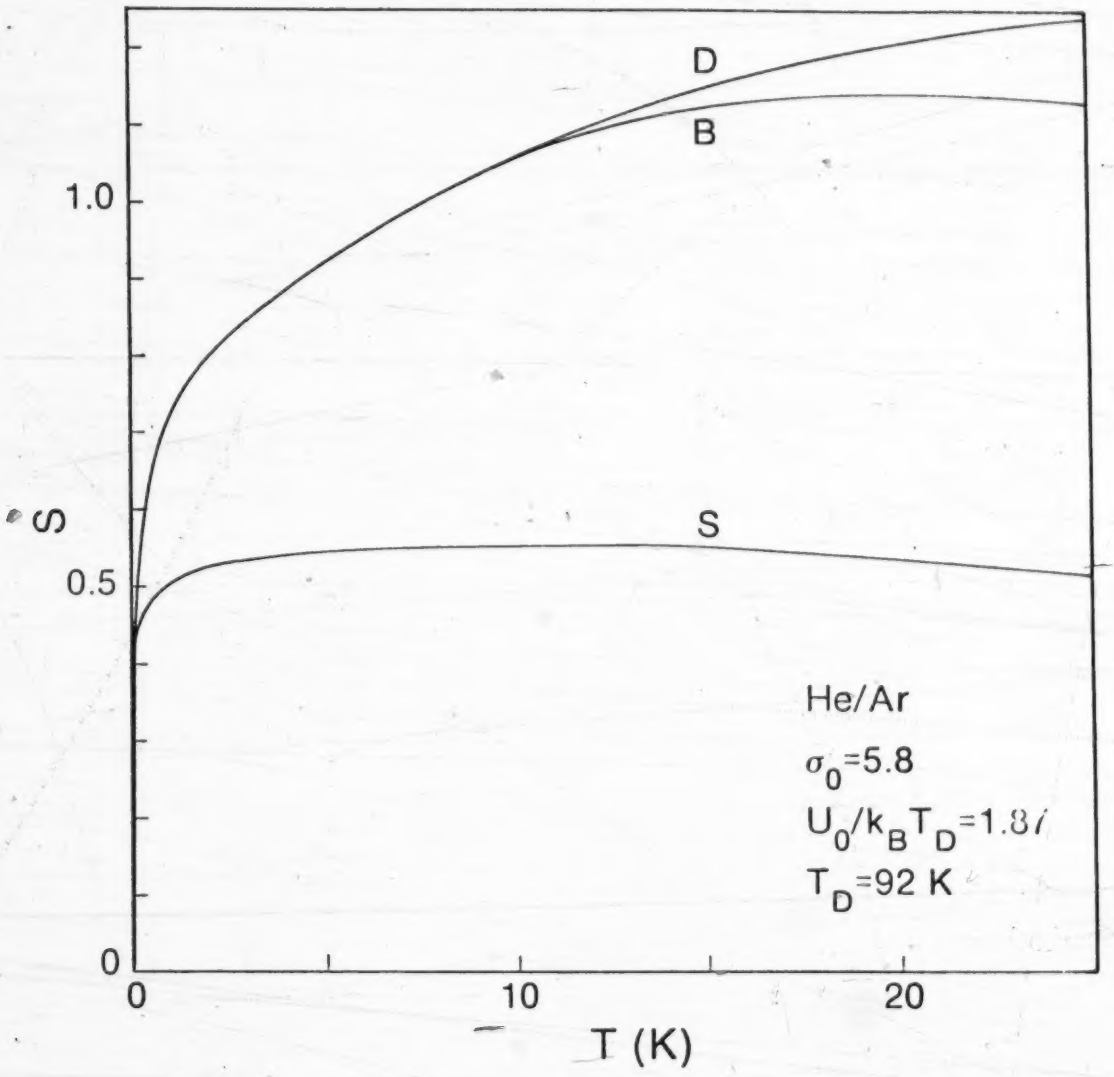
D
B
S
1.0
0.5
0
0
10
20
T (K)
He/Ar
σ_0=5.8
U_0/k_BT_D=1.87
T_D=92 K

FIGURE 14. The (R) readsorption coefficient (3.29), exact (S) sticking coefficient (3.20), and the approximate sticking coefficient (7.6) as functions of temperature for a Xe/W system with 240 bound states. The exact sticking coefficient is shown by the solid curve while the approximate expression is denoted by the dashed curve. The dotted curve is the readsorption coefficient.

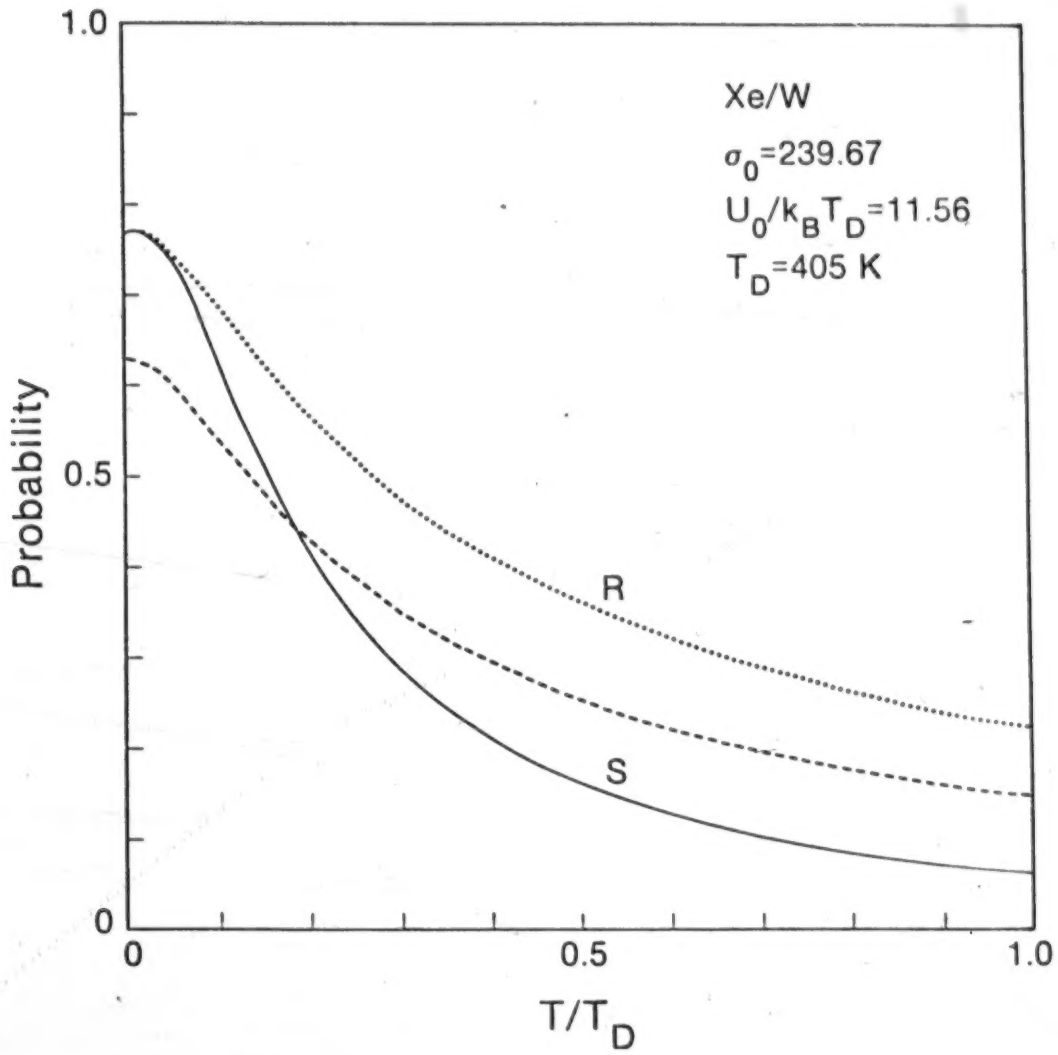
1.0
0.5
0
Probability
0
0.5
1.0
T/T_D
Xe/W
σ_0=239.67
U_0/k_BT_D=11.56
T_D=405 K
R
S

FIGURE 15. The same as Fig. 7.2 but for a Xe/W system with only 80 bound states.

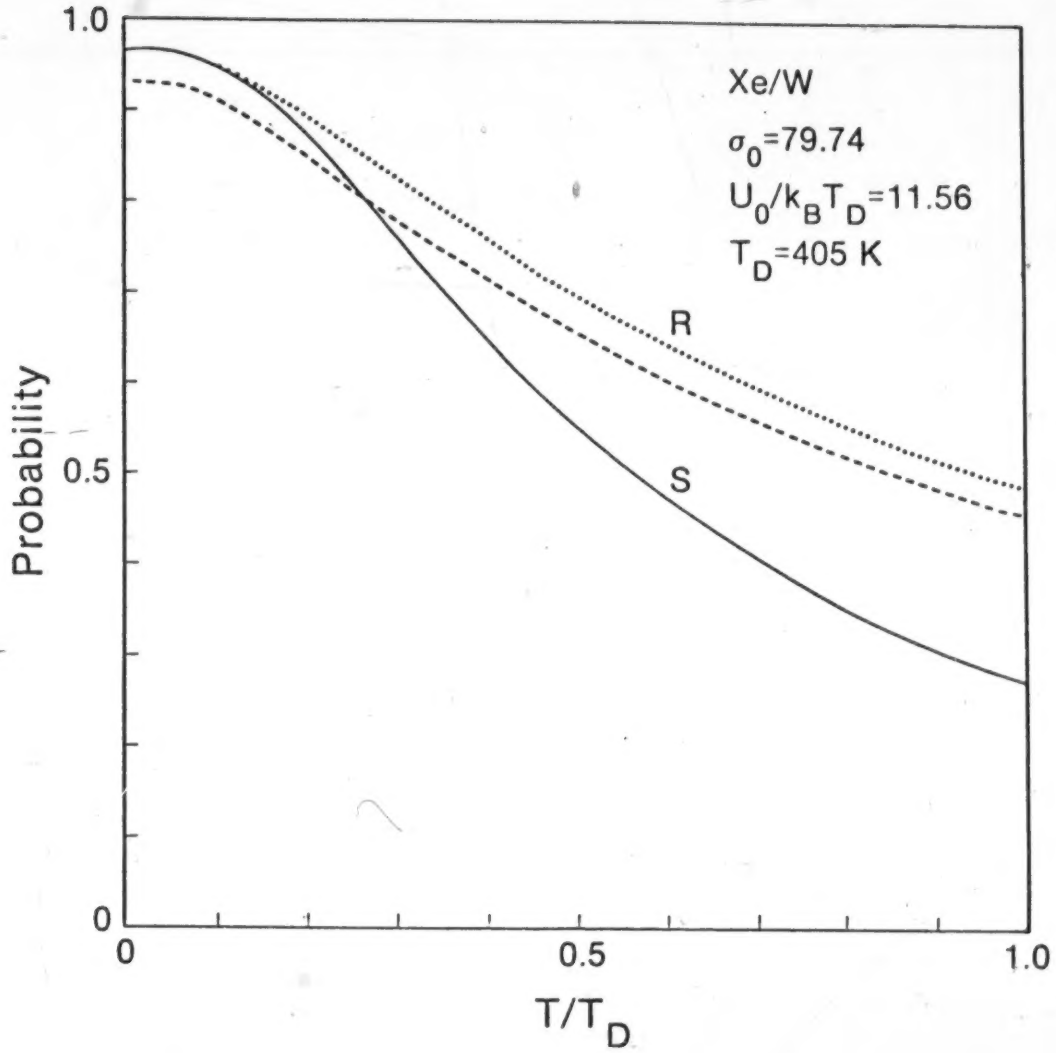
1.0
0.5
0
Probability
0
0.5
1.0
T/T_D
Xe/W
σ_0=79.74
U_0/k_BT_D=11.56
T_D=405 K
R
S

FIGURE 16. The same as Fig. 7.2 but for an Ar/Ag system with 77 bound states.

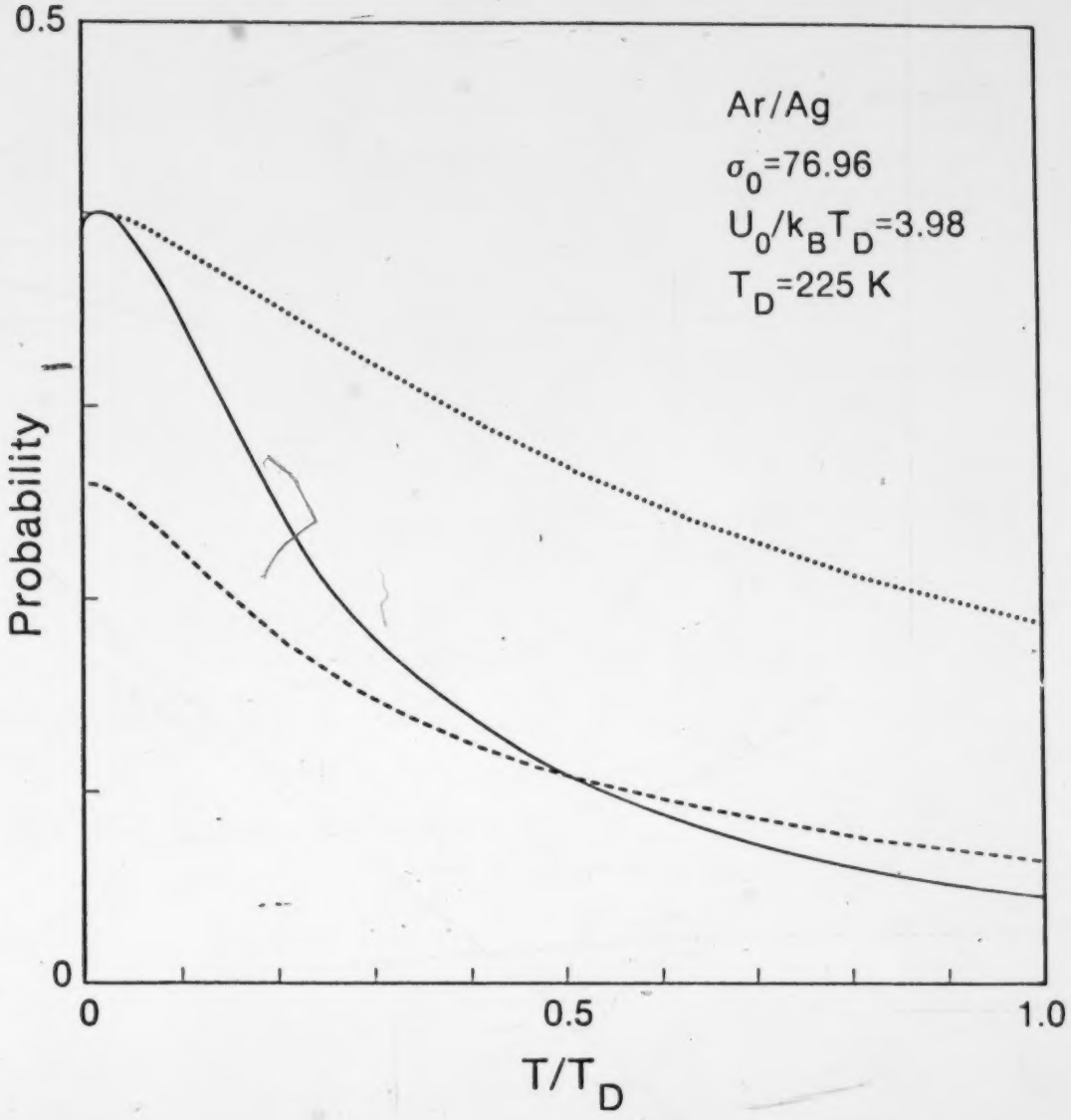
0.5
Ar/Ag
σ_0=76.96
U_0/k_BT_D=3.98
T_D=225 K
Probability
0
0
0.5
1.0
T/T_D

References

1. R.H. Williams and I.T. McGovern, Chap. 6 (Adsorption on Semiconductors) in *The Chemical Physics of Solid Surfaces and Heterogeneous Catalysis, Vol.3B: Chemisorbed Systems*, Eds. D. A. King and D. P. Woodruff (Elsevier, Amsterdam, 1984).

2. A. Clark, *The Theory of Adsorption and Catalysis*, (Academic, New York, 1970).

3. H. J. Kreuzer and Z. W. Gortel, *Physisorption Kinetics*, (Springer, Berlin, 1986).

4. T. N. Rhodin and D. L. Adams, Chap. 6 (Adsorption of Gases on Solids) in *Treatise on Solid State Chemistry, Vol.6A:Surfaces 1* Ed. N. B. Hannay, (Plenum, New York, 1976).

5. T.B. Grimley, Chap. 6 (Theory of Chemisorption) in *The Chemical Physics of Solid Surfaces and Heterogeneous Catalysis, Vol.2: Adsorption at Solid Surfaces*, Eds. D. A. King and D. P. Woodruff, (Elsevier, Amsterdam, 1984).

6. *Theory of Chemisorption*, Ed. J. R. Smith, (Springer-Verlag, Berlin, 1980).

7. J.E. Inglesfield and B. W. Holland, Chap. 3 (Electrons at Surfaces) in *The Chemical Physics of Solid Surfaces and Heterogeneous Catalysis, Vol.1: Adsorption at Solid Surfaces*, Eds. D. A. King and D. P. Woodruff, (Elsevier, Amsterdam, 1984).

8. J. R. Smith, Chap. 1 (Theory of Electronic Properties of Surfaces) in *Interactions on Metal Surfaces*, Ed. R. Gomer, (Springer, Berlin, 1975).

9. T.E. Madey, J.T. Yates Jr., D.R. Sandstrom, and R. J. H. Voorhoeve, Chap. 1 (Catalysis by Solid Surfaces) in *Treatise on Solid State Chemistry, Vol.6B:Surfaces 2*, Ed. N. B. Hannay, (Plenum, New York, 1976).

10. *The Chemical Physics of Solid Surfaces and Heterogeneous Catalysis, Vol.4: Fundamental Studies of Heterogeoneous Catalysis* Eds. D. A. King and D. P. Woodruff, (Elsevier Amsterdam, 1984).

11. R. J. H. Voorhoeve, Chap. 4 (Molecular Beam Deposition of Solids on Surfaces) in *Treatise on Solid State Chemistry, Vol.6A:Surfaces 1*, Ed. N. B. Hannay, (Plenum, New York, 1976).

12. G. N. Patterson, *Molecular Nature of Aerodynamics*, (University of Toronto Institute of Aerospace Studies, Toronto, 1981).

13. S. R. Morrison, Chap. 3 (Semiconductor Surfaces) in *Treatise on Solid State Chemistry, Vol.6B: Surfaces 2*, Ed. N. B. Hannay, (Plenum, New York, 1976).

14. M. W. Cole, D. R. Frankel, and D. L. Goodstein, Rev. Mod. Phys. **53**, 199 (1981).

15. A. A. Maradudin, E. W. Montroll, G. H. Weiss, and I. P. Ipatova, *Theory of Lattice Dynamics in the Harmonic Approximation* 2nd. Ed. (Academic, New York, 1971).

16. I. Langmuir, Phys. Rev. **2**, 329 (1913).

17. I. Langmuir, J. Am. Chem. Soc. **40**, 1361 (1918).

18. C. Wang and R. Gomer, Surf. Sci. **84**,329 (1979).

19. K. Christmann and J. E. Demuth, Surf. Sci. **120**, 291 (1982).

20. I. Frenkel, Z. Phys. **26**, 117 (1924).

21. H. J. Kreuzer and P. Summerside, Surf. Sci. **111**, 102 (1981).

22. P. Summerside, E. Sommer, H. J. Kreuzer, and R. Teshima, Phys. Rev. B **25**, 6235 (1982).

23. E. Sommer and H. J. Kreuzer, Phys. Rev. B **26**, 658 (1982).

24. E. Sommer and H. J. Kreuzer, Phys. Rev. B **26**, 4094 (1982).

25. E. Sommer and H. J. Kreuzer, Phys. Rev. Lett. **49**, 61 (1982).

26. E. Sommer and H. J. Kreuzer, Surf. Sci. **119**, L331 (1982).

27. M. Sinvani, P. Taborek, and D. L. Goodstein, Phys. Rev. Lett. **48**, 1259 (1982).

28. D. Menzel, Chap. 4 (Desorption Phenomena) in *Interactions on Metal Surfaces*, Ed. R. Gomer (Springer, Berlin, 1975).

29. Z. W. Gortel, H. J. Kreuzer, and R. Teshima, Phys. Rev. B **22**, 5655 (1980).

30. Z. W. Gortel, H. J. Kreuzer, R. Teshima, and L. A. Turski, Phys. Rev. B **24**, 4456 (1981).

31. H. J. Kreuzer and R. Teshima, Phys. Rev. B **24**, 4470 (1981).

32. J. E. Lennard-Jones and C. Strachan, Proc. Roy. Soc.(London)A **150**, 442 (1935).

33. C. Strachan, Proc. Roy. Soc.(London)A **150**, 456 (1935).

34. J. E. Lennard-Jones and A. F. Devonshire, Proc. Roy. Soc.(London)A **156**, 6 (1936).

35. J. E. Lennard-Jones and A. F. Devonshire, Proc. Roy. Soc.(London)A **156**, 29 (1936).

36. A. F. Devonshire, Proc. Roy. Soc. (London) A **156**, 37 (1936).

37. J. E. Lennard-Jones and A. F. Devonshire, Proc. Roy. Soc.(London)A **158**, 242 (1937).

38. J. E. Lennard-Jones and A. F. Devonshire, Proc. Roy. Soc.(London)A **158**, 253 (1937).

39. A. F. Devonshire, Proc. Roy. Soc. (London) A **158**, 269 (1937).

40. C. Strachan, Proc. Roy. Soc.(London)A **158**, 591 (1937).

41. Z. W. Gortel and H. J. Kreuzer, Surf. Sci. **133**, L359 (1985).

42. Z. W. Gortel and H. J. Kreuzer, Surf. Sci. **133**, 484 (1983).

43. Z. W. Gortel, H. J. Kreuzer, M. Schäff, and G. Wedler, Surf. Sci. **134**, 577 (1983).

44. H. J. Kreuzer and D. N. Lowy, Chem. Phys. Lett. **78**, 50 (1981).

45. Z. W. Gortel, H. J. Kreuzer, P. Piercy, and R. Teshima, Phys. Rev. B **27**, 5066 (1983).

46. Z. W. Gortel, H. J. Kreuzer, P. Piercy, and R. Teshima, Phys. Rev. B **28**, 2119 (1983).

47. Z. W. Gortel and H. J. Kreuzer, Phys. Rev. B **29**, 6926 (1984).

48. C. Jedrzejek, K. F. Freed, S. Efrima, and H. Metiu, Chem. Phys. Lett. **74**, 43 (1980).

49. C. Jedrzejek, K. F. Freed, S. Efrima, and H. Metiu, Chem. Phys. Lett. **79**, 227 (1981).

50. G. Koreniewski, E. Hood, and H. Metiu, J. Vac. Sci. Technol. **20**, 594 (1982).

51. K. F. Freed, H. Metiu, E. Hood, and C. Jedrzejek, in *Intramolecular Dynamics*, Eds. J. Jortner and B. Pullman (Reidel, Dordrecht, 1982).

52. S. Efrima, C. Jedrzejek, K. F. Freed, E. Hood, and H. Metiu, J. Chem. Phys. **79**, 2436 (1983).

53. E. Hood, C. Jedrzejek, K. F. Freed, E. Hood, and H. Metiu, J. Chem. Phys. **81**, 3277 (1984).

54. E. Hood and H. Metiu, in *Many-Body Phenomena at Surfaces*, Ed. D. Langreth and H. Suhl, (Academic, San Francisco, 1984).

55. F. O. Goodman, Surf. Sci. **24**, 667 (1971).

56. B. L. Bonch-Bruevich, Usp. Fiz. Nauk. **40**, 369 (1950).

57. N. Cabrera, V. Celli, F. O. Goodman, and R. Manson, Surf. Sci. **19**, 67 (1970).

58. F. O. Goodman, Surf. Sci. **19**, 93 (1970).

59. F. O. Goodman and J. D. Gillerlain, J. Chem. Phys. **54**, 3077 (1971).

60. N. Garcia, V. Celli, and R. F. Manson, J. Chem. Phys. **67**, 3436 (1980).

61. F. O. Goodman, Prog. Surf. Sci. **5**, 261 (1975).

62. F. O. Goodman, Surf. Sci. **111**, 279 (1981).

63. W. L. Schaich, J. Phys. C **11**, 2519 (1978).

64. E. Montroll and K. E. Shuler, Adv. Chem. Phys. **1**, 361 (1958).

65. H. A. Kramers, Physica **7**, 284 (1940).

66. S. K. Kim, J. Chem. Phys. **28**, 1057 (1958).

67. S. C. Ying and B. Bendow, Phys. Lett. A **37**, 91 (1971).

68. B. Bendow and S. C. Ying, J. Vac. Sci. Technol. **9**, 804 (1972).

69. B. Bendow and S. C. Ying, Phys. Rev. B **7**, 622 (1973).

70. S. C. Ying and B. Bendow, Phys. Rev. B **7**, 637 (1973).

71. E. G. d'Agliano, P. Kumar, W. L. Schaich, and H. Suhl, in *Nobel Symposium Twenty Four: Collective Properties of Physical Systems*, Eds. B. Lundqvist and S. Lundqvist, (Academic, New York, 1973).

72. E. G. d'Agliano, P. Kumar, W. L. Schaich, and H. Suhl, Phy. Rev. B **11**, 2122 (1975).

73. W. L. Schaich, J. Chem. Phys. **60**, 1087 (1974).

74. P. Mazur and I. Oppenheim, Physica (Utr.)**50**, 241 (1970).

75. I. Oppenheim and S. K. Kim, Physica (Utr.)**57**, 469 (1972).

76. R. Zwanzig, J. Chem. Phys. **33**, 1338 (1960).

77. R. Kubo J. Phys. Soc. Japan **12**, 570 (1957).

78. W. Brenig, Z. Phys. B **36**, 81 (1979).

79. J. Böheim and W. Brenig, Z. Phys. **41**,243 (1981).

80. G. Iche and P. Nozières, J. Phys. (France) **37**, 1313 (1976).

81. R. Sedlmeir and W. Brenig, Z. Phys. B **36**, 245 (1980).

82. W. Brenig, Z. Phys. B **36**, 227 (1980).

83. J. Böheim, W. Brenig, and J. Stutzki, Z. Phys. B **48**, 43 (1982).

84. J. Stutzki and W. Brenig, Z. Phys. B **45**, 49 (1981).

85. J. Böheim, Surf. Sci. **148**, 463 (1984).

86. W. Brenig, Z. Physik B **48**, 127 (1982).

87. U.Leuthäusser, Z. Phys. B **44**, 101 (1981).

88. U.Leuthäusser, Z. Phys. B **50**, 65 (1983).

89. U.Leuthäusser, Surf. Sci. **145**, 48 (1984).

90. D. B. Jack and H. J. Kreuzer, Phys. Rev. B **26**, 6516 (1982).

91. D. B. Jack and H. J. Kreuzer, Phys. Rev. B **31**, 2514 (1985).

92. J. E. Lennard-Jones, Proc. Roy. Soc. (London) A **163**, 127 (1973).

93. N. B. Slater, Proc. Roy. Soc. (London) A **194**, 112 (1948).

94. N. Cabrera, Discuss. Far. Soc. **28**, 16 (1959).

95. R. W. Zwanzig, J. Chem. Phys., **32**, 1173 (1960).

96. B. McCarroll and G. Ehrlich, J. Chem. Phys. **38**, 523 (1963).

97. F. O. Goodman, Surf. Sci. **3**, 386 (1965).

98. F. O. Goodman, Surf. Sci. **5**, 283 (1966).

99. F. O. Goodman, Surf. Sci. **11**, 283 (1968).

100. G. Armand, Surf. Sci. **9**, 145 (1968).

101. G. Armand, Surf. Sci. **66**, 321 (1977).

102. J. L. Beeby and L. Dobrzynski, J. Phys. C **4**, 1269 (1971).

103. J. L. Beeby and E. G. Thomas, J. Phys. C **7**, 2157 (1974).

104. S. Hollway and J. L. Beeby, J. Phys. C **8**, 3531 (1975).

105. P. Jewsbury and J. L. Beeby, J. Phys. C **8**, 3541 (1975).

106. S. Holloway and P. Jewsbury, J. Phys. C **9**, 1907 (1976).

107. P. Jewsbury and S. Holloway, J. Phys. C **9**, 3205 (1976).

108. S. Holloway, P. Jewsbury, and J. L. Beeby, Surf. Sci. **63**, 339 (1977).

109. P. Jewsbury, J. Phys. C **10**, 671 (1977).

110. J. L. Beeby and B. K. Agrawal, Surf. Sci. **122**, 447 (1982).

111. R. M. Logan and R. E. Stickney, J. Chem. Phys. **44**, 195 (1966).

112. W. H. Weinberg and R. P. Merill, J. Vacuum Sci. Tech. **8**, 718 (1971).

113. R. M. Logan and J. C. Keck, J. Chem. Phys. **49**, 860 (1968).

114. R. M. Logan, Surf. Sci. **15**, 387 (1969).

115. P. J. Pagni and J. C. Keck, J. Chem. Phys. **58**, 1162 (1973).

116. P. J. Pagni, J. Chem. Phys. **58**, 2940 (1973).

117. A. T. Modak and P. J. Pagni, J. Chem. Phys. **59**, 2019 (1973).

118. A. T. Modak and P. J. Pagni, J. Chem. Phys. **65**, 1327 (1976).

119. C. Caroli, B. Roulet, and D. Saint-James, Phys. Rev. B **18**, 545 (1978).

120. T. A. Bak and K. Anderser., Mat. Fys. Medd. Dan. Vid. Selsk. **33**, Art. no. 7 (1961).

121. T. A. Bak, *Contributions to the Theory of Chemical Kinetics*, (Munksgaard, Copenhagen, 1963).

122. V. M. Zatsepin, Teor. Eksper. Khim. **14-4**, 522 (1979).

123. W. Brenig and K. Schönhammer, Z. Phys. B **24**, 91 (1976).

124. H. Müller and W. Brenig, Z. Phys. B **34**, 165 (1979).

125. A. C. Diebold, S. A. Adelman, and C. Y. Mou, J. Chem. Phys. **71**, 3236 (1979).

126. S. A. Adelman, Adv. Chem. Phys. **44**, 43 (1980).

127. J. Doll, in *Aerosol Microphysics*, Ed. W. H. Marlow (Springer, New York, 1980).

128. J. C. Tully, J. Chem. Phys. **73**, 1975 (1980).

129. J. C. Tully, Annu. Rev. Phys. Chem. **31**, 319 (1980).

130. J. C. Tully, Surf. Sci. **111**, 461 (1981).

131. J. C. Tully, Acc. Chem. Res. **14**, 188 (1981).

132. E. Zaremba and W. Kohn, Phys. Rev. B **13**, 2270 (1976).

133. E. Zaremba and W. Kohn, Phys. Rev. B **15**, 1769 (1977).

134. G. Vidali and M. W. Cole, Surf. Sci. **110**, 10 (1981).

135. G. Vidali, M. W. Cole, and J. R. Klein, Phys. Rev. B **28**, 3064 (1983).

136. G. Vidali, M. W. Cole, and J. R. Klein, Phys. Rev. B **29**, 6736 (1984).

137. X. P. Jiang, F. Toigo, M. W. Cole, Surf. Sci. **145**, 281 (1984).

138. X. P. Jiang, F. Toigo, M. W. Cole, Surf. Sci. **148**, 21 (1984).

139. G. P. Brivio and T. B. Grimley, Surf. Sci. **131**, 475 (1983).

140. G. P. Brivio and T. B. Grimley, Surf. Sci. **161**, L573 (1985).

141. N. G. van Kampen, Can. J. Phys. **39**, 551 (1961).

142. N. G. van Kampen, Adv. Chem. Phys. **14**, 245 (1976).

143. N. G. van Kampen, *Stochastic Processes in Physics and Chemistry*, (North-Holland, Amsterdam, 1981).

144. N. G. van Kampen and I. Oppenheim, J. Math. Phys. **13**, 842 (1972).

145. R. F. Pawula, Phys. Rev. **162**, 186 (1967).

146. R. Courant and D. Hilbert, *Methods of Mathematical Physics*, (Interscience, New York, 1953).

147. P. M. Morse and H. Feshbach, *Methods of Theoretical Physics*, (McGraw-Hill, New York, 1953).

148. N. G. van Kampen, Physica Norvegica, **5**, 279 (1971).

149. J. C. Keck, J. Chem. Phys. **46**, 4211 (1965).

150. *Handbook of Mathematical Functions*, Eds. M. Abramowitz and I. A. Stegun, (National Bureau of Standards(U.S.A.), Washington, 1972).

151. T. J. Lee, Surf. Sci. **44**, 389 (1974).

152. M. Sinvani, M. W. Cole, and D. L. Goodstein, Phys. Rev. Lett. **48**, 1259 (1983).

153. G. Ehrlich, Advan. Catalysis **14**, 225 (1963).

154. M. J. Dresser, T. E. Madey, and J. T. Yates Jr., Surf. Sci. **42**, 533 (1974).

155. J. T. Yates Jr., and N. E. Erikson, Surf. Sci. **44**, 489 (1974).

156. C. Wang and R. Gomer, Surf. Sci. **84**, 329 (1979).

157. I. S. Gradsteyn and I. M. Ryzhik, *Table of Integrals, Series, and Products*, 4th. ed. (Academic, New York, 1980).

Appendix A

Properties of the Desorption Eigenvectors and Eigenvalues

This appendix lists the properties of the eigenvectors and eigenvalues of the master equation modified for desorption. The master equation is altered from its full form through the exclusion of continuum to bound state transitions, i.e.

$$\dot{n}_i(t) = \sum_{j=0}^{N-1} W_{ij} n_j(t) - \sum_{j=0}^{N-1} W_{ji} n_i(t) - \sum_{k=-\infty}^{\infty} W_{ki} n_i(t) \ . \qquad (A.1)$$

Solutions of this equation may be expressed as

$$n_i(t) = \sum_{\nu=0}^{N-1} \sum_{j=0}^{N-1} n_j(0) e_j^{(\nu)} e_i^{(\nu)} e^{-\lambda_\nu t} \ , \qquad (A.2)$$

where the left and right hand eigenvectors, and their associated eigenvalue satisfy

$$\sum_{i=0}^{N-1} \tilde{e}_i^{(\nu)} \left\{ W_{ij} - \sum_{i'=0}^{N-1} W_{ij} \delta_{ij} - \sum_{k=-\infty}^{\infty} W_{kj} \delta_{ij} \right\} = - \lambda_\nu \tilde{e}_j^{(\nu)} \ , \qquad (A.3)$$

and

$$\sum_{j=0}^{N-1} \left\{ W_{ij} - \sum_{i'=0}^{N-1} W_{i'j} \delta_{ij} - \sum_{k=-\infty}^{\infty} W_{kj} \delta_{ij} \right\} e_j^{(\nu)} = - \lambda_\nu e_i^{(\nu)} \ , \qquad (A.4)$$

respectively. The left and right hand eigenvectors are orthonormal

$$\sum_{i=0}^{N-1} \tilde{e}_j^{(\nu)} e_i^{(\nu')} = \delta_{\nu\nu'} \ , \qquad (A.5)$$

satisfy the completeness relation

$$\sum_{\nu=0}^{N-1} \tilde{e}_i^{(\nu)} e_i^{(\nu)} = \delta_{ij} \ , \qquad (A.6)$$

and are related through the expression

$$e_i^{(\nu)} = \left(\sum_{j=0}^{N-1} n_j^{eq} \right)^{-1} \tilde{e}_i^{(\nu)} n_i^{eq} \quad . \tag{A.7}$$

This last relation is a consequence of the bound state to bound state transition rates satisfying the principle of detailed balance

$$W_{ij} n_j^{eq} = W_{ji} n_i^{eq} \quad , \tag{A.8}$$

as may be seen by inserting Eq. (A.7) into (A.4). It is easily shown that for equilibrium, $\lambda_0 = 0$, the right eigenvector is given by the Boltzmann distribution, i.e.

$$e_i^{(o)} = n_i^{eq} \quad . \tag{A.9}$$

Using Eq. (A.7) it is then apparent that the left hand eigenvector associated with the equilibrium state is simply a vector whose elements are all equal to one, i.e.

$$\tilde{e}_i^{(o)} = 1 \quad . \tag{A.10}$$

By summing over the free index in Eqs. (A.3) and (A.4) the eigenvalue may be expressed as

$$\lambda_\nu = \left(\sum_{j=0}^{N-1} e_j^{(\nu)} \right)^{-1} \sum_{i=0}^{N-1} \sum_{k=-\infty}^{\infty} W_{ki} e_i^{(\nu)} \quad , \tag{A.11}$$

or

$$\lambda_\nu = \left(\sum_{j=0}^{N-1} n_j^{eq} \tilde{e}_j^{(\nu)} \right) \sum_{i=0}^{N-1} \sum_{k=-\infty}^{\infty} W_{ki} n_i^{eq} \tilde{e}_i^{(\nu)} \quad . \tag{A.12}$$

Appendix B

The Use of Laplace Transforms

In this appendix the technique of Laplace Transforms is used to solve the master equation for the gas phase as well as the integral equation for the adsorbate distribution function, Eq. (3.13).

The discrete rate equation for the gas phase (3.3) is

$$\dot{n}_k(t) = \sum_i \left[W_{ki} n_i(t) - W_{ik} n_k(t) \right] + \frac{\dot{n}_k}{mL} \left[n_k^{eq} - n_k(t) \right] . \qquad (B.1)$$

The Laplace transform of (B.1) is

$$sN_k(s) - n_k(o) = \sum_i \left[W_{ki} N_i(s) - W_{ik} N_k(s) \right] + \frac{\dot{n}_k}{mL} \left[\frac{1}{s} n_k^{eq} - N_k(s) \right] , \qquad (B.2)$$

where $N_k(s)$ is the Laplace transform of $n_k(t)$, i.e.

$$N_k(s) = \int_0^\infty dt \; e^{-st} n_k(t) , \qquad (B.3)$$

and the inverse transform is

$$n_k(t) = \frac{1}{2\pi i} \int_{c-i\infty}^{c+i\infty} ds \; e^{st} N_k(s) , \qquad (B.4)$$

where c is a positive constant. A rearrangement of terms in Eq. (B.2) yields

$$N_k(s) = \frac{\left(\frac{\dot{n}_k}{mL}\right) n_k^{eq}}{s \left(s + \sum_i W_{ik} + \frac{\dot{n}_k}{mL} \right)} + \frac{n_k(0)}{\left(s + \sum_i W_{ik} + \frac{\dot{n}_k}{mL} \right)} + \frac{\sum_k W_{ki} N_i(s)}{\left(s + \frac{\dot{n}_k}{mL} + \sum_i W_{ik} \right)} . \qquad (B.5)$$

The inverse transform of Eq. (B.5) is

$$n_k(t) = n_k(0)e^{-\mu_k t} + \sum_i W_{ki} e^{-\mu_k t} \int_0^t dt' e^{\mu_k t'} n_i(t')$$

$$+ \frac{n_k^{eq}}{2\pi i} \int_{c-i\infty}^{c+i\infty} ds\, e^{st} \left[\frac{1}{s} - \frac{1}{(s+\mu_k)} \right] \frac{\dot{m}_k}{mL\mu_k} , \qquad \text{(B.6)}$$

or

$$n_k(t) = n_k(0)e^{-\mu_k t} + \frac{\dot{m}_k}{mL}\left(1 - e^{-\mu_k t}\right) + \sum_k W_{ki} e^{-\mu_k t} \int_0^t dt' e^{\mu_k t'} n_i(t'), \qquad \text{(B.7)}$$

where

$$\mu_k = \frac{\dot{m}_k}{mL} + \sum_i W_{ik} . \qquad \text{(B.8)}$$

Equation (B.6) occurs in chapter 3 as Equation (3.5).

The Laplace transform is also useful for solving the following integral equation (3.13),

$$n(t) = \frac{1}{\lambda_o}\left(1 - e^{-\lambda_o t}\right) \sum_j \sum_k \tilde{e}_j W_{jk} \frac{\dot{m}_k}{mL} n_k^{eq} \frac{1}{\mu_k}$$

$$+ \sum_j \sum_k \sum_i \tilde{e}_j W_{jk} \frac{1}{\mu_k} W_{ki} e^{-\lambda_o t} \int_0^t dt' e^{\lambda_o t'} n(t'). \qquad \text{(B.9)}$$

The Laplace transform of Eq. (B.9) is

$$N(s) + \frac{1}{\lambda_o}\left[\frac{1}{s} - \frac{1}{s+\lambda_o}\right]\sum_j\sum_k \tilde{e}_j W_{jk}\frac{\hbar k}{mL}\frac{n_k^{eq}}{\mu_k}$$

$$+\sum_i\sum_j\sum_k \tilde{e}_j W_{jk}\frac{1}{\mu_k}W_{ki}e_i\frac{N(s)}{s+\lambda_o} . \qquad (B.10)$$

A rearrangement of terms yields

$$\frac{N(s)}{(s+\lambda_o)}\left[s+\lambda_o - \sum_i\sum_j\sum_k \tilde{e}_j W_{jk}\frac{1}{\mu_k}W_{ki}e_i\right] = \frac{1}{s+\lambda_o}\sum_j\sum_k \tilde{e}_j W_{jk}\frac{\hbar k}{mL}\frac{n_k^{eq}}{\mu_k} , \qquad (B.11)$$

or

$$N(s) = \frac{1}{\lambda_o(1-R)}\left[\frac{1}{s} - \frac{1}{s+\lambda_o(1-R)}\right]\cdot\left[\sum_j\sum_k \tilde{e}_j W_{jk}\frac{\hbar k}{mL}\frac{n_k^{eq}}{\mu_k}\right] , \qquad (B.12)$$

where

$$R = \frac{1}{\lambda_o}\sum_j\sum_k \tilde{e}_j W_{jk}\frac{1}{\mu_k}W_{ki}e_i . \qquad (B.13)$$

The inverse transform of Eq. (B.12) is

$$n(t) = \frac{1}{\lambda_o(1-R)}\left(1 - e^{-\lambda_o(1-R)t}\right)\left[\sum_j\sum_k \tilde{e}_j W_{jk}\frac{\hbar k}{mL}\frac{n_k^{eq}}{\mu_k}\right] . \qquad (B.14)$$

By multiplying (B.14) by e_i, Eq. (3.14) is obtained.

Appendix C

The Phonon Mediated Transition Rates

In this appendix the phonon mediated transition rates, for both the discrete and continuous case are listed. Originally derived by Lennard-Jones, Strachan, and Devonshire the following forms used by Gortel and Kreuzer are listed.

The transition rate between the discrete bound states i and j of a Morse potential (See Eq. (1.5)) is

$$W_{ij} = \frac{3\pi}{2}\omega_D \frac{m}{M}\left(\frac{U_o}{\hbar\omega_D}\right)^4 \sigma_o^{-6}\,(2\sigma_o-2i-1)(2\sigma_o-2j-1)(2\sigma_o-i-j-1)^3$$

$$\left\{\Theta(i-j)\,\Theta\left(1-\frac{U_o(i-j)(2\sigma_o-i-j-1)}{\hbar\omega_D\sigma_o^2}\right)\frac{i!}{j!}\frac{\Gamma(2\sigma_o-i)}{\Gamma(2\sigma_o-j)}(i-j)^3\right.$$

$$\left[\exp\left(U_o(i-j)(2\sigma_o-i-j-1)/\sigma_o^2\,k_BT\right)-1\right]^{-1}$$

$$+\Theta(j-i)\,\Theta\left(1-\frac{U_o(j-i)(2\sigma_o-i-j-1)}{\hbar\omega_D\sigma_o^2}\right)\frac{j!}{i!}\frac{\Gamma(2\sigma_o-j)}{\Gamma(2\sigma_o-i)}(j-i)^3$$

$$\left.\left[\left[\exp\left(U_o(j-k)\,(2\sigma_o-j-i-1)/\sigma_o^2\,k_BT\right)-1\right]^{-1}+1\right]\right\}, \qquad (C.1)$$

where Θ is the step function. The transition rate from a discrete bound state j to a continuum state k is

$$W_{kj} = \frac{\pi}{\gamma L}\frac{3\pi}{2}\omega_D\frac{m}{M}\left(\frac{U_o}{\hbar\omega_D}\right)^4\sigma_o^{-6}\,\frac{(2\sigma_o-2j-1)}{j!\Gamma(2\sigma_o-1)}\,\frac{\left(\frac{\pi k}{\gamma L}\right)\sinh\left(\frac{2\pi^2 k}{\gamma L}\right)\left|\Gamma\left(\frac{1}{2}+\sigma_o+i\frac{\pi k}{\gamma L}\right)\right|^2}{\left[\cos^2(\pi\sigma_o)+\sinh^2\left(\frac{\pi^2 k}{\gamma L}\right)\right]}$$

$$\left[(\sigma_o-j-\tfrac{1}{2})^2+\left(\frac{\pi k}{\gamma L}\right)^2\right]^3\left[\exp\left(\frac{U_o}{\hbar\omega_D\sigma_o^2}\left((\sigma_o-j-\tfrac{1}{2})^2+\left(\frac{\pi k}{\gamma L}\right)^2\right)\right)-1\right]^{-1}, \qquad (C.2)$$

while the transition rate from a continuum state k to a bound state j is given by

$$W_{jk} = \frac{\pi}{\gamma L}\frac{3\pi}{2}\omega_D \frac{m}{M}\left(\frac{U_o}{\hbar\omega_D}\right)^4 \sigma_o^{-8} \frac{(2\sigma_o - 2j - 1)}{j!\,\Gamma(2\sigma_o - j)} \frac{\left(\frac{\pi k}{\gamma L}\right) \sinh\left(\frac{\pi^2 k}{\gamma L}\right) \left|\Gamma\left(\frac{1}{2} + \sigma_o + i\frac{\pi k}{\gamma L}\right)\right|^2}{\left[\cosh^2(\pi\sigma_o) + \sinh^2\left(\frac{\pi^2 k}{\gamma L}\right)\right]}$$

$$\left[(\sigma_o - j - \tfrac{1}{2})^2 + \left(\frac{\pi k}{\gamma L}\right)^2\right]^3 \left[1 + \left[\exp\left(\frac{U_o}{\hbar\omega_D \sigma_o^2}\left((\sigma_o - j - \tfrac{1}{2})^2 + \left(\frac{\pi k}{\gamma L}\right)^2\right)\right) - 1\right]^{-1}\right]. \quad \text{(C.3)}$$

The factor L is the length of the chamber which confines the gas particles.

The continuous form of the above transition rates may be written conveniently in terms of the dimensionless energy

$$\varepsilon = E/U_o \,. \quad \text{(C.4)}$$

The bound state energies are then

$$\varepsilon = \varepsilon_j = -(\sigma_o - j - \tfrac{1}{2})^2/\sigma_o^2 \,, \quad \text{(C.5)}$$

and the continuum state energies are

$$\varepsilon = \varepsilon_k = \frac{\hbar^2\pi^2 k^2}{2mU_o L^2} \,. \quad \text{(C.6)}$$

The bound state ϵ' to bound state ϵ transitions are then

$$W(\epsilon,\epsilon') = 6\pi\omega_D \frac{m}{M}\left(\frac{U_o}{\hbar\omega_D}\right)^4 (\epsilon'\epsilon)^{\frac{1}{2}}(\epsilon-\epsilon')^3 \left[\exp\left(\frac{U_o}{k_BT}(\epsilon-\epsilon')\right) - 1\right]^{-1}$$

$$\cdot\left\{\theta(\epsilon-\epsilon')\,\theta\left(1 - \frac{U_o}{\hbar\omega_D}(\epsilon-\epsilon')\right) \frac{\Gamma\left(\sigma_o(1-\sqrt{-\epsilon}) + \frac{1}{2}\right)\Gamma\left(\sigma_o(1+\sqrt{-\epsilon}) + \frac{1}{2}\right)}{\Gamma\left(\sigma_o(1-\sqrt{-\epsilon'}) + \frac{1}{2}\right)\Gamma\left(\sigma_o(1+\sqrt{-\epsilon'}) + \frac{1}{2}\right)}\right.$$

$$\left. + \theta(\epsilon'-\epsilon)\,\theta\left(1 - \frac{U_o}{\hbar\omega_D}(\epsilon'-\epsilon)\right) \frac{\Gamma\left(\sigma_o(1-\sqrt{-\epsilon'}) + \frac{1}{2}\right)\Gamma\left(\sigma_o(1+\sqrt{-\epsilon'}) + \frac{1}{2}\right)}{\Gamma\left(\sigma_o(1-\sqrt{-\epsilon}) + \frac{1}{2}\right)\Gamma\left(\sigma_o(1+\sqrt{-\epsilon}) + \frac{1}{2}\right)}\right\}, \qquad \text{(C.7)}$$

where $\epsilon<0$ and $\epsilon'<0$. The bound state, $\epsilon<0$, to continuum state, $\epsilon'>0$, transitions are

$$W(\epsilon',\epsilon) = 3\pi\omega_D \frac{m}{M}\left(\frac{U_o}{\hbar\omega_D}\right)^4 (-\epsilon'\epsilon)^{\frac{1}{2}}(\epsilon'-\epsilon)^3 \left[\exp\left(\frac{U_o}{k_BT}(\epsilon'-\epsilon)\right) - 1\right]^{-1}$$

$$\frac{\theta\left(1+\frac{U_o}{\hbar\omega_D}(\epsilon-\epsilon')\right)\,\sinh\left(2\pi\sigma_o\sqrt{\epsilon'}\right)}{\left[\sinh^2\left(\pi\sigma_o\sqrt{\epsilon'}\right) + \cos^2(\pi\sigma_o)\right]} \frac{\left|\Gamma\left(\sigma_o(1+i\sqrt{\epsilon'}) + \frac{1}{2}\right)\right|^2}{\Gamma\left(\sigma_o(1+\sqrt{-\epsilon})+\frac{1}{2}\right)\Gamma\left(\sigma_o(1-\sqrt{-\epsilon})+\frac{1}{2}\right)}, \qquad \text{(C.8)}$$

and the continuum state, $\epsilon>0$, to bound state, $\epsilon'<0$, transitions are

$$W(\epsilon,\epsilon') = 3\pi\omega_D \frac{m}{M}\left(\frac{U_o}{\hbar\omega_D}\right)(-\epsilon'\epsilon)^{\frac{1}{2}}(\epsilon'-\epsilon)^3 \left[\left[\exp\left(\frac{U_o}{k_BT}(\epsilon'-\epsilon)\right) - 1\right]^{-1} + 1\right]$$

$$\frac{\theta\left(1+\frac{U_o}{\hbar\omega_D}(\epsilon-\epsilon')\right)\,\sinh\left(2\pi\sigma_o\sqrt{\epsilon'}\right)}{\left[\sinh^2\left(\pi\sigma_o\sqrt{\epsilon'}\right) + \cos^2(\pi\sigma_o)\right]} \frac{\left|\Gamma\left(\sigma_o(1+i\sqrt{\epsilon'}) + \frac{1}{2}\right)\right|^2}{\Gamma\left(\sigma_o(1+\sqrt{-\epsilon})+\frac{1}{2}\right)\Gamma\left(\sigma_o(1-\sqrt{-\epsilon})+\frac{1}{2}\right)}. \qquad \text{(C.9)}$$

It may be readily seen that Eqs. (C.8) and (C.9) satisfy the principle of detailed

balance; i.e.

$$W(\varepsilon,\varepsilon')\, e^{-\varepsilon'\beta U_o} = W(\varepsilon',\varepsilon)\, e^{-\varepsilon\beta U_o} . \qquad (C.10)$$

It should also be noted that the continuous forms of the transition rates do not contain the factor L that the discrete forms contain. In particular, the discrete form (C.2) contains an overall factor of L^{-1} which is absent in the continuous form (C.8). This factor has in effect been cancelled by a factor of L which appears in the passage from the sum over the k states to its integral form; i.e.

$$\sum_{k=0}^{\infty} \to \frac{\sigma_o}{2}\frac{\gamma L}{\pi}\int_0^{\infty} d\varepsilon\, \frac{1}{\sqrt{\varepsilon}} \qquad (C.11)$$

so that

$$\sum_{k=0}^{\infty} W_{kj} \to \frac{\sigma_o}{2}\int_0^{\infty} d\varepsilon\, \frac{1}{\sqrt{\varepsilon}}\, W(\varepsilon,\varepsilon') = \int_0^{\infty} d\varepsilon \rho(\varepsilon)\, W(\varepsilon,\varepsilon') \qquad (C.12)$$

where

$$\rho(\varepsilon) = \frac{\sigma_o}{2}\frac{1}{\sqrt{|\varepsilon|}} . \qquad (C.13)$$

Appendix D

Calculation of the Moments of the Transition Rates

The moments of the transition rates occur in the Kramers-Moyal expansion of the Master equation and are defined as

$$\alpha_k(\varepsilon) = \int_{-1}^{\infty} d\varepsilon' \rho(\varepsilon')(\varepsilon'-\varepsilon)^k W(\varepsilon',\varepsilon) \qquad (D.1)$$

where the transition rates are given in App. C . Since only the bound state energies, $\epsilon<0$, are studied, only Eqs. (C.7) and (C.8) are needed. In order to calculate the integral in Eq. (D.1) the transition rates must be simplified . Equation (C.8) may be by noting that one of its constituent factors may be written as follows[157]

$$\frac{\sinh(2\pi\sigma_o\sqrt{\varepsilon})}{\left[\sinh^2(\pi\sigma_o\sqrt{\varepsilon}) + \cos^2(\pi\sigma_o)\right]} = 2 + 4\sum_{n=1}^{\infty}(-1)^n e^{-2\pi n\sigma_o\sqrt{\varepsilon}}\cos(2\pi\sigma_o). \qquad (D.2)$$

For $\sigma_o\sqrt{\epsilon}>1$, Eq. (D.2) may be approximated by the first term in the series; i.e.

$$\frac{\sinh(2\pi\sigma_o\sqrt{\varepsilon})}{\left[\sinh^2(\pi\sigma_o\sqrt{\varepsilon}) + \cos^2(\pi\sigma_o)\right]} \approx 2 . \qquad (D.3)$$

With this approximation Eq. (C.8) becomes the analytic continuation of Eq. (C.7). To proceed, the gamma functions must be simplified by using the asymptotic formula[150]

$$\Gamma(az+b) \simeq (2\pi)^{\frac{1}{2}}(az)^{az+b-\frac{1}{2}}e^{-az} , \qquad (D.4)$$

where $z>>1$. When $\sigma_o>>1$ the products and ratios of the gamma functions may be

approximated as

$$\frac{\Gamma\left(\left(\sigma_o(1-\sqrt{-\varepsilon}\right)+\tfrac{1}{2}\right)\Gamma\left(\sigma_o(1+\sqrt{-\varepsilon})+\tfrac{1}{2}\right)}{\Gamma\left(\sigma_o(1-\sqrt{-\varepsilon'})+\tfrac{1}{2}\right)\Gamma\left(\sigma_o(1+\sqrt{-\varepsilon'})+\tfrac{1}{2}\right)} \approx e^{-\sigma_o f(\varepsilon,\varepsilon')} , \tag{D.5}$$

and

$$\frac{\left|\Gamma\left(\sigma_o(1+i\sqrt{\varepsilon})+\tfrac{1}{2}\right)\right|^2}{\Gamma\left(\sigma_o(1-\sqrt{-\varepsilon'})+\tfrac{1}{2}\right)\Gamma\left(\sigma_o(1+\sqrt{-\varepsilon'})+\tfrac{1}{2}\right)} \approx e^{-\sigma_o f(\varepsilon,\varepsilon')} , \tag{D.6}$$

where

$$f(\varepsilon,\varepsilon') = \ln\left(\frac{1+\varepsilon'}{1+\varepsilon}\right) - 2\sqrt{-\varepsilon}\,\tanh^{-1}\left(\sqrt{-\varepsilon}\right) + 2\sqrt{-\varepsilon'}\,\tanh^{-1}\left(\sqrt{-\varepsilon'}\right) . \tag{D.7}$$

With these approximations the moments (D.1) may now be written as

$$\alpha_k(\varepsilon) = \frac{\eta\sigma_o^4}{6}\int_{\varepsilon}^{\varepsilon+\hbar\omega_D/U_o} d\varepsilon'\rho(\varepsilon')\sqrt{\varepsilon\varepsilon'}\,(\varepsilon'-\varepsilon)^{k+3}\,\frac{e^{-\sigma_o f(\varepsilon,\varepsilon')}}{e^{(\varepsilon'-\varepsilon)\beta U_o}-1}$$

$$+\frac{\eta\sigma_o^4}{6}\int_{\max(\varepsilon-\hbar\omega_D/U_o,-1)}^{\varepsilon} d\varepsilon'\rho(\varepsilon')\sqrt{\varepsilon\varepsilon'}\,(\varepsilon'-\varepsilon)^{k+3}\,\frac{e^{-\sigma_o f(\varepsilon',\varepsilon)}}{e^{(\varepsilon'-\varepsilon)\beta U_o}-1} , \tag{D.8}$$

where

$$\rho(\varepsilon') = \frac{\sigma_o}{2}\frac{1}{\sqrt{|\varepsilon'|}} , \tag{D.9}$$

and

$$\eta = 36\,\pi\omega_D\,\frac{m}{M}\left(\frac{U_o}{\sigma_o\hbar\omega_D}\right)^4 . \tag{D.10}$$

The two integrals in Eq. (D.8) are largely controlled by the exponential terms which contain the factor $\sigma_o f(\epsilon,\epsilon')$. When ϵ approaches -1 then $\sigma_o f(\epsilon,\epsilon')$ goes to infinity thus damping the integral very rapidly. The lower integration limit of the second integral in Eq. (D.8) can, therefore, be taken to be $\epsilon - h\omega_D/2\pi U_o$ for all values of ϵ'.

The introduction of the change of variable $x=\epsilon'-\epsilon$ into the first integral and $x=\epsilon-\epsilon'$ into the second integral of Eq. (D.8) yields

$$\alpha_k(\varepsilon) = \frac{\eta\sigma_o^5}{12}\sqrt{\varepsilon}\int_0^{\hbar\omega_D/U_o} dx\; x^{k+3}\left\{\frac{e^{-\sigma_o f(\varepsilon,\varepsilon+x)}}{\left[e^{x\beta U_o}-1\right]} + (-1)^k\frac{e^{-\sigma_o f(\varepsilon-x,\varepsilon)}}{\left[e^{-x\beta U_o}-1\right]}\right\}. \qquad (D.11)$$

The main contribution to the integral in Eq. (D.11) comes from around the point $x=0$. An expansion of $f(\epsilon,\epsilon+x)$ and $f(\epsilon-x,\epsilon)$ around $x=0$ yields

$$f(\varepsilon,\varepsilon+x) = \left[\frac{\tanh^{-1}(\sqrt{-\varepsilon})}{\sqrt{-\varepsilon}}\right]x + \left[\frac{1}{1+\varepsilon} - \frac{\tanh^{-1}(\sqrt{-\varepsilon})}{\sqrt{-\varepsilon}}\right]\frac{x^2}{2\varepsilon} + \cdots \qquad (D.12)$$

and

$$f(\varepsilon-x,\varepsilon) = \left[\frac{\tanh^{-1}(\sqrt{-\varepsilon})}{\sqrt{-\varepsilon}}\right]x - \left[\frac{1}{1+\varepsilon} - \frac{\tanh^{-1}(\sqrt{-\varepsilon})}{\sqrt{-\varepsilon}}\right]\frac{x^2}{2\varepsilon} + \cdots \qquad (D.13)$$

The substitution of Eqs. (D.12) and (D.13) into (D.11) gives

$$\alpha_k(\varepsilon) \approx \frac{\eta\sigma_o^4}{6}\sqrt{\varepsilon}\int_0^{\hbar\omega_D/U_o} dx\; x^{k+3}\exp\left(-\sigma_o\frac{\tanh^{-1}(\sqrt{-\varepsilon})}{\sqrt{-\varepsilon}}x\right)\left\{\frac{1-(-1)^k e^{x\beta U_o}}{\left[e^{x\beta U_o}-1\right]}\right.$$

$$\left. + \sigma_o\left[\frac{1}{1+\varepsilon} - \frac{\tanh^{-1}(\sqrt{-\varepsilon})}{\sqrt{-\varepsilon}}\right]\frac{x^2}{2\varepsilon}\left[\frac{1+(-1)^k e^{x\beta U_o}}{\left[e^{x\beta U_o}-1\right]}\right]\right\}. \qquad (D.14)$$

The moments may now be evaluated. If $k=1$ then

$$\alpha_1(\varepsilon) \approx \frac{\eta\sigma_o^5}{12}\sqrt{\varepsilon}\int_0^{\hbar\omega_D/U_o} dx\; x^4 \exp\left(-\sigma_o \frac{\tanh^{-1}(\sqrt{-\varepsilon})}{\sqrt{-\varepsilon}}\, x\right)$$

$$\cdot\left\{-1 + \sigma_o\left[\frac{1}{1+\varepsilon} - \frac{\tanh^{-1}(\sqrt{-\varepsilon})}{\sqrt{-\varepsilon}}\right]\frac{x}{\varepsilon\beta U_o}\right\}, \qquad \text{(D.15)}$$

where in the second term of the integrand the approximation

$$\coth(x\beta U_o) \approx \frac{2}{x\beta U_o} \qquad \text{(D.16)}$$

has been used. Performing the integrations in Eq. (D.15) to the lowest order in σ_o^{-1} yields

$$\alpha_1(\varepsilon) = 2\eta\sqrt{-\varepsilon}\, F_5(\tanh^{-1}(\sqrt{-\varepsilon})/\sqrt{-\varepsilon})$$

$$+ \frac{5\eta k_B T}{U_o\sqrt{-\varepsilon}}\left[\frac{1}{1+\varepsilon} - \frac{\tanh^{-1}(\sqrt{-\varepsilon})}{\sqrt{-\varepsilon}}\right]F_o(\tanh^{-1}(\sqrt{-\varepsilon}/\sqrt{-\varepsilon}) + O(\sigma_o^{-5}), \qquad \text{(D.17)}$$

where

$$F_n(s) = s^{-n}\left[1 - e^{-\sigma_o \hbar\omega_D s/U_o}\sum_{k=0}^{n-1}\frac{s^k}{k!}(\sigma_o\hbar\omega_D/U_o)^k\right]. \qquad \text{(D.18)}$$

By following the above procedure for $k=2$ one obtains

$$\alpha_2(\varepsilon) = \frac{4\eta k_B T}{U_o}\sqrt{-\varepsilon}\, F_5(\tanh^{-1}(\sqrt{-\varepsilon})/\sqrt{-\varepsilon}) + O(\sigma_o^{-5}). \qquad \text{(D.19)}$$

The function $F_n(s)$ satisfies the following property

$$\frac{\partial}{\partial s} F_n(s) = -n\, F_{n+1}(s), \qquad \text{(D.20)}$$

which is needed to obtain the relation

$$\alpha_1(\varepsilon) = -\frac{U_o}{2k_BT}\alpha_2(\varepsilon) + \frac{1}{2\rho(\varepsilon)}\frac{\partial}{\partial\varepsilon}\left(\rho(\varepsilon)\alpha_2(\varepsilon)\right) \quad . \tag{D.21}$$

This relation ensures that the Boltzmann distribution is the equilibrium solution of the Fokker-Planck equation.

Appendix E

Evaluation of Integrals from the Small Eigenvalue Method

The integrals occurring in the small eigenvalue method are evaluated. This involves the use of the asymptotic form of Dawson's integral[150],

$$D(z) = e^{-z^2} \int_0^z dt\, e^{t^2} \sim \frac{1}{2z} . \tag{E.1}$$

The integrals to be calculated are

$$I_1 = \int_0^1 ds\, e^{s^2 \beta U_o} , \tag{E.2}$$

and

$$I_2 = \int_y^1 ds \frac{s e^{-s^2 \beta U_o}}{(1-s^2)(1 - \frac{2}{3} s^2)} \int_s^1 dr\, e^{\beta U_o r^2} . \tag{E.3}$$

The integral I_1 may be written as

$$I_1 = \frac{e^{\beta U_o}}{\sqrt{\beta U_o}} D(\sqrt{\beta U_o}) , \tag{E.4}$$

and evaluated immediately

$$I_1 \sim \frac{e^{\beta U_o}}{2\sqrt{\beta U_o}} . \tag{E.5}$$

The second integral may be rewritten as follows

$$I_2(y) = \frac{1}{\sqrt{\beta U_o}} \int_y^1 ds \frac{s e^{-s^2 \beta U_o}}{(1-s^2)(1 - \frac{2}{3} s^2)} \left[e^{\beta U_o} D(\sqrt{\beta U_o}) - e^{y^2 \beta U_o} D(s\sqrt{\beta U_o}) \right] . \tag{E.6}$$

The dominant contribution to Eq. (E.6) comes near s=0. By expanding around this point one

obtains

$$L_2(y) \approx \frac{e^{\beta U_o}}{\sqrt{\beta U_o}} D(\sqrt{\beta U_o}) \int_y^1 ds\ s\ e^{-s^2 \beta U_o} \tag{E.7}$$

which with the change of variable $x = s^2 \beta U_o$ becomes

$$L_2(y) \approx \frac{e^{\beta U_o}}{2(\beta U_o)^{3/2}} D(\sqrt{\beta U_o}) \int_{y^2 \beta U_o}^{\beta U_o} dx\ e^{-x} \tag{E.8}$$

$$\approx \frac{D(\sqrt{\beta U_o})}{2(\beta U_o)^{3/2}} e^{\beta U_o (1-y^2)} \tag{E.9}$$

$$\sim \frac{e^{\beta U_o (1-y^2)}}{4(\beta U_o)^2}, \tag{E.10}$$

where exponentially small terms have been dropped and Eq. (E.1) has been used.

Appendix F

Evaluation of Integrals needed for the Sticking Coefficient

The two dimensional integrals occurring in the approximate expression (7.2) of the sticking coefficient are evaluated in this appendix. The integrals to be evaluated are

$$I_o = \int_0^{\infty} d\varepsilon \int_{-1}^{0} d\varepsilon' \, \frac{1}{\sqrt{-\varepsilon'}} \, W(\varepsilon', \varepsilon) \, e^{-\varepsilon \beta U_o} , \qquad (F.1)$$

and

$$I_1 = \int_0^{\infty} d\varepsilon \int_{-1}^{0} d\varepsilon' \, \frac{1}{\sqrt{-\varepsilon'}} \, W(\varepsilon', \varepsilon) \, e^{\varepsilon' \beta_s U_o - \varepsilon \beta_g U_o} , \qquad (F.2)$$

where the subscript s and g indicate whether the solid or gas are being referred to. Using the expressions and notation of App. C and D, the first integral may be written as

$$I_o = \int_0^{\hbar\omega_D/U_o} d\varepsilon \int_{\varepsilon - \frac{\hbar\omega_D}{U_o}}^{0} \frac{(\varepsilon - \varepsilon')^{3} \, e^{-\sigma_o f(\varepsilon', \varepsilon) - \varepsilon \beta_g U_o + (\varepsilon - \varepsilon') \beta_s U_o}}{e^{(\varepsilon - \varepsilon')\beta_s U_o} - 1} . \qquad (F.3)$$

This integral is more easily evaluated if the change of variables

$$x = (\varepsilon - \varepsilon') \qquad (F.4)$$

$$y = (\varepsilon + \varepsilon') \qquad (F.5)$$

is made so that Eq. (F.3) becomes

$$I_o = \frac{1}{2} \int_0^{\hbar\omega_D/U_o} dx \, x^3 \, \frac{e^{-\sigma_o x + (\beta_s - \beta_g/2) U_o x}}{\left[e^{x \beta U_o} - 1 \right]} \int_{-x}^{x} dy \, e^{-y \beta_g U_o/2} . \qquad (F.6)$$

The integration over y may be done exactly so that after some manipulation Eq. (F.6)

becomes

$$I_o = \frac{k_B T_g}{U_o} \int_0^{\hbar\omega_D/U_o} dx\, x^3 \, \frac{\sinh\left(xU_o/2k_B T_g\right)}{\sinh\left(xU_o/2k_B T_s\right)} \, e^{-x\left(\sigma_o + (\beta_g - \beta_s)U_o/2\right)} . \qquad \text{(F.7)}$$

Taking only the first term of the Taylor series of the hyperbolic sine yields

$$I_o \approx \frac{k_B T_s}{U_o} \int_0^{\hbar\omega_D/U_o} dx\, x^3 \, e^{-\left(\sigma_o + \frac{1}{2}U_o(\beta_g - \beta_s)\right)} \qquad \text{(F.8)}$$

$$\approx \frac{6k_B T_s}{U_o \sigma_o^4} F_4 \left(1 + \frac{U_o}{2k_B \sigma_o} \left(\frac{1}{T_g} - \frac{1}{T_s}\right)\right) , \qquad \text{(F.9)}$$

where the function F_4 is defined by Eq. (D.18).

By following an identical procedure the other integral (F.2) may be evaluated approximately as

$$I_1 \sim \frac{k_B T_s}{U_o} \int_0^{\hbar\omega_D/U_o} dx\, x^3 \, e^{-x(\sigma_o + \beta_g U_o/2)} \qquad \text{(F.10)}$$

$$\sim \frac{6k_B T_s}{U_o \sigma_o^4} F_4 \left(1 + \frac{U_o}{2\sigma_o k_B T_g}\right) . \qquad \text{(F.11)}$$